Haptic assistance to mitigate damaging vertical accelerations of fast ships in head waves

MSc Thesis - Delft University of Technology

Roy Kok

Supervisors:
Dr. A. Vrijdag
Prof. Dr. A. P. van 't Veer
Prof. Dr. D. A. Abbink

TU Delft

Department of Biomechanical Design,
Department of Offshore and Dredging Engineering,
Faculty of Mechanical, Maritime and Materials Engineering

September 20^{th}, 2018

-

- This page has been intentionally left blank -

-

Preface

"Navegare necesse est, vivere non necesse est"

This saying originates form the roman empire in the year 56 B.C. and can be freely translated as "To sail is necessary, to be alive is not". Although a bit dramatic the saying is still used also as the motto of the city of Rotterdam to convey the importance of being able to operate under any conditions. In the context of current research can be explained as that it is known that it is dangerous to sail in harsh weather conditions at high speeds but the operators do not always have a choice and serve a greater good by risking their life for mission success. The current research will investigate a way to make the mission more safe for operators and crew and thereby increasing the chances of mission success.

Acknowledgements

In this section I would like to take the time to thank the persons that supported me throughout the project and without whom I could not have achieved the current level of work. First of all many thanks to Frank Hoeckx for developing the first version of the haptic simulator and providing me with an excellent base from which to continue my work. Next I would like to thank Henri Boessenkool and Timo Melman for helping me out with the experimental setup and statistics. A special thanks to the people at MARIN for providing the necessary support and updates when needed. I would also like to thank all participants that took the time to help me out with the pilot study and the experiment. Most of all I would also like to thank dedicated daily supervisor Arthur Vrijdag for always taking the time to discuss any issue that came up during the whole project and my Haptics professor David Abbink for providing high quality feedback when needed.

Contents

List of Figures

Haptic assistance to mitigate damaging vertical accelerations of small fast ships in head waves

R. Kok, A. Vrijdag*, A.P. van 't Veer*, D.A. Abbink**
*Department of Maritime and Transport Technology, Delft University of Technology, Mekelweg 2, 2628 CD, Delft, the Netherlands
**Department of Cognitive Robotics, Delft University of Technology, Mekelweg 2, 2628 CD, Delft, the Netherlands

***Abstract*— Crew of small fast ships often experience excessive vertical accelerations when sailing in waves, leading to discomfort and injuries. In an attempt to avoid this, in good visibility experienced operators reduce speed voluntarily when they anticipate that the next vertical peak acceleration will be unacceptably large. However, at night and during excessive spray, the operator can hardly see the environment which makes it almost impossible to anticipate wave driven events. On top of that, this approach carries the risk of operator misjudgment due to loss of concentration or fatigue. In this paper, the potential of haptic feedback to support the operator in preventing dangerously large vertical accelerations is investigated. A stochastic based approach was used in combination with a high end ship simulator to construct a haptic algorithm which gives a maximum advisable propeller speed setting based on an estimate of the current sea state. In order to test the effectiveness of this approach, a human-in-the-loop experiment was conducted using a within-subject design with 24 conveniently sampled participants. In this experiment the effect of haptic assistance is compared to manual control under both good and reduced visibility conditions. A key advantage of implemented haptic feedback algorithms is that the human remains in the control loop and can continuously decide to overrule the haptic advice. From the experiment it is found that the workload experienced by the operators is significantly decreased when using haptic feedback. However, no significant decrease in the number of excessive vertical accelerations was found using the current setup. A possible explanation for this result is the lack of motion cues and the inexperience of the participants. Therefore, it is recommended to extend the setup with a motion platform and conduct future experiments with experienced operators.**

Keywords - small fast ships, excessive vertical accelerations, haptic feedback, human-in-the-loop experiment, within-subject

I. INTRODUCTION

The FRISC or Fast Raiding Interception and Special forces Craft is a small fast (45kts) special forces craft that is used by the Royal Netherlands Navy for anti-smuggling, anti-piracy, counter-terrorism and patrol missions. In Fig. 1 the raiding craft version of the FRISC is shown. A tactical advantage of the FRISC is its ability to operate at high speeds in adverse weather conditions. However, the physical strain that accompanies operating high speed vessels in adverse conditions now proves the limiting factor in the employability of the FRISC. Operating in extreme conditions, the crew can experience dangerously high slamming impact forces, potentially causing severe injuries to the crew, as well as damage to the structure.This problem is not exclusive to the FRISC but holds for most small fast vessels [4], [14].

Fig. 1. The FRISC raiding craft in action [19].

The FRISC is operated by a minimum of two crew members: a navigator and a helmsman. In restricted waters the navigator communicates the directions to the helmsman who is standing with one hand on the wheel and one hand on the lever and has to keep all of his/her attention on the water, especially at high speeds. Due to the high load on the visual system of the helmsman, additional information is preferably provided through other sensory channels. Therefore, in this paper the potential of using haptic shared control (HSC) to assist the operators of small fast ships when sailing in waves is investigated.

Several measures have been taken in an effort to reduce the possibility of injuries due to wave induced vertical accelerations. These measures include shock absorbing chairs, a responsible sailing behaviour table and an extensive exercise program for the FRISC crew. Furthermore, the exposure time is limited by implementing strict deck cycles and resting periods.

When operators control a complex machine, the addition of force feedback on the controls reduces the workload, increase task performance and situational awareness [6]. When using haptic shared control not only visual but also the tactile and proprioceptive senses are used, which allows for fast control using reflexes and increased awareness. Although literature has shown the benefits of applying force feedback for driving, flying and remote operation (tele-operation), little attention has been directed towards implementing this promising technology in the maritime domain. The human-

in-the-loop maritime simulator setup used by Hoeckx et al. [1] is one of the first attempts to apply haptic shared control in the maritime domain. Their main goal was to see if it is possible to increase safety of shipping by the introduction of haptic ship control. Towards this end, two actuated 2-DOF azimuth control levers were designed. In this paper the same levers are used to control a small fast ship.

A. Vertical accelerations

From previous work on fast ships in waves [2], [3], [4], [14] it is known that the excessive vertical accelerations are the limiting factor in operations. Furthermore, from on-board measurements it was found that vertical peak accelerations have a very short duration and a relatively low frequency of occurrence [4]. It can be concluded that not all wave encounters will lead to an excessive vertical acceleration.

Understanding exactly what influences the vertical accelerations is the first step towards finding a mitigation measure. Peaks in vertical acceleration levels are the result of complex interplay between geometry, incoming wave characteristics, motion before impact and forward speed at impact [20]. Of these variables the incoming wave characteristics and the relative ship speed are most dominant. The largest accelerations occur in head seas at high forward speed with a low average wave period, which causes steep waves [8], [9].

The injuries that result from extremes in accelerations and excessive exposure can range from joint pain to severe kidney injury and fractured vertebrae. However, not only the extremes in vertical acceleration can cause injury to the human body but also the vibration dose and exposure time affect injury severity. The vibration dose can be reduced by significantly reducing the vessel speed and exposure time, which is undesirable given the type of operations that are typical for the FRISC and similar small fast ships. Therefore, the focus of this paper lies on reducing the extremes in vertical acceleration level.

Identifying the damaging accelerations is a key point in finding a solution to the wave slamming problem. When measuring onboard accelerations in practice, the acceleration signals are normally measured by an accelerometer mounted on the structure of the vessel. The resulting raw signal needs to be processed to find the accelerations that can cause injuries to the human body. For this purpose a set of three signal processing steps as proposed by Coe et al. [10] is used in this paper.

- *A 10 Hz low-pass filter:*
  This filter gets rid of the the high frequency vibrations of the deck and other components that might locally have the same magnitude but a much higher frequency. These high frequency deck vibrations are not damaging to the human body.
- *A vertical threshold:*
  This threshold signifies the minimum acceleration magnitude that is required to count it as being an acceleration. Usually this threshold is set to the Root-Mean-Square (RMS) of the signal.
- *A horizontal threshold:*
  This threshold is used to signify that there cannot be multiple harmful accelerations within one wave encounter. Usually this threshold is set to 0.5 [sec] for analyzing small fast ship accelerations.

The harmful accelerations can be distinguished from the raw signal using the signal processing steps defined above. Note that in this paper these signal processing steps are applied to the vertical acceleration signal generated by the ship simulator and the results are used to construct the Rayleigh database, which is explained later.

B. Control strategies

Experienced operators tend to reduce speed when a large wave, which is expected to cause an unacceptable acceleration, is approaching [3]. This way of sailing is called active throttle control. The difficulty with this approach is that the operator has to see the wave, perform an estimation based on intuition/experience and reduce speed several seconds before the wave is encountered to allow the vessel to slow down significantly and reduce the severity of impact. This active throttle control was the inspiration for a mitigation measure called proactive thrust control, which was extensively researched at Delft University of Technology by Deyzen [3] and Rijkens [2]. In their solution the system can be divided into three subsystems: (1) A wave measurement/prediction system, (2) A computational model that calculates the response of the ship to the predicted wave field in real-time for different speeds and (3) A control system, which automatically adjusts the propeller speed when required. Although this work is a valuable source of inspiration and proved that accelerations could be reduced using proactive thrust control, current (radar) technology has not been shown to be able to observe waves from a small fast moving ship.

Another possible approach, used in this paper, is to adjust the ship speed according to the sea state that is encountered. The FRISC sails in conditions up to sea state 5, which is equal to 4 m significant wave height. In the VCZSK [5] (Voorschrift Commando Zeestrijdkrachten) a 'responsible' ship speed table for the critical sea states (3-5) is provided. Application of the table has three drawbacks. First of all the table does not discriminate between different waveheight-waveperiod combinations nor does it consider the sailing direction with respect to the waves. Secondly, it requires the operator to estimate the wave characteristics. Finally, operators need to remember and use the table correctly in the heat of the moment, which is not ideal. In this paper the drawbacks of the described table are countered by using onboard sensors to estimate the wave characteristics and by using haptic shared control to communicate the advised maximum ship speed.

Summarizing, the aim of this study is to investigate the effects of providing a haptic speed advice on the excessive accelerations encountered. Thus, the research question reads:

"To what extend can haptic feedback on the lever assist the operators of small fast ships in mitigating the excessive vertical accelerations due to wave slamming?"

It was hypothesized that when sailing with the haptic assistance the operator would experience less excessive accelerations compared to manual sailing. Because the operator currently almost fully relies on visual information the effect of reduced visibility when applying shared control is also investigated. Each condition was assessed with respect to three categories of measures: Performance, Safety and Workload.

II. METHOD

A. Participants

Twenty-four participants (4 female) between the ages of 22 and 57 (M=26.9, SD = 7.5) volunteered in a human-in-the-loop ship simulator experiment. More than half of the participants claimed to have significant experience on the water (sailing or motor boat). However, only 3 participants were in possession of a navigation licence.

B. Apparatus

The haptic ship simulator setup was designed and built at Delft University of Technology. The setup as originally described by Hoeckx et al [1] was extended with the Fast Ship Simulator (FSSS) model from the E-Dolphin software developed by MARIN. The layout of the setup is shown in Fig. 2. The full setup consists of the following elements:

- *Ship simulator*
  The FSSS as part of the MARIN E-Dolphin software was developed with the aim to perform training runs of potentially difficult and dynamic situations that are difficult to perform in real life. The high accuracy in the hydrodynamic behaviour of the simulated vessel is required because most risk factors are related to complex non-linear hydrodynamic ship behaviour such as slamming, planing, broaching, ship-ship interactions, etc. The model used for the forces in the planing condition is based on slender body theory (2.5D). This method is an extended method of Zarnick's strip theory [11], later extended to small fast vessels by Keuning [4], in which the hull is divided up into a number of segments for which the sum of the forces is calculated separately after which all of the forces are summed up to arrive at the total force acting on the hull. The simulated wave field follows a JONSWAP distribution. The behaviour of the model was validated using the measured ship response to regular waves. The final model used was E-Dolphin 5.2, which was modified to send the acceleration information directly over NMEA (National Maritime Electronics Association) protocol.
- *Haptic levers*
  The haptic levers are custom-made by the Delft Haptics Lab by using the two 1 Degree of Freedom (DoF) levers from the Gemini (2014) project [18]. These levers are mounted to rotational discs such that they resembled 2 DoF azimuth thrusters. Both DoF's are connected via a steel cable capstan mechanisms to separate Maxon motors. This connection allows for efficient force translation with zero noticeable slip. In this paper only a single degree of freedom is used.
- *Operator*
  The operator controls the vessel using the visual and auditory information provided on the screen and the tactile and proprioceptive feedback from the haptic functionalities provided in the levers.
- *Real-time processor*
  The Bachmann real-time processor has multiple functions. First of all it runs the haptic algorithm, which is constructed in MATLAB Simulink before it is compiled. Secondly, it acts as a bidirectional interface between the haptic algorithm and the FSSS. That means that it decodes the NMEA messages coming from the FSSS to variables that can be used in the haptic algorithm. It encodes outputs of the haptic algorithm to NMEA messages that are sent to the FSSS. The haptic algorithm runs at 1kHz to ensure haptic fidelity and prevent any noticeable delays. The simulator is connected to the real-time processor via an Ethernet connection, which sends and receives the NMEA sentences using UDP protocol. Finally, the real-time processor gets input from the motor encoders that are mounted on the lever actuators and controls the PWM motor drives.
- *Control computer*
  A control computer is used to adjust the settings on the real-time processor via a custom made Graphic User Interface (GUI) using Matlab Simulink. The powerful graphics card of this computer is also used to run the visualization model of the simulator computer.

All systems are connected together via Ethernet cables and a network switch.

C. The haptic algorithm

The haptic algorithm as shown in Fig. 5 consists of five modules: 1. Sea state estimation, 2. The Rayleigh database, 3. The speed RPM relation, 4. RPM to lever position and 5. Haptic force. First, the average wave height is estimated based on the heave displacement of the vessel. After that the safe speed corresponding to that average wave height is determined from the Rayleigh database using the defined probability of exceedance and acceleration threshold. Then this safe speed is translated to a setpoint RPM. This setpoint RPM is translated to setpoint lever position. Finally, this setpoint lever position is communicated to the helmsman using the haptic levers. In the following sections a detailed description of the construction of the haptic algorithm is provided.

1.) For the estimation of the sea state parameters the heave response of the vessel is used. For each sea state the interval between the boundaries of the response motion are defined. Then the peaks in the response motion are averaged and this average value is compared to the different intervals.

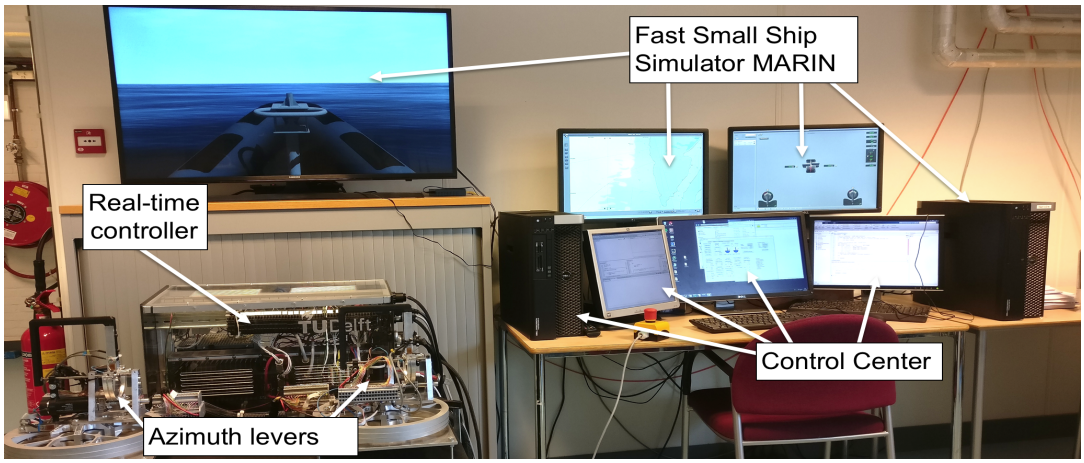

Fig. 2. The haptic demonstrator setup.

In this way the sea state is selected and changed if the average response value changes significantly. An update rate of this estimation is defined because a dynamic sea state estimation is required to generate a dynamic speed advice. For this update rate a moving time window of 30 seconds is used because this is used in the FSSS model as a standard initializing time for sea state changes.

2.) A safe sailing speed is found using the relation between the sea state and the vessel responses. The method developed is based on a stochastic approach that uses a database of response history. This database is constructed using the simulated vessel responses to different wave conditions and at different speeds. Knowing that the FRISC will operate in sea states from 0 to 5, only these sea states will be investigated. Taking a wave scatter diagram that is typical to the northern part of the North Sea the most relevant wave heights and periods can be found for that region. The largest vertical accelerations occur at short steep waves as was found by Keuning [4] and therefore these short steep waves are of most importance. From a wave scatter diagram of the northern part of the north sea the following wave height and period relations were chosen to be covered by the model [1]:

- Hs = 1 m, Tp = 7 sec.
- Hs = 1.5 m, Tp = 7 sec.
- Hs = 2 m, Tp = 7 sec.

A Rayleigh plot is constructed for each combination of wave height and period considered. The Rayleigh plot is used as a tool to estimate the probability that the wave height will exceed a certain level. Assuming that the wave height is sufficiently narrow banded and normally distributed the wave crests and troughs follow a Rayleigh distribution as was found by Longuet-Higgens [12]. If a linear relation between the wave height and vessel response is assumed, it follows that the accelerations also approximate the Rayleigh distribution. The nonlinear behavior will show up as deviations from the Rayleigh line. The simulated vessel responses to the sea states given above are measured for speeds ranging from 10 to 40 kts. For each speed and each sea state a recording of the vessel motions (velocities and accelerations) of 50 minutes (eq 3000 wave encounters) was taken. For the current model this was deemed good enough statistics.

In the resulting Rayleigh plot a user defined threshold acceleration and a probability of exceedance (PoE) can be set. Using the work of Keuning and Walree [7] who found that the crew of small fast rescue craft tolerated vertical accelerations up to $13 m/s^2$ at the wheelhouse and 25 m/s^2 at the bow a threshold was defined. It has to be noted that the threshold acceleration is very much dependent on the crew and mission, therefore, this threshold is made adjustable in the final model. However, for the experiment the threshold is fixed at using the values above. The operator is able to select a PoE of this threshold between 10^{-1} and 10^{-6}. For the experiment the PoE is fixed at 0.001. The probability that acceleration x_n exceeds threshold value α is shown in Eq. (1).

$$P(x_n > \alpha) = exp(\frac{-\alpha^2}{2\sigma_x^2}) \tag{1}$$

Where,

- x_n is the acceleration signal.
- α is the acceleration threshold.
- σ_x is the standard deviation of signal x.

$$\alpha = \sigma_x \sqrt{-2ln(P(x_n > a))} \tag{2}$$

Rewriting Eq. (1) to Eq. (2) makes using the Rayleigh plot more straightforward because linear lines of constant speed through the measured data can be drawn as can be shown in Fig. 4. At the crossing of the red lines in Fig. 4, which signify the acceleration threshold and PoE, the resulting advice speed is found using quadratic interpolation.

[1]Gathering statistically significant response data for each sea state at multiple speeds is time consuming. Therefore, a limited number of sea state conditions is used to provide a prove of principle of this way of providing speed advice.

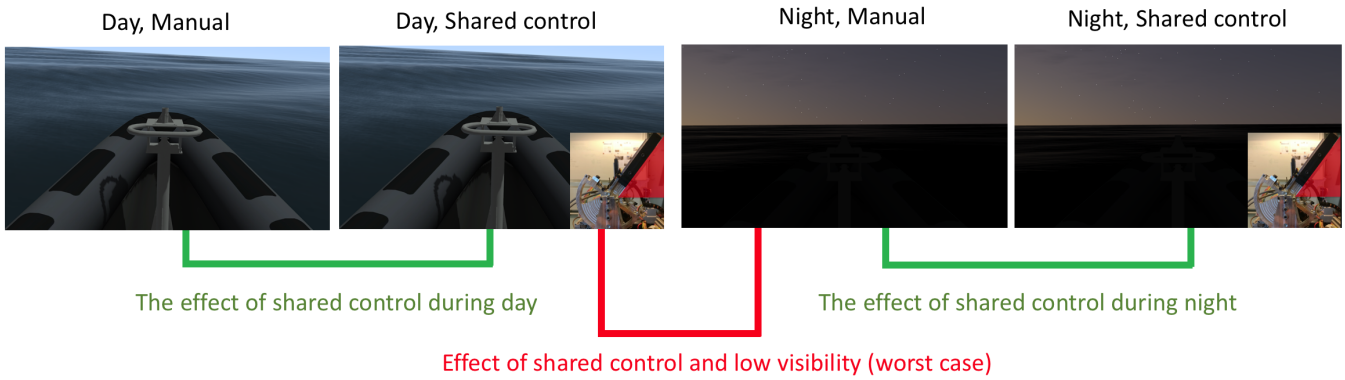

Fig. 3. The four conditions: Manual day, Shared control day, Manual night and Shared control night shown respectively as well as the pairwise comparisons considered in this research.

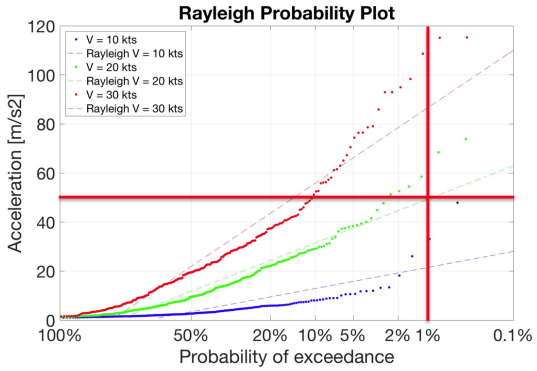

Fig. 4. An example of the one of the Rayleigh plots used in the database showing the probability of exceedance of an acceleration level at different speeds. The dots are actual measured acceleration peaks while the dotted lines are used as the Rayleigh approximation of the data.

3.) The speed advice is translated to a setpoint RPM using a look-up table that is constructed using the FSSS simulator.

4.) The setpoint RPM is translated to a lever angle setpoint using another look-up table.

5.) The haptic force, which is felt when the lever position exceeds the advised position, is modeled as a virtual spring with spring stiffness K_s. In Fig. 6 this force is illustrated showing the advice lever position X_{Adv} and the boundaries between which the advice can vary.

D. Environment conditions

All participants sailed four conditions (Manual day, Shared control day, Manual night or Shared control night) inn a marked strip of deep water. These conditions are shown in Fig. 3. The track is 4 nm in length and because only the effect of head waves is considered an autopilot was used to fix the heading. A significant wave height of 2 m and a peak period of 7 seconds was chosen for the experiment to provide the participant with a challenging but realistic wave field. When starting each run a wave field comprised of (pseudo-) random components, with desired significant wave height and peak period, was generated. The randomness of the wave field ensures that the participants cannot adopt a position dependent control strategy. The length of the run is chosen such that for an average speed of 22 kts an equal number of wave groups is encountered, which makes the average wave conditions for all participants relatively equal. Before starting the experiment the participants got one full run of manual control to familiarize with the dynamics of the vessel and the wave conditions. A drawback of this experiment is that the participants could not feel the (excessive) acceleration. To partly replace this missing motion cue, a vibration signal was provided by the levers every time an excessive acceleration occurred.

E. Experimental design

Before the experiment commenced all participants were asked to read and sign an informed consent form, explaining the purpose, instructions, procedures and agreements of the study. A fully counterbalanced within-subject design was used to mitigate the learning effects. The participants were asked to maintain a firm grip on both levers. The negative RPM direction of levers was blocked to maintain realistic control strategy behaviour. In reality reversing propeller speed when moving forward at relatively high speed will cause the engines to shut down. Participants were informed about the availability of the speed advice and warning vibrations. No advice on a operating strategy was given.

The participants were asked to complete the trial as fast as possible while aiming to minimize the number of excessive accelerations. After each trial the completion time and number of excessive accelerations were marked on the whiteboard. In order to motivate the participants a score of a (fictive) experienced operator was set as the first score.

After each trial the participants were asked to fill out a NASA Task Load Index form (NASA-TLX) [13] to assess the experienced workload. The NASA-TLX had an extra item to assess the simulator sickness on a scale of 1 to 6 (1 = not experiencing any nausea, no sign of symptoms, 2 = arising symptoms, 3=slightly nauseous, 4 = nauseous, 5 = very nauseous, retching, 6 = vomiting). Because it is the first time that a human-in-the-loop experiment is conducted with the haptic ship simulator this item was added to avoid any issues. If a response of 4 or higher would be given

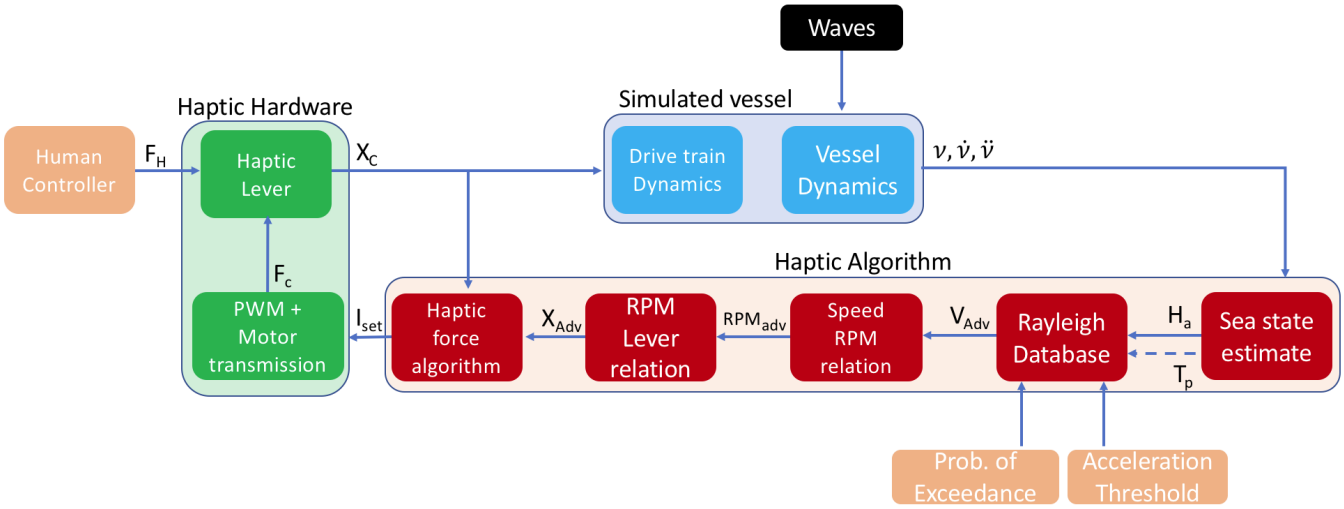

Fig. 5. A block diagram showing the human controller acting on the haptic hardware, which controls the simulated vessel and the haptic algorithm used to provide a haptic speed advice.

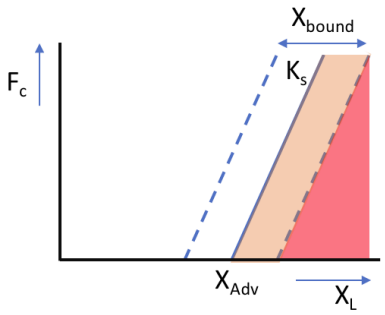

Fig. 6. A schematic visualization of the haptic force algorithm showing that the virtual spring force with spring constant K_s is only generated once the lever position (X_L) reaches the advised maximum position (X_{Adv}).

the experiment would be stopped. Fortunately, non of the participants experienced any kind of nausia during the trials. In total the experiment including the training and NASA-TLX took approximately 45 minutes.

F. Dependent measures

The data was measured from when the vessel crossed the starting line until the finish was reached at a frequency of 1kHz. The vessel had some time to accelerate before the starting line and no deceleration at the finish was needed. However, it was found that in many cases the haptic algorithm was not completely initialized when the starting line was crossed. Therefore, it was decided to discard the first 10% of the track for every participant. The dependent measures were categorized into performance, safety and effort.

Performance

To assess the performance of the participants the average speed over the trial is used. Average speed was taken because in literature on the mitigation of excessive accelerations [2][3] the difference in average speed is used as a measure of performance.

Safety

Mean acceleration level $[m/s^2]$*:* The means are used to investigate the change of operator behaviour when using shared control, because the advice is only generated when the system assumes the vessel is on the boundary of the threshold acceleration level. The means will give an idea if the acceleration levels are increasing on average.

Excessive accelerations [-]: The number of excessive accelerations is counted and compared because the shared control system was designed to mitigate these. If the participants would perfectly follow the shared control advice on average an excessive acceleration is encountered every 1000 waves, given a PoE setting of 0.001.

The significant acceleration levels ($A_{1/3}$, $A_{1/10}$, $A_{1/100}$) are used to gain insight in the distribution and the change in distribution of the acceleration levels. It is deemed important to investigate if/how this changes when implementing shared control.

$A_{1/3}$ $[m/s^2]$*:* the one third highest accelerations or significant accelerations. This metric is related to the significant wave height and therefore deemed interesting.

$A_{1/10}$ $[m/s^2]$*:* the one tenth highest accelerations.

$A_{1/100}$ $[m/s^2]$*:* the one hundredth highest accelerations. This metric gives an insight on the distribution of the acceleration in the tail of the spectrum.

Workload

Throttle reversals: The number of times the participant reverses the direction of the throttle with a magnitude greater than 2 degrees [15]. From literature it is known that shared control generally decreases the workload when compared to manual control. However, without respiratory or EEG measurements an alternative objective metric for workload needs to be found. Johanson et al. [16] found that when looking at user input on the system, the number of reversals

and the reversal rate give an indication of the workload experienced by the participants. A reversal is signified by a significant change in the movement direction of the lever. To make sure the reversal is an intended movement and not subjected to sensory noise a minimum difference between peaks is used. The number of reversals is determined by only counting the reversals if the value between the calculating local minima and maxima of the throttle angle signal were greater than 2 degrees.

NASA TLX (%): At the end of every trial the participants were asked to grade their workload on a 21-points scale for six categories: Mental Demand, Physical Demand, Performance, Effort and Frustration. Each question was scaled from very low to very high with the exception of Performance, which was scaled from perfect to failure. The total workload was calculated by taking the mean of the percentages.

G. Statistical analysis

A 24x4 matrix of each dependent measure was obtained resulting from the 24 participants each completing 4 conditions. Not all dependent measures are normally distributed and therefore the matrix was rank transformed according to Conover and Iman [17]. This rank transformation rewrites all scores to a scale of 1 to n (where n is the number of scores) to account for possible violation of the normality assumption that comes with using parametric tests. A repeated measures ANOVA with the four conditions as within-subject factor was used to to analyze the matrix that now consist of numbers between 1 and 96. For the three pairwise comparisons that were deemed relevant Bonferroni corrections were applied. To determine the effect sizes (d_z) Eq. (3) was used, where the μ_{x-y} is the mean of the difference and σ_{x-y} is the standard deviation of this difference. Spearman rank-order correlation coefficients were used to assess the associations between the dependent measures.

$$d_z = \frac{|(\mu_{x-y})|}{\sigma_{x-y}} \tag{3}$$

III. Results

For all dependent measures the means, standard deviations, the results of the repeated measured ANOVA and the pairwise comparisons are provided in Table I. No recordings were made during the training run. An example of the speed advice was introduced near the end of the run. Furthermore, the experimental results of two participants were excluded from further analysis after it was found that during some trial these participants experienced 10 times more excessive accelerations than average. Fig. 7 shows the throttle angle, speed and accelerations for a typical participant over the 4 trials.

A. Performance

In Table I shows the results of the statistical analysis. No significant difference was found between the average speed with manual control compared to shared control.

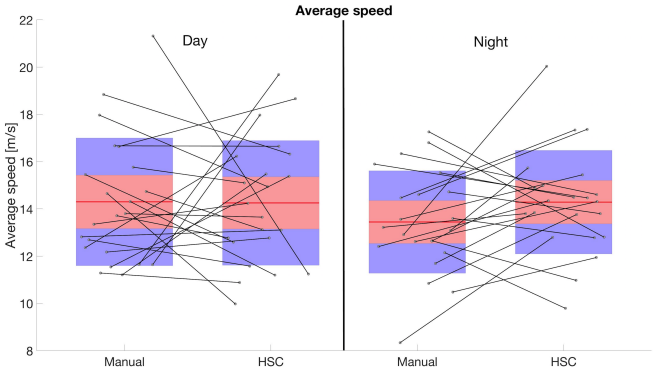

Fig. 7. The average speed showing the groups of raw data, the mean (red line), the SEM (pink square) and the 95% confidence interval (blue square) for each of the four conditions. The lines show the difference for the same person due to different conditions.

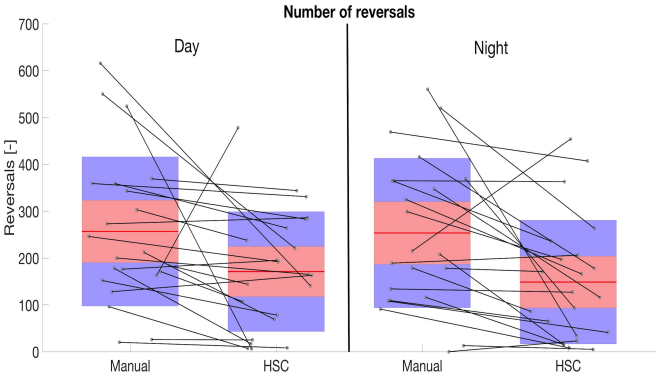

Fig. 8. The number of reversals showing the groups of raw data, the mean (red line), the SEM (pink square) and the 95% confidence interval (blue square) for each of the four conditions. The lines show the difference for the same person due to different conditions.

B. Safety

The mean acceleration level does not show a significant difference between the different conditions.

The number of excessive accelerations was found to vary significantly between the conditions. The effect size during night time was found to be medium and a significant effect (p=0.039) was found when comparing the shared control day to the manual night (best/worst scenario comparison).

For the $A_{1/3}$ no significant effect of shared control was found.

The $A_{1/10}$ accelerations also do not show a significant effect of shared control. In the manual case the $A_{1/10}$ are about 10% higher on average.

In the tail of the acceleration distribution ($A_{1/100}$) a significant effect is shown when comparing the different conditions. When comparing the best/worst case again a significant effect (p=0.034) was found. In general when approaching the tail of the acceleration distribution the effect sizes are observed

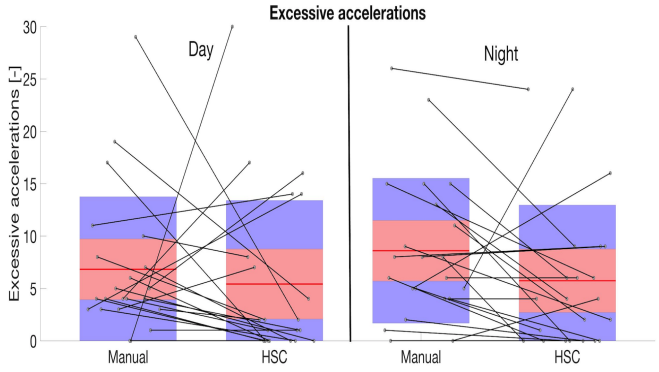

Fig. 9. The number of excessive accelerations showing the groups of raw data, the mean (red line), the SEM (pink square) and the 95% confidence interval (blue square) for each of the four conditions. The lines show the difference for the same person due to different conditions.

to be growing for the different comparisons.

C. Workload

Participants' reversal show a significant difference between the conditions. Where on average a reversal difference during day time between the shared control and the manual condition of 33% was found during night time it was 42%. The reversals for each condition are shown in Fig. 8.

The NASA-TLX questionnaire results indicate higher reported workload for the manual condition compared to the shared control conditions. For the pairwise day time comparison a significant difference between the conditions was found (p=0.014). For the night time comparison this was also found to be significantly different (p=0.045). The strongest effect was found when comparing the best/worst case scenarios (p=0.007). The results of the NASA-TLX are shown in Fig. 10.

IV. Discussion

A human-in-the-loop experiment was conducted to investigate the effect of a haptic shared control compared to manual when sailing in waves, on the operators average speed, vertical acceleration levels, reported workload and lever reversals. The 24 participants considered in the within-subject design experiment sailed a 4nm track in head waves in both good and poor visibility conditions. The effect of reduced visibility on the effect of the system was tested because the operator currently almost fully relies on visual information to support his control actions.

The application of shared control in the experiment considered showed a reduction in both the reported workload (NASA-TLX), 20% in day and 10% in night, and the measured workload (reversals), 33% in day and 42% in night, without effecting the average speed or the number of excessive accelerations. This effect measured during an experiment with a limited duration could prove to be beneficial in reality since FRISC missions can consist of hours of sailing.

The fact that there was no significant difference between manual and shared control in terms average speed and number of reversals could be attributed to the large differences between individual subjects. For example Fig. 9 shows the lines comparing individual performance, here it can be seen that 16 out of 22 tend to experience less excessive accelerations using haptic shared control during for the day condition and in the night condition this number is even 17 out of 22. However, for a few participants the lines go up, which indicates a different strategy, namely taking more risks by exceeding the speed advice more. For the average speed this effect is not observed, which indicates that taking more risk in the form of excessive accelerations does not always translate in a higher average speed.

Furthermore, the results do show a significant reduction of the number of excessive accelerations between manual night and haptic shared control day. This indicates that haptic shared control does influence the number of excessive accelerations, however, the effect size is low and thus only observable for the most extreme condition comparison (i.e. low visibility for manual and high visibility and haptic assistance). An increase in the number of participants could increase the statistical significance between the different runs.

It was found that when looking at the reversals metric a significant decrease was found during the night condition. The reversals seem to decrease when using haptic shared control compared to manual for both day an night. However, a only for night time a significant effect was found. The results from the NASA-TLX indicated that the participants experienced less control workload when using the shared control system compared manual control. This reduction in of both reported and measured workload corresponds to the expectations based on literature [6] on haptic shared control in other domains.

The haptic speed advice is felt once the maximum advised lever position and correspondingly the maximum safe speed is reached. The fact that the mean acceleration level, the $A_{1/3}$, and the $A_{1/10}$ accelerations did not vary significantly between the conditions is considered to be a positive outcome of the experiment, since an increase in these acceleration levels when using shared control could have meant an increase in acceleration dose sustained because participants choose to operate more closely to the limits.

A. Effect of experimental design choices

When preparing the experiment choices and simplifications needed to be made due to time and resources constraints. In this section the impact of these simplifications on the outcome of the experiment are discussed.

Simulator setup: From literature it is known that the operators tend to react after a (excessive) vertical acceleration is felt [4]. The lack of this motion cue in the current experimental setup could have had an effect on the results. The vibration that was implemented on the levers when an

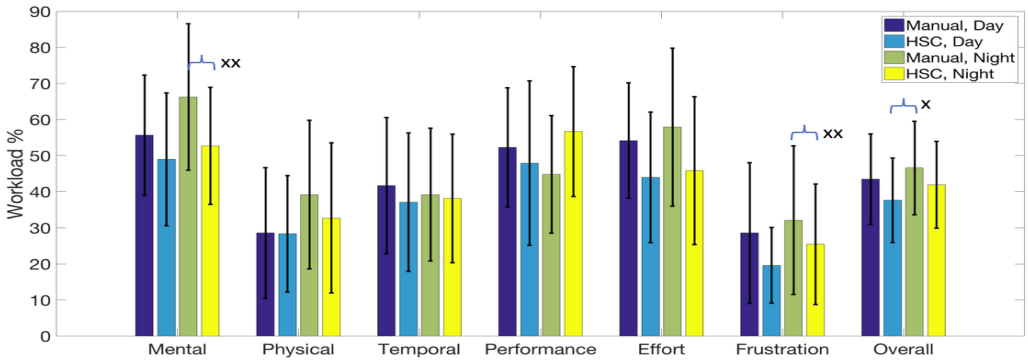

Fig. 10. The results and the standard deviation of the NASA-TLX for all participants with x:p=0.01, xx:p=0.001.

excessive acceleration was encountered is much more easily dismissed than a full body vibration. Using the FSSS motion platform at MARIN together with the haptic levers could lead to different results. However, the aim of the experiment to investigate the effect of applying haptic shared control when sailing in waves. If valuable insights could be gained using the current simplified setup it would be beneficial compared to a expensive motion platform.

Participants: For the experiment 24 conveniently sampled participants were selected from among the students and staff of Delft University of Technology. After analyzing the raw data two participants were excluded from further analysis. Of the remaining participants only two were in possession of a navigation license. The lack of sailing experience and the relatively small size of the group could have effected the outcome of the experiment. However, if experienced operators would have been selected for the current setup, the lack of motion cues and the presence of a navigator could have interfered with the operators strong internal model gained from experience. This could also have had a significant impact on the results.

Wave field: Although the wave characteristics in general, the peak period and significant wave height, are similar for every participant it can happen that some participants encounter somewhat more long and shallow waves rather than steep high waves. In some cases this could have lead to a more difficult wave environment. If full insight into the wave field components could have been provided it could be used to normalize the score of the participants with for example the spectral power of the wave signal. However, with the current simulator information available this was not possible.

Sea state estimator: The sea state estimation was kept simple to show the prove of principle of this method of providing advice based solely on the heave response of the vessel. However, if the pitch motion of the vessel would also be included in the estimation it could be used to estimate the wave steepness next to the wave height and base the sea state estimation on this combination. Experiments will need to show the usefulness of this combined method. Furthermore, the current approach makes use of simple sensors that are mostly available on the current vessels. However, using sensors that could potentially make a more precise estimate of the sea state, such as radar or smart camera's, could also increase the model quality in the future.

Warnings: To partly replace the missing motion cue a vibration signal was implemented on the lever when an excessive acceleration was reached. It could have happened that the vibration is easily dismissed or that the the signal did not carry enough information about the severity and the duration of the acceleration signal. Therefore, if the vibration would be made dependent on the severity and/or the duration of the excessive acceleration it could give the operator more information and potentially influence behavior. Conveying a signal that contains more information than a warning signal could be useful. However, this will also require more training and effort to get familiar with.

Order effects: When looking at the order effects for number of excessive accelerations it can be seen that a substantial decrease in the number excessive accelerations occurs when the participants become more experienced. This indicates that the participants are not fully trained when the experiment commenced. The large number of excessive accelerations could potentially partly be explained by training trials that were not recorded, so the participants did not get feedback on their performance before the experiment commenced. This was done intentionally because the participants were urged to explore the boundaries of what was possible with the simulated vessel and thereby get a feel for the dynamics and the acceleration and deceleration capabilities. However, providing feedback on the training run could have helped in avoiding the outliers that occurred during some of the first runs. To compensate for these learning effects the Latin-square approach was used. However, testing the model with experienced operators could reduce these differences in individual prior skill level. For future experiments a longer training run could also help to further mitigate the learning effects.

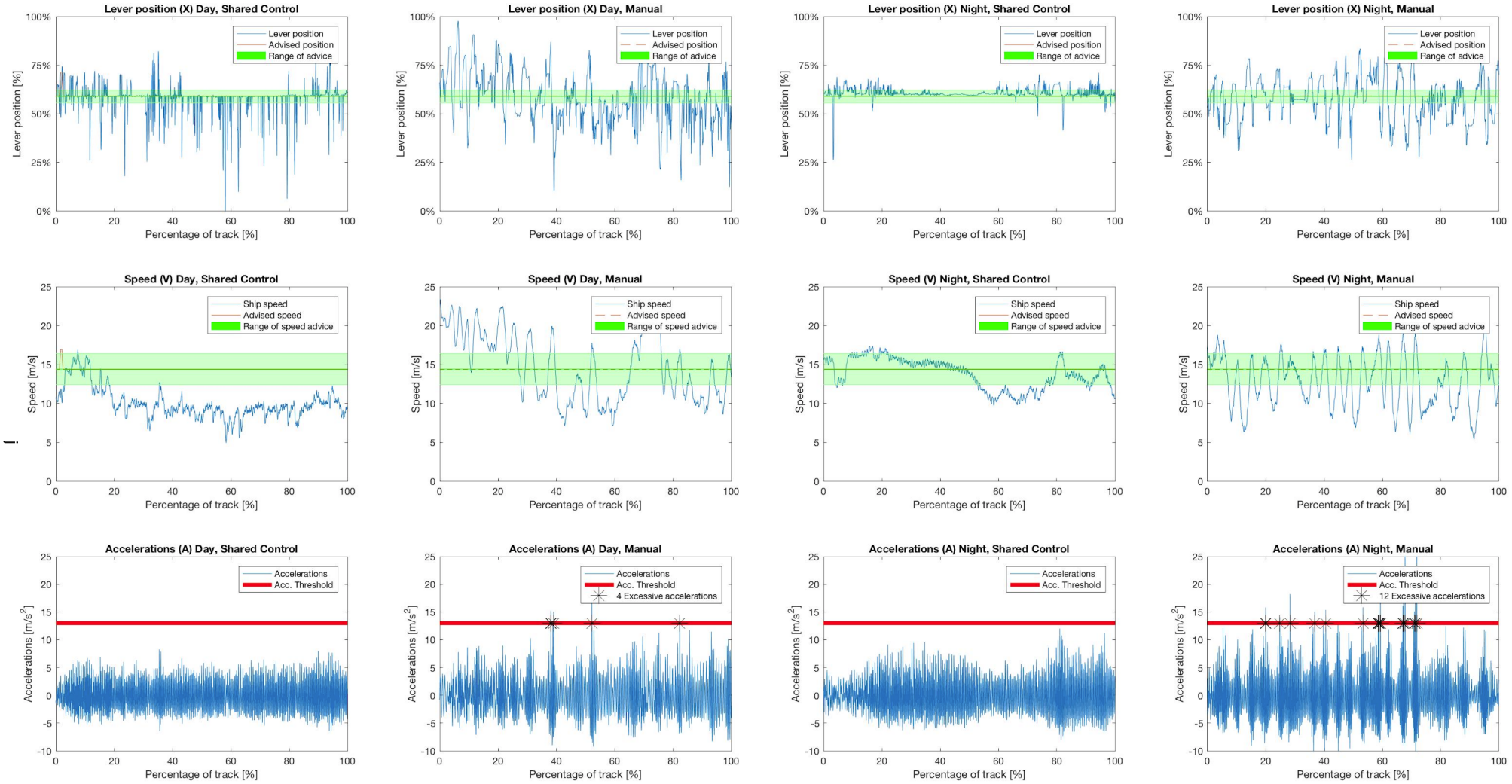

Fig. 11. The most important mectrics: lever angle (X), ship speed (V) and acceleration (A) for a typical participant over the four trials.

Headwaves: In the experiment is was chosen to sail in head waves because this is generally considered to be the most limiting condition. However, a much voiced argument, especially from the persons with sailing experience and a navigation licence, was that the inability to maneuver did not feel natural. What experienced operators tend to do is to maintain an angle of attack with respect to the approaching wave of about 30^o. This leads to a zigzag sailing pattern in which the chance of excessive vertical accelerations due to wave slamming is decreased. The reason to set the simulated ship to autopilot is to have similar conditions for every participant and make the experiment less sensitive to operator experience. In an experiment with experienced (FRISC) operators and a more realistic simulation environment it could be useful to have also manoeuvring capabilities.

V. Conclusion

In the beginning of this paper it was hypothesized that when sailing with the haptic assistance the operator would encounter less excessive accelerations compared to manual sailing. The results from the current experiment only show a significant decrease in the number of excessive accelerations when comparing the best/worst case scenario. However, 16 out of 22 participants experienced less excessive accelerations when sailing shared control. The lack of significance indicates a difference in control strategy between the participants. Furthermore, a significant decrease in the workload reported and the number of reversals was found when shared control was used.

This study is the first to consider human-in-the-loop experiments for reducing the vertical accelerations of small fast vessels. Furthermore, it was the first time a haptic ship simulator was used to perform experiments. Valuable insights were gained on operator response and applying human-in-the-loop experiments for maritime applications. Further research could expand the way operator response is measured and how best to apply shared control within the maritime domain.

VI. Recommendations

In this section some recommendations for future work are given. These recommendations can be split up into improvements upon the current model and steps needed to implement this model in the FRISCs.

Firstly some recommendations regarding the current model and experiment are given. These recommendations are meant as improvements to strengthen the current experiment.

- *Connect to motion base platform*
  Firstly, it is recommended to connect the existing haptic controls setup to the FSSS simulator with motion base platform, which is currently based at MARIN. The participants are expected to perform in a much more realistic manner when really feeling the effect that the waves have on the vessel.
- *Test with trained/experienced operators*
  The measuring the response of the persons that are the end user of this technology will be valuable. Also their feedback on how the system functions and what could be improved can be very useful. In this way the model can be tuned using the experience of the operators. However, testing with experienced operators will be most beneficial when the simulation environment most closely resembles real life operations.
- *Maneuvering*
  In the improved experiment it is recommended to allow the operator to maneuver up and down the waves as would also be done in reality. This will improve the operators sense of immersion in the simulation. Using the FSSS simulator from MARIN the current steering wheel could be used to manoeuvre or it could even be extended with a haptic steering wheel that would help to navigate the waves.

In this section the steps that are needed to implement the current model aboard the FRISC fleet is provided. First of all the FRISCs need to be equipped with high precision sensors and robust shock resistance data storage units. Collecting the response and operator input data will besides constructing the database but also grand and insight in operator behaviour, which could be very valuable when performing preventive maintenance strategies, but also accident analysis and many other applications.

Most importantly for implementation of haptic for this application would be to test the effectiveness of the levers and the sensory threshold of the operators when wearing protective gear. The haptic advice provided can only be as subtle what the operator is able to sense. A version of the haptic handles that is small but yet powerful enough to provide meaningful force feedback to the operator even when wearing protective gear and in a high vibration environment could prove to be a challenge. The handles will also have to be redundant that when the haptic functionality fails the engines can still be controlled.

ACKNOWLEDGEMENTS

The authors would first of all like to thank Frank Hoeckx for developing the first version of the haptic simulator and providing an excellent base from which to continue. Next, thanks to Henri Boessenkool and Timo Melman for assisting with the experimental setup and statistics. A special thanks to the people at MARIN for providing the necessary support and updates when needed. Also the authors would very much like to thank all participants that took time off to partake in the pilot study and the experiment.

This research was part of the ”Haptic control for small fast ships MIIP project, which was partly supported by NML and the Dutch Ministry of Economic Affairs.

TABLE I

MEANS (M), STANDARD DEVIATIONS (SD), EFFECT SIZES (d_z), AND RESULTS OF THE REPEATED MEASURES ANOVA (F, P) PER DEPENDENT MEASURE.

	Manual Day M(SD)	Shared control Day M(SD)	Manual Night M(SD)	Shared Control Night M(SD)	p-value (F=3.94)	Pairs 1-2 $p(d_z)$	3-4 $p(d_z)$	2-3 $p(d_z)$
Performance								
Average speed	14.3(2.7)	14.2(2.6)	13.4(2.2)	14.3(2.2)	p=0.58 F=0.65	0.02	0.35	0.23
Safety								
Mean acc.	5.3 (1.2)	5.1 (1.1)	5.3 (1.2)	4.9 (1.1)	p=0.59 F=0.64	0.08	0.33	0.0.16
Excessive acc.	7.9 (11.0)	5.5 (8.0)	8.6 (6.9)	5.7 (7.2)	p=0.033 F=3.11	0.32	0.54	0.64 (x=0.039)
$A_{1/3}$	8.6 (2.1)	8.0 (1.9)	8.7 (1.9)	7.9 (1.6)	p=0.17 F=1.74	0.23	0.4	0.42
$A_{1/10}$	11.8 (3.7)	10.4 (2.8)	11.8 (2.7)	10.7 (3.0)	p=0.060 F=2.59	0.30	0.46	0.55
$A_{1/100}$	1.6.6 (6.5)	14.2 (5.0)	17.3 (5.6)	15.4 (5.3)	p=0.041 F=3.0	0.43	0.35	0.62 (x=0.034)
Workload								
Reversals	256.7 (159.2)	171.3 (127.8)	253.4 (159.6)	148.6 (132.0)	p=$1.39 * 10^{-4}$ F=7.9	0.56	0.78 (x=0.009)	0.53
NASA TLX (%)	45.1 (11.9)	36.4 (10.4)	47.4 (15.2)	42.2 (13.4)	p=$3.82 * 10^{-4}$ F=7.01	0.73 (x=0.014)	0.63 (x=0.045)	0.80 (x=0.007)

REFERENCES

[1] Hoeckx, F., Vrijdag, A., Abbink, D.A., (2017). "Developing of a test setup for exploring the potential of haptic feedback for maritime operations", MECSS Conference Proceedings, Glasgow, UK.

[2] Rijkens, A.A.K., (2016), "Proactive Control of Fast Ships: Improving the seakeeping behaviour in head waves". PhD Thesis, Delft University of Technology.

[3] Deyzen, A.F.J., (2014), "Improving the operability of planing monohulls using proactive control: From idea to proof of concept", PhD Thesis, Delft University of Technology.

[4] Keuning, J.A., (1994), "Nonlinear Behaviour of Fast Monohulls in Head Waves", PhD Thesis, Delft University of Technology.

[5] Directie operaties NLMF, (2014), "Voorschrift Commando Zeestrijdkrachten","Zeemanschap deel 1".

[6] Abbink, D. A., Mulder, M., Boer, E.R.,(2012),"Haptic shared control: smoothly shifting control authority?",In: Cognition, Technology Work 14.1: 19-28..

[7] Keuning, J.A. and Walree F.,(2005), "The comparison of the hydrodynamic behaviour of three fast patrol boats with special hull geometries.", In Proceedings of the 5th International Conference on High-Performance Marine Vehicles, Newnham, Australia.

[8] Coe, T.E., Dyne, S., Hirst, J., (2012), "Whole body vibration mitigation: maintaining capability while complying with legislation and protecting crew from high speed craft motions, Edinburgh, Scotland", Conference Proceedings of INEC.

[9] Coe, T.E., King, P.D., Hirst, J., (2014), "Understanding Whole Body Vibration Exposures on High Speed Marine Craft", Conference Proceedings of INEC, Amsterdam, Netherlands.

[10] Coe, T.E. et al., (2014), "Development of an International Standard for comparing shock mitigating boat seat performance", Proceedings of Innovation in Small Craft Technology, London, UK.

[11] Zarnick, E.E., (1978), "A nonlinear mathematical model of motions of a planing boat in regular head waves, 86.", David W. Taylor Ship RD Center, USA.

[12] Longuet-Higgins, M. S., (1952), "On the statistical distribution of the heights of sea waves.", Journal of Marine Research, 11: $245-246$.

[13] Hart, S.G., Staveland, L.E., (1988), "Development of NASA-TLX (Task load index): results of emperical and theoretical research." In: Meshkati, P.A.H.N. (Ed.), Human Mental Workload, vol. 1: $139-183$.

[14] de Jong, P., (2011), "Seakeeping behaviour of high speed ships", PhD Thesis, Delft University of Technology.

[15] McLean, J.R., Hoffmann, E.R., (1975), "Steering reversals as a measure of driver performance and steering task difficulty.", Human Factors 17: $248-256$.

[16] Johansson, E., Engstrom, J., Cherri, C., Nodari, E., Toffetti, A., Schindhelm, R., Gelau, C., (2004), "Review of existing techniques and metrics for IVIS and ADAS assessment" (AIDE IST-1-507674-IP). Retrieved from www.aide-eu.org/pdf/sp2 deliv new/aide d2 2 1.pdf.

[17] Conover, W.J., Iman, R.L., (1981), "Rank transformations as a bridge between parametric and nonparametric statistics.", Am. Stat. 35: 124 129.

[18] Kuiper, R., Boerefijn, E., Heij, W., Flipse, M., Vreugdenhil, W., Wang, K. (2014) http://www.delfthapticslab.nl/device/gemini-1dof-master-slave/, accessed on $20-7-2018$

[19] https://www.defensie.nl/onderwerpen/materieel/schepen/frisc-motorboot-fast-raiding-interception-and-special-forces-craft. Accessed on $05-3-2018$, in Dutch.

[20] Townsend, N.C., Wilson, P.A., Austen, S., (2008), "What influences rigid inflatable boat motion?", Proceedings of the Institution of Mechanical Engineers, Part M: Journal of Engineering for the Maritime Environment 222.4 : 207-217

Chapter 1

Introduction

Since the invention of the torpedo boats in 1880's man has been able to traverse the seas at high speeds and during the world wars the development of such high speed craft got high priority. However, little thought was given to the workability of these crafts, only in the 1980's people started talking about seakeeping behaviour and the comfort of the crew. Efforts towards increasing the workability are found in the Bow Enlargement Concept, which later resulted in the axe bow concept. Also multi-hull designs were suggested to increase workability and crew comfort. However, the large majority of today's small fast ships are and for the foreseeable future will remain mono-hulls because of their cost efficiency and relatively easy construction. The problem with monohull designs is that there is relatively little that can be done to mitigate the slamming impact of the hull on waves. An example of such a fast monohull is the FRISC or Fast Raiding Interception and Special forces Craft, which is a fast (up to 45 kts), small (up to 10 crew), special forces craft that is used by the Royal Netherlands Navy for anti-smuggling, anti-piracy, counter terrorism and patrol missions. Speed, agility and the capability to operate in all conditions are what gives the FRISC its tactical advantage. Built to operate in any environment, the FRISC can achieve relatively high speeds in large wave conditions.

However, the physical strain that accompanies operating high speed vessels in adverse conditions now proves the limiting factor in the employability of the FRISC. Operating in extreme conditions, the crew can experience dangerously high slamming impact forces, potentially causing severe injuries, as well as damage to the structure. This problem is not exclusive to the FRISC but holds for most small fast vessels [20][10]. The FRISC is operated by a minimum of two crew members: a navigator and a helmsman. In restricted waters the navigator communicates the directions to the helmsman who is standing with one hand on the wheel and one on the lever and has to keep all of his/her attention on the water, especially at high speeds. Due to the high load on the visual system of the helmsman, additional information is preferably provided trough other (non-visual) sensory channels. Therefore, this report investigates the potential of using haptic feedback to assist the operators of small fast ships when sailing in waves is investigated.

When operators control a complex machine, the addition of force feedback on the controls might reduce the workload, increase task performance and situational awareness. Although literature has shown the benefits of applying force feedback for driving, flying and remote operation [2] (tele-operation), little attention has been directed towards implementing this promising technology in the maritime domain. The human-in-the-loop maritime simulator setup used by Hoeckx et al. [18] is one of the first attempts to apply shared control in the maritime domain. Their main goal was to see if it is possible to increase safety of shipping by the introduction of haptic ship control. Towards this end, two actuated 2-DOF azimuth control levers were designed. Next to commanding engine speed and thruster orientation, these levers could also provide haptic feedback by generating forces in both degrees of freedom. In this report the same levers are used for to control a small fast ship.

From previous work on fast ships in waves [20], [10], [4], [1] it is known that the excessive vertical accelerations are the limiting factor in operations. Furthermore, from on-board measurements it was found that vertical peak accelerations have a very short duration and a relatively low frequency of occur-

rence [20]. It can be concluded that not all wave encounters will lead to an excessive vertical acceleration. Before coming up with mitigation measures it was decided to look at how the operators of small fast vessels currently try to mitigate slamming events. Experienced operators tend to reduce speed when a large wave, which is expected to cause an unacceptable acceleration, is approaching [4]. This way of sailing is called active throttle control. The difficulty with this approach is that the operator has to see the wave, perform a calculation based on intuition/experience and reduce speed several seconds before the wave is encountered to allow the vessel to slow down significantly and reduce the severity of impact. This active throttle control was the inspiration for a mitigation measure called proactive thrust control, which was extensively researched at Delft University of Technology by Deyzen [4] and Rijkens [1]. Although this work is a valuable source of inspiration and proved that accelerations could be reduced using proactive thrust control, current technology cannot predict waves up to the level of accuracy which is needed for such a system.

Another method is to adjust the ship speed according to previously experienced motions (stochastic approach). This method will continuously provide a maximum safe sailing speed according to the motions experienced. Using on-board sensors the system can make an estimation on the wave characteristics and using a database of past motions give a speed advice to stay below a certain threshold acceleration level. Due to the risks of injuries being caused by wave slamming to current vessels, it is very important to develop a method which can be implemented as soon as possible. Therefore, in the current work a haptic speed advice algorithm will be used that provides the operator with a speed advice based on the wave field in which the vessel currently resides. The aim of this study is to investigate the effects of providing a haptic speed advice to the helmsman in terms of performance, safety and workload. Thus, the research question reads:

"To what extend can haptic feedback on the lever assist the operators of small fast ships in mitigating the excessive vertical accelerations due to wave slamming ?"

It was hypothesized that when sailing with the haptic assistance the operator would encounter less excessive accelerations compared to manual sailing. Furthermore, because the operator currently fully relies on visual information it was hypothesized that the effect of reduced visibility would increase the effect of the advised speed. Each condition was assessed with respect to three categories of measures: Performance, Safety and Workload.

This hypothesis will be tested using a human-in-the-loop simulator setup. This experiment will be conducted using the following constraints:

- Sailing in head waves.
- Only RPM control (no modifications to the vessels exterior).
- No maneuvering (straight line sailing).
- Simulation environment based on the FRISC.

In Chapter 2 the necessary background information on the FRISC and the operational problems that it encounters are discussed. Furthermore the current acceleration mitigation measures are discussed. In Chapter 3 the vertical acceleration signal is analyzed and all parameters are discussed. Chapter 4 discusses the Fast Small Ship Simulator that was used during this research. The model that was constructed to provide the speed advice using haptic feedback is discussed in Chapter 5. In Chapter 6 the human-in-the-loop experiment that was conducted to test the effect of the model is discussed in detail. The results of the experiment can be found in Chapter 7. Chapter 8 compares the expectations to the results from the experiment and discusses differences. The conclusion of the work can be found in Chapter 9. Finally, in Chapter 10 recommendations for future work are given.

Chapter 2

The FRISC

Since this thesis assignment is centered around the FRISC and finding a solution for its operational problems, this chapter will give a general overview of characteristics and the purpose / general mission description. This chapter will provide a detailed description of the FRISC in terms of versions, layout, engines, mission scope and the current vertical acceleration mitigation measures prescribed by the Navy.

2.1 The FRISC

The Rigid Hull Inflatable Body (RHIB) concept was first conceived in 1964 by a team of the Royal National Lifeboat Institution and is nowadays most used for rescue and safety boats but also as tender vessels for larger ships. The RHIBs advantages lie in its speed, high maneuverability, shallow draught and its resistance to damage for collisions at low speeds.

The Fast Raiding Interception and Special forces Craft (FRISC) of the Royal Netherlands Navy is a heavy duty high speed military RHIB craft depicted in Figure 2.1. These crafts are build by the British company Marine Specialised Technology (MST) Limited and designed for a wide range of operations from special and shaping operations to maritime counter terrorism and river operations. The minimum manning of each craft is two persons, one navigator and one helmsman, behind which there is additional seating for up to 8 embarking crew is provided. The FRISC fleet consists of 48 craft that can be divided into the following 5 main variants:

- Support Craft Caribbean - designated as the MST960SCC.
- Boarding Craft Interceptor - designated as the MST1200BC-INT
- Boarding Craft Maritime Counter Terrorism - designated as the MST1200BC-MCT
- Boarding Craft Special Operations - designated as the MST1200BC-SO
- Raiding Craft - designated as the MST1200RC

For this research the boarding craft version of the FRISC is selected because that is the variant that is implemented in the simulator from MARIN, which is explained in Chapter 4. Although the research uses the FRISC interceptor Craft as a primary focus the resulting model will not be limited in applicability solely to this craft but can be used for similar craft as well.

Figure 2.1: The FRISC in action during a training in the Atlantic Intercoastal Waterway.

Type FRISC	Interceptor INT	Raiding Craft RC	Support craft carribean SCC	Maritime counter terrorism MCT	Special Operations SO
Lengte over alles (M)	12.00	12.00	9.50	12.00	12.00
Breedte over alles (M)	3.30	3.30	3.50	3.30	3.30
Max snelheid Kn.	40	40	40	40	40
Inzet afstand	240 Nm met 40 Kn	200 Nm met 30 KN	200 Nm met 30 Kn	240 Nm met 40 Kn	240 Nm met 40 Kn
Voortstuwing	Diesel/Schroef	Diesel/Waterjet	Diesel/Schroef	Diesel/Schroef	Diesel/ Schroef
Brandstof capaciteit	2X 480 ltr.	2X 480 ltr	2x480 ltr	2x 440 ltr	2x 480 ltr
Gewicht	7060	7270	6540	7360	7120
Belading	440	600	700	440	900
Bemanning	2	2	2	2	2
Opstappers	6	8	8	8	6
Hoogte mast op	3.70	3.70	3.70	3.70	3.70
Hoogte mast neer	2.80	2.80	2.80	2.80	2.80
Hoogte A frame achter	2.50	2.50	2.50	2.50	2.50
Hoogte console	1.90	1.90	1.90	1.90	1.90
Diepgang	1.15	1.15 (70)	1.15	1.15	1.15

Figure 2.2: An overview of the typical characteristics of the different types of FRISC. Note that all FRISCs have a maximum of 10 chairs and it is not allowed to take more persons than chairs available. [30]

In Figure 2.2 the specifications of the different versions of the FRISC are provided. As can be seen the FRISC is quite heavy for a RHIB, which lends the vessel its stability in high speed maneuvers. The powerful twin diesel engines lend the FRISC a combined power of 544 kW (or 740hp). These engines are Volvo-Penta D6 370 A engines that power the dual counter rotating propellers as can be seen in Figure 2.3.

Sailing profile

The typical sailing profile of the FRISC when it was designed is provided below [30] [1]. From this design sailing profile it follows that the FRISC is traveling at relatively high speeds for 65% of the time. This shows the relevance of the current research in trying to mitigate the excessive vertical accelerations at mostly occur at high speeds.

1. 10 kts: 10 % in port or when calmly approaching a suspicious vessel
2. 10-25 kts: 25 % bad weather and on patrol
3. 25-30 kts: 55 % cruising speed
4. 30-max kts: 10 % calm weather or during missions

[1] Whether this is a realistic profile now that the FRISCs are in operation is unknown to the author.

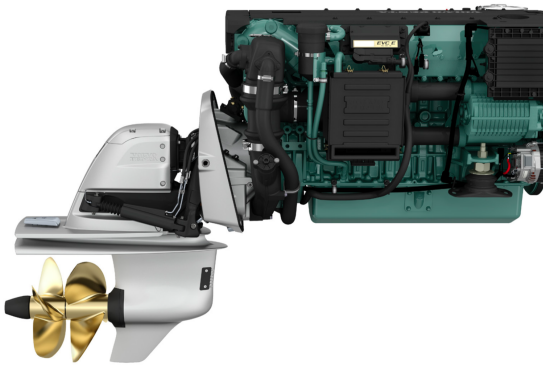

Technical Data

Engine designation	D6-370 A
Crankshaft power, kW (hp)	272 (370)
Propeller shaft power, kW (hp)	261 (355)
Engine speed, rpm	3500
Displacement, l (in^3)	5.5 (336)
Number of cylinders	6
Bore/stroke, mm (in.)	103/110 (4.06/4.33)
Compression ratio	17.5:1
Volvo Penta Duoprop drive	DPH
Ratio	1.63:1
Dry weight with DP, incl. prop. & PS, kg (lb)	770 (1698)
Rating	R5*
Emission compliance	IMO NOx, EU RCD Stage II, US EPA Tier 3

Figure 2.3: On the left: The engine with the dual propeller, On the right: The engine specifications.

Source	*Event*	*Injury*
Wild[12]	Splash down of airborne RIB after crossing wake of another ship in calm conditions.	Wedge fracture of vertebra T12
MAIB Report into injury to passenger on RIB Celtic Pioneer[13]	Slam event in RIB being used for corporate 'thrill ride'	Wedge fracture of vertebra in the lower back
MAIB Report into injury to passenger on an 8.5m RIB[14]	Slam event in working RIB, passenger was seated on a FRP locker	Lower back compression fracture

Figure 2.4: Three events that led to acute injuries due to whole body vibrations [6].

2.2 Problems with the FRISC

The main topic of this research is the reaction of the FRISC to adverse weather conditions. Because of powerful twin diesel engines the FRISCs can operate with speeds of up to 45 kts. The combination of this high speed and a flat bottom hull make the FRISCs vulnerable to high impact forces (slamming) when operating in waves [11], [12], [25], [26], [34]. Since the introduction of the FRISC the CZSK (Commando Zeestrijdkrachten) is faced with complaints regarding both the physical strain and minor to severe injuries from the FRISC operators. The CZSK concluded that the main origin of these complaints center around exposure to repeated shocks (RS) and whole body vibrations (WBV) [30]. It was found that in extreme cases the impact forces can go up to 15g. The damage from these repeated impacts can have short-term but also long term consequences [6], [7], [31], [14]. The injuries range from joint and lower back pain to damage to the central nervous system and kidney-bladder system [30]. It has to be noted that this problem is not limited to the FRISC but holds for all similar vessels. In Figure 2.4 several examples of acute injuries sustained while in operation on small fast crafts in waves is given.

Besides causing potential harm also the athletic abilities of the crew can be significantly hampered by rough transit. This was first observed by Meyers et al. [29] who compared post transit performance for groups with and without suspension seats.

	gebruik	9,6 meter FRISC	12 meter FRISC
Seastate 1/ 2 (golfhoogte tot 0,5 meter)	Max. vaart	3000 RPM – 35 Kn	Geen beperkingen
	Max. roeruitslag	75% (erboven kan wel maar dan gaat de boot driften	Geen beperkingen
	Pacen	Geen beperkingen	Geen beperkingen
	Landen	Geen beperkingen	Geen beperkingen
	Tijdsduur	4 uur zonder fysiek ongemak, daarna pauze gewenst i.v.m. concentratie en inspanning	NTB

	gebruik	9,6 meter FRISC	12 meter FRISC
Seastate 3 (golfhoogte 0,5 tot 1,5 meter)	Max. vaart	2300 RPM – 25 Kn doordat de boot kort is valt hij tussen elke golf wat oncomfortabel varen veroorzaakt.	3000 RPM – 35 Kn
	Max. roeruitslag	50%	50%
	Pacen	Max. 25 Kn	Max. 25 Kn
	Landen	Veilig landen is niet mogelijk bij een golfhoogte van meer dan 0,5 meter	Veilig landen is niet mogelijk bij een golfhoogte van meer dan 0,5 meter
	Tijdsduur	2 uur daarna gaat men het lichaam steeds meer aanspannen om de klappen op te vangen en krijgt men last van knieën, rug, nek	NTB
	gebruik	9,6 meter FRISC	12 meter FRISC
Seastate 4 (golfhoogte 1,5 tot 2,5 meter)	Max. vaart	1700 RPM –15 Kn	2300 Kn- 25Kn afhankelijk van de hoek van de golven.
	Max. roeruitslag	40%	40%
	Pacen	Max. 15 Kn mits voldoende lij.	Max. 25 Kn mits voldoende lij.
	Landen	Uitgesloten	Uitgesloten
	Tijdsduur	1,5 uur hierna fysiek uitgeput	NTB

	gebruik	9,6 meter FRISC	12 meter FRISC
Seastate 5 (golfhoogte 2,5 tot 4 meter)	Max. vaart	1500 RPM – 10 Kn eigenlijk is normaal varen niet meer mogelijk	1700 RPM – 15 Kn
	Max. roeruitslag	50%	30%
	Pacen	Max. 15 Kn mits voldoende lij.	Max. 15 Kn mits voldoende lij.
	Landen	Uitgesloten	Uitgesloten
	Tijdsduur	0,5 uur fysiek zeer belastend	NTB

Figure 2.5: The responsible sailing behaviour as defined by the CZSK.

Mitigation measures

The severity of the vertical accelerations are for the largest part dependent on the speed of the craft, hullshape and the sea state. Large impact forces are the main reason for operators to perform voluntary speed reductions [20]. Other factors that contribute are the exposure time and the operating behaviour. Several measures were taken to mitigate the negative consequences of the vertical accelerations such as:

- *Shock damping chairs*
  Special saddle shape chairs were designed that can partly reduce the vertical accelerations.

- *A responsible sailing profile*
  The CZSK established for the range of sea states in which the FRISCs are used a responsible sailing

table, which is shown in Figure 2.5. This table gives the limits of safe speed according to the sea state.

- *Deck cycles*
  The CZSK established strict deck cycles that consist of a period of 24 hours. Of these 24 hours the mission time may be no more than 14 hours. The resting period should be no less then 10 hours, of which the crew get a minimum stretch of 8 hours of rest, such that the body can recover.

- *Planning and preparation*
  Planning of operations and responsible operating behaviour will further reduce the risks of excessive vertical accelerations. Responsible operating behaviour includes taking note of the environmental conditions, the health of the crew and possible boarders during the trip.

- *Training and selection*
  The FRISC crew is specially selected on their physical abilities. Furthermore, special mandatory training schedules are provided that focus on important muscle groups such as lower back and legs.

Conclusion

In this chapter the FRISC was discussed together with the operational problem it faces. The concept of vertical accelerations was shortly introduced and some mitigation measures were discussed. The next chapter will treat the vertical acceleration signal in more detail.

Chapter 3

Accelerations

As determined in the previous chapter the impact forces that are the result of the hull slamming on waves at high speeds are the most limiting factor in the operability of the FRISC. Before trying to make any steps in mitigating the accelerations the first step is to understand the phenomena and the causes. In this chapter the following is discussed: what is a vertical acceleration, what is the typical frequency, duration, frequency of occurrence, what types of accelerations are there, how should an acceleration signal be documented. A measured acceleration signal was provided by Defensie Materieel Organizatie (DMO) from recordings aboard a FRISC. In this chapter the DMO signal is post-processed using signal processing steps from literature to extract the relevant content.

3.1 Understanding the vertical accelerations

In this section the basics of vertical accelerations such as: variables, duration, severity and types of accelerations will be treated. Peak vertical accelerations are the result of complex interplay between: hull geometry, incoming wave characteristics, vessel motion before impact and forward speed at impact. Of these variables the incoming wave height and the relative ship speed are most dominant. The largest accelerations occur in head seas for steep waves (relatively high wave and short period) at high forward speed [6]. The response of monohull crafts at high speed can be considered to be nonlinear to wave amplitude [4]. Of the most dominant factors contributing to these accelerations ship speed is the only one the operator can influence [5], assuming no changes to the vessel exterior such as the trim flaps used by Rijkens [1] are made.

It is known from onboard measurement that vertical peak accelerations have a very short duration and a relatively low frequency of occurrence [20]. From this it can be concluded that not all wave encounters will lead to an excessive vertical acceleration. When an impact occurs it was found to result in either a bow-up or a bow-down motion depending on the location of the center of gravity relative to the wave crest upon impact as depicted in Figure 3.1. The use of RPM setpoint control could make the difference between bow-up and bow-down motion in this situation and increase the comfort of the crew [33].

During on-board recordings accelerometers and rotational sensors are the primary sensors used to characterize the vessel motions. The acceleration signal requires post processing due to the frequency range of the accelerometers, since structural vibrations of the hull are also recorded and can be of the same order of magnitude as the heave accelerations. The Fourier transform of a recording done by Coe et al. [14] is shown in Figure 3.2. As can be seen there are quite some high frequency disturbances caused by the structural vibrations of the vessel. The wave slams are in the order of 1-10Hz while the different modes of structural vibrations are around 25 to 55 Hz depending on the specific craft.

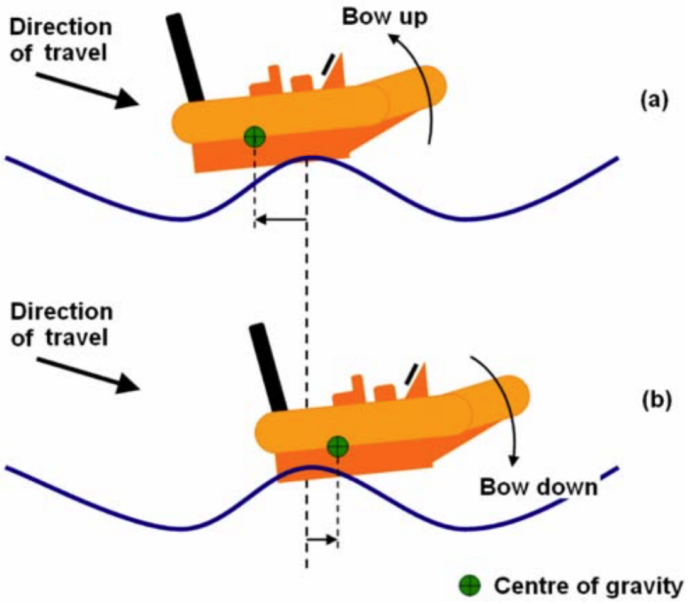

Figure 3.1: (a) the CoG is located behind the crest upon impact resulting in a bow-up motion, (b) the CoG is located in front of the crest upon impact resulting in a bow-down motion. [33].

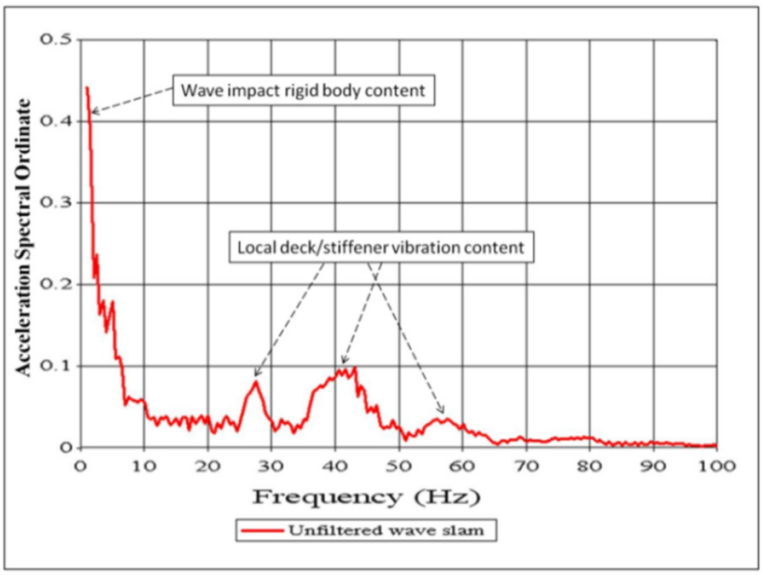

Figure 3.2: A Fourier transform of an acceleration signal as measured by Coe et al. [14].

Coe et al. [14] also looked at the relation between the duration and severity of the impact. In Figure 3.3 a scatter plot with three weight categories of fast crafts are shown. Using this scatter plot it can be seen that the accelerations mainly have a duration between 150-400 milliseconds and an average acceleration duration around 250 milliseconds. All signals with a duration of less than 100 milliseconds are assumed to be caused by structural vibrations.

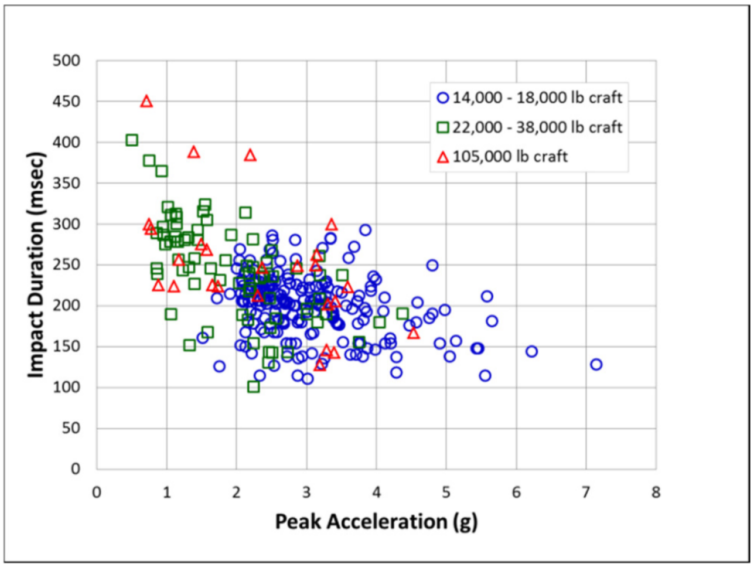

Figure 3.3: The duration of the acceleration plotted against the intensity for three different weight classes of fast ships as measured by Coe et al. [14].

Signal processing example

In Figure 3.4 the sequence of events that comprise a wave impact are shown for both the displacement of the vessel and the acceleration. The bottom figure was made from measurements conducted by DMO and is showing the raw unfiltered vertical acceleration signal. On the top the heave displacement of the vessel in the center of gravity is shown, while in the bottom the unfiltered acceleration signal is shown. The letters A to E mark the different phases of the acceleration.

From A to B the vessel is falling downwards thus the sensor needs to indicate -9.81 until point B is reached. However, the sensor used in this measurement always tried to get back to zero, which causes a drift in the signal. This is not a serious problem since the phenomenon is understood and can be corrected for.

The impact occurs at time B with an almost instantaneous increase to the maximum acceleration level, which is reached in approximately 0.2 seconds in this example.

From point B to C the craft still moves downwards into the wave. The acceleration again decreases fast, which is characteristic of an impact event with an initial peak force, to about $10 m/s^2$. At point C the craft has reached its lowest point and the impact event has come to an end. From point C on the forces acting on the craft will turn positive and the hull will be forced upwards.

From C to D the combined forces result in a positive force that continues to push the craft out of the wave. However, the positive upward force is rapidly being balancing by the gravity force. At point D the gravity force has restored the balance and the total acceleration acting on the craft becomes zero.

From D to E the vessel rises with the wave to another maximum in vertical displacement. When E is reached the vessel is ready to start another impact cycle.

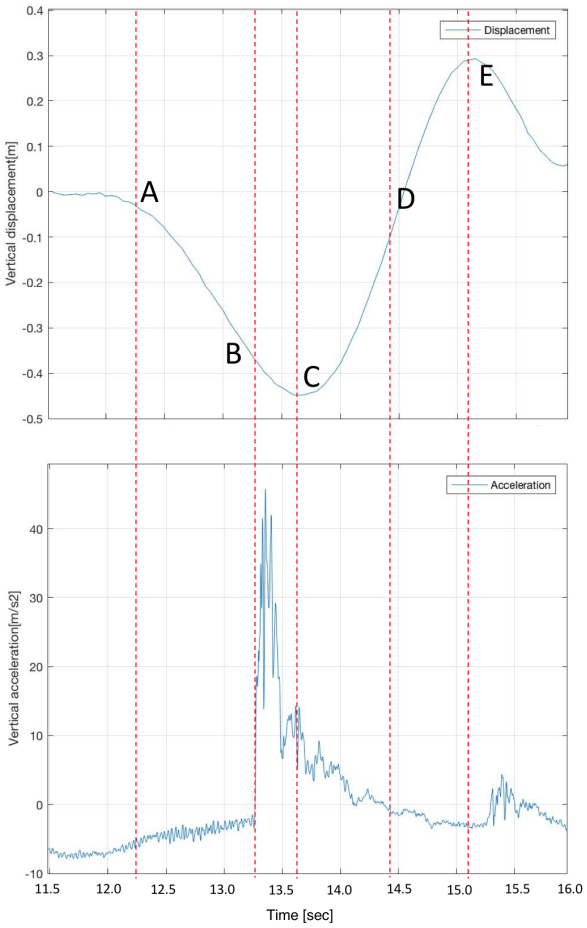

Figure 3.4: The acceleration and displacement of the FRISC shown for a single acceleration cycle.

3.2 Human tolerance to vertical accelerations

The impacts encountered on high speed voyages exceed the limits set for the safe working environment. But what is a too high vertical acceleration? Unfortunately, there is not a single simple answer to this question, the level of vertical accelerations accepted is largely dependent on human elements such as physical fitness and mission purpose. During a critical rescue mission the acceptable level of accelerations will be much higher than on a regular patrol or transit voyage. To illustrate the complexity of this problem Townsent et al. [33] is quoted:

Human tolerance to vibration primarily depends on the complex interactions of motion duration, direction, frequency, magnitude and biodynamical, psychological, physiological, pathological and intra- and inter-subject variabilities. The complex interactions and their effects on humans are not fully understood. However, whole body vibration, especially those associated with rough vehicle rides, can damage the human body.

Various injuries and injury mechanisms are associated with whole body vibrations and repeated shock. With very few studies into the effects of repeated impacts associated with high speed marine craft motions, inspite of the reported significant risk of injury, limited data is available to identify the injury mechanisms. This is further compounded by the ethical difficulties in reproducing the dangerous motions in a laboratory.

3.3 Acceleration quantifiers

When analyzing vertical accelerations levels one can either choose to quantify it as an acceleration level sustained over a period of time (dose) or only pick the accelerations that come above a certain threshold. In this section both quantifiers will be explained.

Exposure and dose

Inspite of the difficulties that full body vibrations (or vertical accelerations) present several attempts have been made to classify them. The daily dose of whole body vibrations was defined by the European parliament and council [7]. This resulted in a daily Exposure Action Value (EAV) and a daily Exposure Limit Value (ELV), which are currently set at 0.5 $m/s^2A(8)$ and 1.15 $m/s^2A(8)$ respectively. The A(8) corresponds to a T_0 reference exposure time of a normal working day, which is considered to be 8 hours. This exposure value can be defined either as a Root Mean Square (RMS) value or Vibration Dose Value (VDV). It was found that in high shock environments like the one under consideration the VDV is a better metric [7]. This VDV can be expressed as given in equation (3.1). In a similar fashion the time to reach the limit exposure value can be expressed as given in equation (3.2). These equations are specifically determined for quantifying the effects of repeated shock in the maritime environment by Coe et al. [7]. For high speed craft it is difficult to comply with these regulations since they are very easily exceeded. Therefore, the choice was made to apply an As Low As Reasonably Practical (ALARP) approach for vibration and slamming reduction. In Figure 3.5 an example of the vibration dose with the most important contributing factors is shown.

$$VDV = (\int_0^T [a_w(t)]^4 dt)^{1/4} \tag{3.1}$$

where,

- VDV is the vibration dose value $[m/s^{-1.75}]$.
- a_w is the weighted acceleration. The weighting is the k-weighting curve defined in ISO 2631-1 [16].

$$T_{LimitValue} = T_0(\frac{ELV}{vdv_{Measured}})^4 \tag{3.2}$$

where,

- $T_{LimitValue}$ is the maximum exposure time.
- T_0 is the baseline exposure time.
- ELV is the Exposure Limit Value $[m/s^{-1.75}]$.
- $vdv_{measured}$ is the measured vibration dose value.

Threshold

A threshold value of the peak vertical acceleration for high speed craft needs to be defined by the crew. For small crafts $< 20m$ Keuning and Van Walree [22] found a maximum acceleration of $13m/s^2$ at the wheelhouse and $25m/s^2$ at the bow was deemed acceptable by the crew. Assuming that no exterior changes can be made to the vessel for the mitigation of these accelerations the focus comes solely down to speed control. Due to the low frequency of occurrence keeping the ship speed continuously low will not be needed. As observed during the trials experienced operators will decrease the speed if they deem a wave that will cause an excessive acceleration is approaching. This operational control method is called "throttle control" or a more technical description could be "RPM setpoint control".

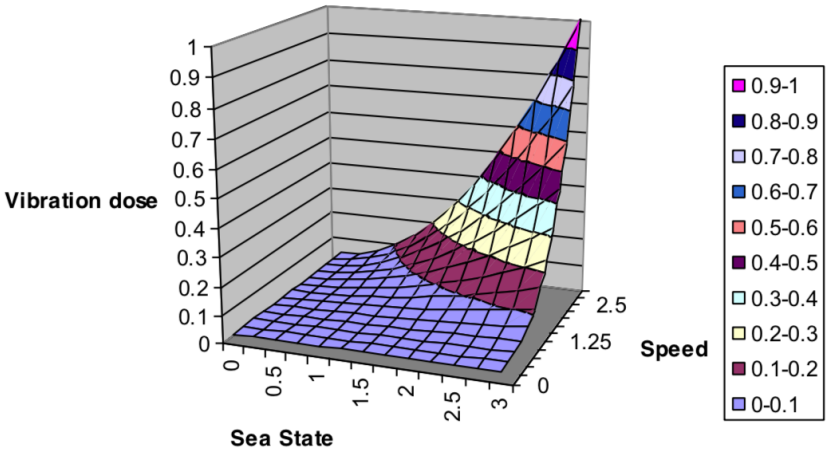

Figure 3.5: Example of a vibration dose as given by Coe et al. [7] showing the speed, sea state and vibration dose relation.

3.4 Documentation of the acceleration signal

In literature several attempts have been made to generalize the acceleration signal and to standardize the procedure to make comparing results more straightforward [27][28]. The unfiltered signal is subjected to the following three signal processing steps:

- *Apply a low pass filter (usually 10Hz):*
  This criterion mostly takes care of the unwanted structural vibrations that are also recorded and can be of the same order of magnitude as the damaging vertical accelerations. Usually also a Fourier transform is applied to the signal to identify the main frequency contributions. The wave slams are in the order of 1-5Hz while the different modes of structural vibrations are around 25 to 55 Hz dependant on the specific craft. The Fourier transform of a recording done by Coe et al. [14] is shown in Figure 3.2. As can be seen there are quite some high frequency disturbances caused by the structural vibrations of the vessel.

- *Apply a horizontal threshold:*
  This threshold signifies the minimum acceleration magnitude that is needed to count it as being an acceleration. Usually this threshold is set to the Root-Mean-Squared (RMS) of the signal.

- *Apply a vertical threshold:*
  This threshold is used to signify that there cannot be multiple harmful accelerations within one wave encounter. Usually this threshold is set to 0.5 [sec] for analyzing small fast ship accelerations.

When describing the acceleration signal Riley [27], [28] proposed some guidelines to always provide a basic number of characteristics of the signal. The acceleration signals used in this report will be documented according to these guidelines as much as possible. Firstly, the signal is described in the 1/3th, 1/10th, and 1/100th highest peaks ($A_{\frac{1}{3}}$,$A_{\frac{1}{10}}$ and $A_{\frac{1}{100}}$) contained within the processed signal. The information provided should also include information about the ship that is was measured on such as: displacement, length, beam, draft, deadrise, LCG, heading, average speed, speed vs time and the environmental conditions such as wave height, period, length. If available the instrumentation specifications also need to be provided.

3.5 Example signal analysis

Analyzing actual ship response data recorded aboard a FRISC vessel is used to gain insight in the current problem but also to validate the acceleration levels from the simulator. The data set provided by DMO was recorded on Wednesday 26th of February 2014 in the waters around the island of Curacao. The data set consists of 6 measurements, each 2 minutes long. The weather conditions at the time of recording were estimated to be winds of 7 to 21 knots and 3 to 5 feet high waves. During the recordings the vessel was sailing in head waves at constant speeds for the duration of the recording. The speeds at which the recordings were made were 10 kts, 20 kts, and 30 kts. Comparing the responses for the different speed ranges was done in Figure 3.6.

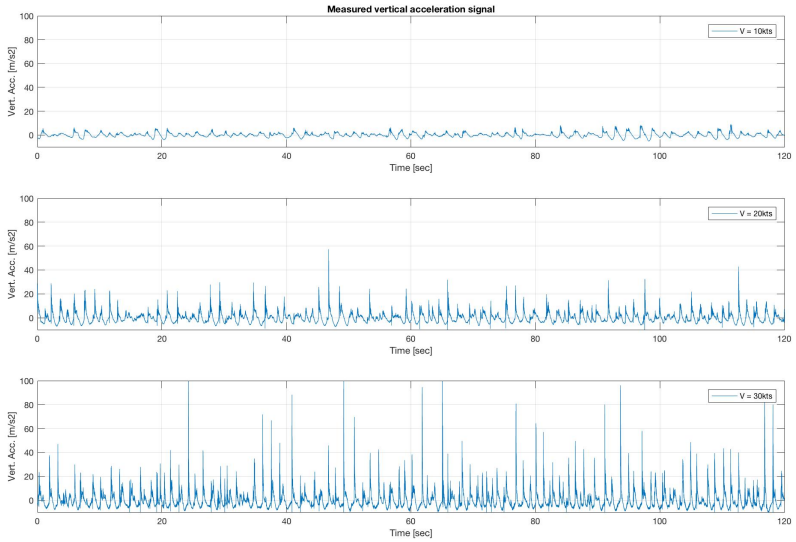

Figure 3.6: The measured vertical acceleration signal recorded for different speeds.

As can be seen from Figure 3.7 the measured signal as expected contains much more than only the harmful acceleration peaks. To get rid of all unwanted content in the signal, the signal processing steps mentioned above are used one by one and the effect on the resulting signal is described. The first step is to apply a 10Hz low-pass filter, which as can be seen on the top of Figure 3.7 still results in a lot of peaks. When the second step is applied the number of peaks identified in the signal decreases significantly, however, still a lot of peaks are identified. Using all three steps results in only the harmful peak values. In Table 3.1, 3.2 and 3.3 the effect of the criteria is shown for the different measurements.

The same signal processing steps are used for the simulator data that will be introduced in Chapter 4. The statistics obtained from these processing steps will be compared to the simulator signal to validate the accuracy of the model.

Table 3.1: The statistics of the acceleration signal measured at 10 kts boat speed.

V = 10	Step 1	Step 1+2	Step 1+2+3
RMS	1.7	1.8	2.3
$A_{\frac{1}{3}}$	1.8	2.6	3.4
$A_{\frac{1}{10}}$	3.1	3.9	5.0
$A_{\frac{1}{100}}$	5.3	5.9	6.9

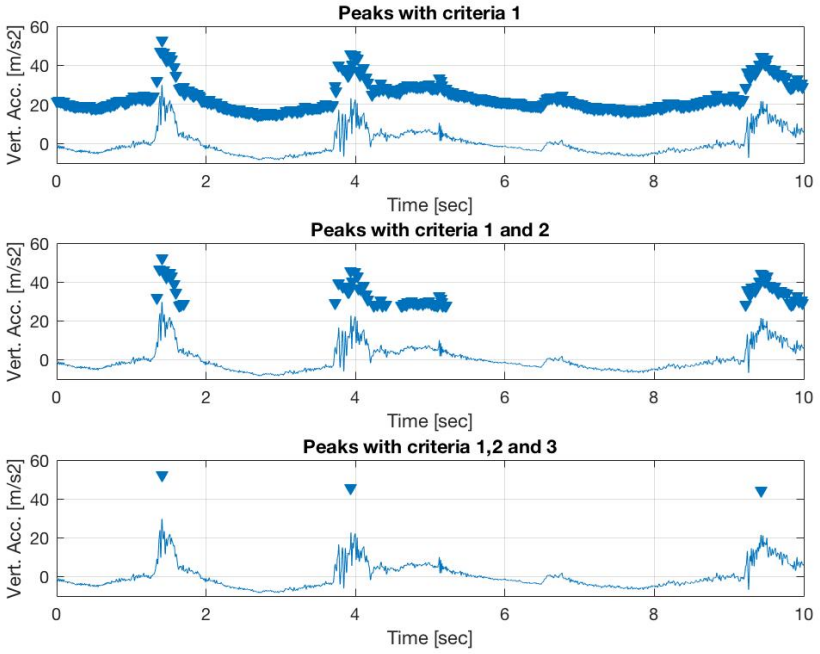

Figure 3.7: The effect of the signal processing steps on the acceleration signal.

Table 3.2: The statistics of the acceleration signal measured at 20 kts boat speed.

V = 20	Step 1	Step 1+2	Step 1+2+3
RMS	3.9	4.5	7.9
$A_{\frac{1}{3}}$	4.5	6.8	12.0
$A_{\frac{1}{10}}$	8.1	10.3	16.2
$A_{\frac{1}{100}}$	14.3	15.8	22.0

Table 3.3: The statistics of the acceleration signal measured at 30 kts boat speed.

V = 30 kts	Step 1	Step 1+2	Step 1+2+3
RMS	6.2	8.2	14.6
$A_{\frac{1}{3}}$	7.0	12.2	21.7
$A_{\frac{1}{10}}$	13.8	19.2	30.0
$A_{\frac{1}{100}}$	27.1	31.4	38.3

Chapter 4

Fast Small Ship Simulator

In this chapter the Fast Small Ship Simulator (FSSS) model from MARIN is analyzed. This model was developed with the aim to train FRISC operators for situations that are difficult or dangerous to practice in real life. The high accuracy needed for the model results from the fact that most risk factors are related to the non-linear hydrodynamic ship behaviour such as slamming, planing, broaching, ship-ship interactions, etc. In this research the slamming and planing behaviour of the simulator are especially of interest and the level of reality will have a significant impact on the test results.

4.1 Structure of the simulator software

MARIN developed the simulator software in an eXtended Model Framework architecture (XMF), which uses graph technology for structuring its application code. This allows for large flexibility and extensibility of the software. The benefit of this is that the resulting application can be integrated in other software or systems without changing the core of the code. This method of using graphs is visualized in Figure 4.1 in which one main file gets its inputs from many separate small files that branch out in a tree-root-like structure. All forces acting on the vessel (hydrodynamic, propulsion, steering etc.) are integrated over time within the XMF structure to obtain the rigid body motions, velocities and accelerations.

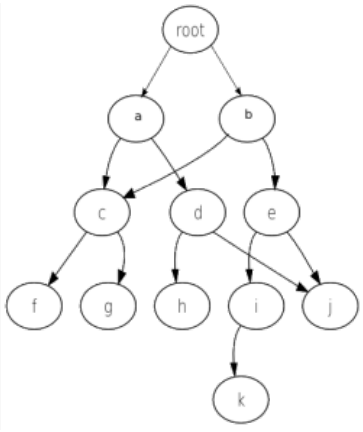

Figure 4.1: The workings of the graphs model presented schematically.

4.2 Forces

When calculating and simulating the vessel motions a trade-off needs to be made between accuracy and computational effort. This leads to some simplifications in the computational model. The forces simulated by the hydrodynamic model can be split up into the following components:

- Buoyancy force due to the displaced water (Archimedes)

- Resistance force in calm water
- Lift that causes planing
- Wave forces due to disturbed and undisturbed waves
- Maneuvering forces in calm water
- Impact forces due to the impact of hull on the waves
- Thrust force
- Steering force
- Damping force (Added damping)

The model used for the forces in the planing condition is based on slender body theory (so called 2.5D because the free-surface condition is 3D but the control equation and the body surface condition are 2D). This method is an extended method of strip theory [13][20] where the hull is divided into a number of segments for which the sum of the forces is calculated separately, after which all of the forces are summed up to arrive at the total force acting on the hull. The forces acting on the hull are schematically represented in Figure 4.2.

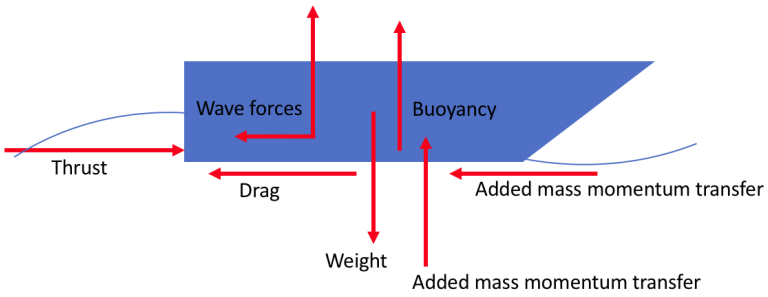

Figure 4.2: The forces acting on the hull.

For this research the wave forces are of importance and therefore it is important to know how the model incorporates those forces. Due to the relatively small size and high forward speed of the ship with respect to the waves, the forces that cause the vessel generated waves, also called radiation and diffraction forces, can be considered to be small in comparison to the external waves. Therefore, it is assumed that the wave forces can be computed using the pressure due to the undisturbed waves on the vessel.

The momentum transfer of the added mass is the mechanism that is responsible for the steady lift developed during planing and the force generation of the impacts in wave encounters. This mechanism is explained as the water mass that is influenced by the presence and movement of the ship in the water as illustrated in Figure 4.3.

Besides the information provided above little is known to the author about the (hydrodynamic) models contained within the software. However, FSSS model was validated using data obtained from model tests in the MARIN Seakeeping and manoeuvring basin. This basin is 170x40x5 meters and equipped with wave-makers along one long and one short side, such that it can generate long and short regular and irregular waves. Thus the model was validated using both regular and irregular wave field. The results said to be promising.

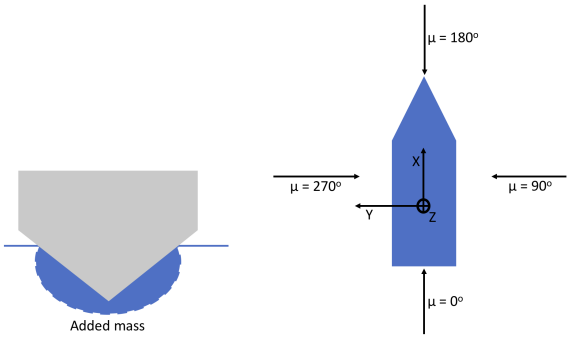

Figure 4.3: On the left: the added mass as is used in the momentum transfer calculations, On the right: the reference system as used in the FSSS calculation model.

4.3 Simulated ship responses

In this section the simulated ship motions are analyzed and later these motions are compared to the measurements provided by DMO, which were treated in 3. The waves that are simulated and used for the ship response calculations follow a JONSWAP distribution and can be calculated by Equation (4.1). In theory when the amplitudes, the phase angles and the reference position is known the waves at each position at any time can be calculated using this equation.

$$h(t, \bar{x}) = \sum_{s=1}^{s} \sum_{i=1}^{N} \zeta_{s,i} cos(\omega_{s,i} t - k_{s,i} \bar{x} + \phi_{s,i}) \tag{4.1}$$

where,

- $\zeta_{s,i}$ is the frequency component i of the spectrum s [m]
- $\omega_{s,i}$ is the frequency component i of the spectrum s [rad]
- t is the simulated temporal time (UTC) [s]
- $k_{s,i}$ is the wave vector (k_x, k_y) frequency component i of the spectrum s [rad/m]
- $\phi_{s,i}$ is the random phase shift of the frequency component i of spectrum s [rad].
- $\bar{x}$ is the ENU position (x,y) [m]

The coordinate system is defined with the x-axis pointing forward, the y-axis pointing to starboard and the z-axis upwards. The wave direction is defined by the angle μ that starts at the bow and circles the vessel in a counter-clockwise direction as can be seen in Figure 4.3.

4.4 Simulator validation

In this section the simulated ship responses are validated using the real FRISC acceleration measurements provided by DMO. Because the measurement location of the DMO measurements is not covered by the JONSWAP spectrum that is used by the FSSS model and the environmental conditions are not described very precisely, the comparison of the results will only function as an indication of the accuracy of the FSSS model. After verification the first version of the FSSS model (Version 3.0) was not deemed satisfying and therefore a updated version (Version 5.2) was supplied by MARIN. The validation of version 3.0 can be found in Appendix C. The FSSS model runs at 60Hz, which is also the highest frequency with which acceleration signal is send.

The same signal processing steps as were used for the measurements provided by DMO are used to find the harmful acceleration peaks. After this the $A_{1/3}$, $A_{1/10}$ and $A_{1/100}$ were identified and compared

to those of the DMO signal at the same speed. The results of this comparison can be found in Figure 4.4, where the sim stands for simulator signal and meas for the the measured DMO signal. Furthermore, in Figure 4.5 part of the time trace of both the simulated and the measured DMO acceleration signal is shown.

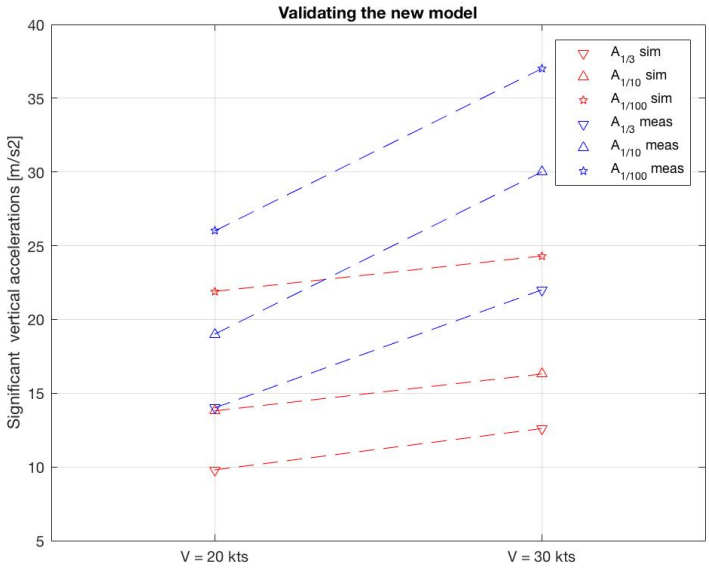

Figure 4.4: Comparing measured signal to simulated results for the significant accelerations.

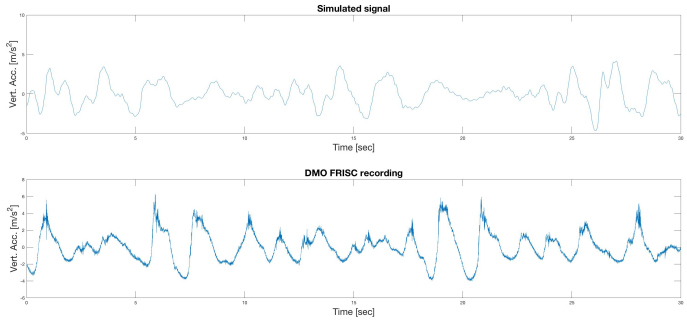

Figure 4.5: Comparing the time traces of the measured signal to the simulated signal.

Although the simulator data does not completely correspond to the acceleration levels measured in a real life situation it is good enough that they are in the same ballpark. The stochastic approach that is under consideration for the current research is designed to reduce the chance of a peak acceleration level rater than to act on each individual peak. The ship responses and the visuals seem realistic to the operator, therefore the simulator will suffice for the current research.

Chapter 5

The haptic assistance algorithm

In this chapter the haptic assistance algorithm that was developed is discussed. The mitigation of the slamming problem can roughly be done using one of two control strategies. One can either use sensors to look ahead at the approaching the wave field and from that predict the resulting ship motions several seconds before occurrence. This control strategy is called **predictive control**. An other control strategy is to use the measured ship responses to the waves to devise an operating strategy for the current wave conditions. This control strategy is called **stochastic control**. While the former model will be more accurate and allow the operator to act on individual waves, the technology that is required for this level of speed and accuracy in wave prediction is not available. Therefore, it was chosen to develop an assisting haptic algorithm that could be implemented using the sensors currently available on the FRISC.

The first work of on-board computation of the wave field from the resulting ship motions spans from the 80s [24], which made use of a pendulum. Later this approach was proven to be not accurate enough, especially at higher speeds. Using a rate gyro and an accelerometer Huss and Olander [19] made a prototype of a guidance system with as output the real-time estimation of the sea state (in the form of a spectrum). The expert system for monitoring dynamic stability of small craft by Kose et al. [23] is more focused on safety in the sense of a capsizing warning system but the philosophy is similar. Using low-cost off-the-shelf sensory equipment the vessel movement can be monitored and suggested actions can be presented to the operator when needed. This system works on rule-based decision making where criteria are defined to identify capsizing modes and others are rules of thumb based on expert operator.

5.1 Working principle

Aboard the FRISC the following sensor information is available: Acceleration information (x,y,z and rotations), vessel speed (GPS and Doppler) and vessel motions (roll,pitch, heave). Using this sensor information a decision support needs to be provided to the operator to allow for the mitigation of the excessive vertical accelerations. The idea about a decision support system originated from the responsible sailing table issued by CZSK [30] in which a sea state is linked to a maximum speed/rpm. This table can be found in Chapter 2.2. However, it has several weak points. How does the operator know what sea state it is? The sea state is defined by a spectrum, which in this case is simplified to a relation between significant wave height (H_s) and peak period (T_P). However, as discussed in Chapter 3 especially the steep waves are likely to cause excessive accelerations and these are currently not given more importance by the table. Furthermore, the operator needs to learn this table by heart, which can lead to errors when remembering the wrong settings. Next to that using a table results in a very static way of speed advice. However, the basic idea of giving an estimate on the safe speed could be valuable and it was estimated that if the information could be provided in a more robust and reliable manner, the advice could work.

Proposed improvements

Knowing the potential of the CZSK approach but also the weaknesses lead to the proposition of improvements that will be discussed in this section. Firstly, the sea state estimation needs to be automated and dynamic such that the speed advice changes when the wave conditions change. Secondly, the advice needs to be more tailored to the situation, instead of classifying the wave field in sea state 3, sea state 4, sea state 5, it should contain information about both wave height and period. Thirdly, the advice speed needs to be communicated to the operator in a robust and elegant way, knowing that the FRISC operators generally are exposed to adverse weather conditions and high workload and therefore do not have time to read values from a table.

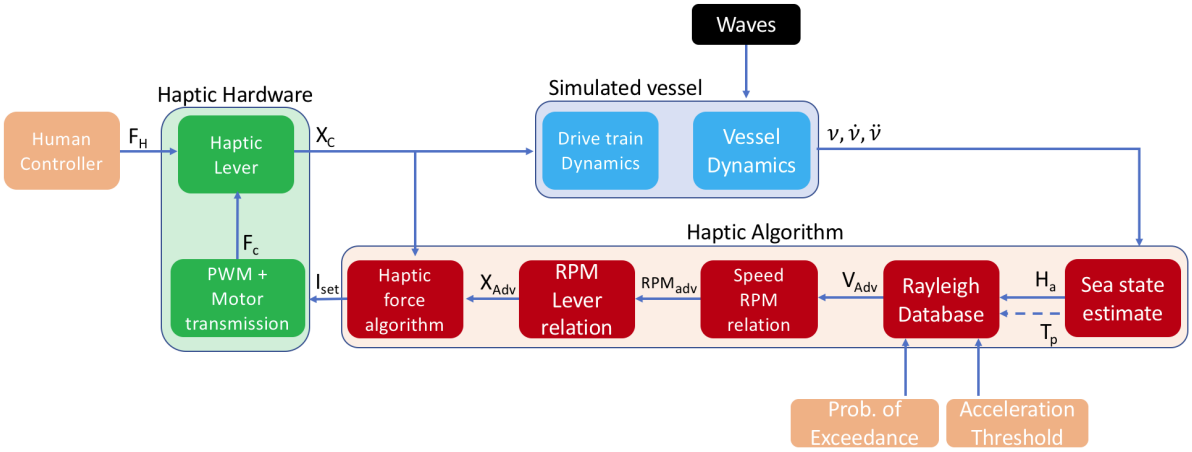

Figure 5.1: A block diagram showing the human controller acting on the haptic hardware, which controls the simulated vessel and the haptic algorithm used to provide a haptic speed advice.

Using the suggested improvements given above the layout of the safe sailing haptic algorithm was constructed, which can be seen in Figure 5.1. The steps that are taken by the algorithm follow the following order: 1. The sea state estimation, 2. The Rayleigh database, 3. The speed to RPM relation, 4. The RPM to lever relation and 5 Haptic force. The construction of the haptic algorithm will be explained following Figure 5.1, starting at the bottom right of the figure with the sea state estimation. The explanation of the haptic levers can be found in Appendix B.

5.2 Sea state estimation

For the estimation of the sea state parameters the heave response of the vessel is used. For each sea state the interval between the boundaries of the response motion are defined. Then the peaks in the response motion are averaged and this average value is compared to the different intervals. In this way the sea state is selected and changed if the average response values change significantly. An update rate of this estimation is defined because a dynamic sea state estimation is required to generate a dynamic speed advice. For this update rate a time window of 30 seconds is used because this is used in the FSSS model as a standard initializing time for sea state changes. Knowing the average wave period is around 7 seconds for the 3 sea states considered in this work (defined below), an estimation of the average number of waves the sea state estimate is based upon can be made. Estimating an average speed of around 45 km/h (from the sailing profile), a wave period of 7 seconds and initializing period of 30 seconds the estimation is made using about 11 full wave encounters. This follows from Equations (5.1) and (5.2) for wave length and wave speed respectively using the deep water wave approximation.

$$\lambda = \frac{2 \cdot pi}{k} = \frac{g \cdot T^2}{2 \cdot pi} \tag{5.1}$$

$$c_0 = \sqrt{\frac{g}{k}} = \frac{g}{\omega} = \frac{g \cdot T}{2 \cdot pi} \tag{5.2}$$

Where,

- λ is the wave length [m].
- c_0 is the wave speed [m/s].
- k is the wave number [-].
- g is the gravitational constant [m/s^2].
- ω is the angular wave frequency [rad/sec].
- T is the wave period [sec].

5.3 Rayleigh database

When the approximation of the sea state is known, this information is used to find a relation between that sea state and the vessel responses. From this relation a safe sailing speed can be found. The method developed is based on statistics and is dependent on a database containing response history. The simulated vessel responses to different wave conditions at different speeds were measured, stored and later used to approximate the vessel responses given the estimated sea state. Because this method depends on past responses generated by the FSSS software it has to be noted that the wave field in the simulator is comprised of a limited number of components where as in reality the wave field will be completely random. Because of this it can happen that a single large wave occurs in an otherwise calm sea. This means that the given advice will not be able to prevent all excessive acceleration peaks.

The wave conditions that will be covered by the haptic algorithm resemble those of the CZSK table but makes a more specific distinction between wave conditions. Knowing that the FRISC will operate in sea states from 0 to 5 only these sea states will be investigated. As the CZSK table has placed no restrictions on the operating speed when in sea states 0 to 2 these will also not be needed in the database and the model will not place restrictions in these conditions. From sea state 3 to 5 the CZSK did place restrictions on the operating speed / the setpoint RPM, while above sea state 5 the advice is to return to a sheltered area at about 15 kts.

		TZ-Seconds											
		5	6	7	8	9	10	11	12	13	14	15	16
Hsig-metres	0.50	0.1%	1.2%	1.6%	1.3%	0.9%	0.6%	0.4%	0.3%	0.2%	0.2%	0.1%	0.1%
	1.00	0.3%	2.4%	5.4%	4.7%	3.6%	1.7%	0.9%	0.2%	0.1%	0.0%	0.0%	0.0%
	1.50	0.1%	1.7%	5.6%	4.8%	3.5%	2.0%	1.2%	0.4%	0.1%	0.0%	0.0%	0.0%
	2.00	0.1%	0.6%	3.5%	4.5%	3.6%	1.9%	1.1%	0.4%	0.2%	0.1%	0.0%	0.0%
	2.50	0.0%	0.2%	1.5%	3.2%	3.2%	1.8%	0.9%	0.3%	0.1%	0.1%	0.0%	0.0%
	3.00	0.0%	0.0%	0.7%	2.2%	2.7%	1.6%	0.9%	0.3%	0.1%	0.1%	0.0%	0.0%
	3.50	0.0%	0.0%	0.3%	0.9%	1.8%	1.2%	0.7%	0.3%	0.1%	0.1%	0.0%	0.0%
	4.00	0.0%	0.0%	0.1%	0.5%	1.2%	1.0%	0.7%	0.3%	0.1%	0.1%	0.0%	0.0%
	4.50	0.0%	0.0%	0.0%	0.2%	0.8%	0.8%	0.6%	0.3%	0.1%	0.1%	0.0%	0.0%
	5.00	0.0%	0.0%	0.0%	0.1%	1.2%	0.6%	0.5%	0.2%	0.1%	0.0%	0.0%	0.0%
	5.50	0.0%	0.0%	0.0%	0.0%	0.8%	0.3%	0.4%	0.2%	0.1%	0.0%	0.0%	0.0%
	6.00	0.0%	0.0%	0.0%	0.0%	0.5%	0.2%	0.3%	0.1%	0.1%	0.0%	0.0%	0.0%
	6.50	0.0%	0.0%	0.0%	0.0%	0.2%	0.1%	0.1%	0.1%	0.1%	0.0%	0.0%	0.0%
	7.00	0.0%	0.0%	0.0%	0.0%	0.1%	0.0%	0.1%	0.0%	0.0%	0.0%	0.0%	0.0%
	7.50	0.0%	0.0%	0.0%	0.0%	0.1%	0.0%	0.1%	0.0%	0.0%	0.0%	0.0%	0.0%
	8.00	0.0%	0.0%	0.0%	0.0%	0.0%	0.0%	0.0%	0.0%	0.0%	0.0%	0.0%	0.0%
	8.50	0.0%	0.0%	0.0%	0.0%	0.0%	0.0%	0.0%	0.0%	0.0%	0.0%	0.0%	0.0%
	9.00	0.0%	0.0%	0.0%	0.0%	0.0%	0.0%	0.0%	0.0%	0.0%	0.0%	0.0%	0.0%
	9.50	0.0%	0.0%	0.0%	0.0%	0.0%	0.0%	0.0%	0.0%	0.0%	0.0%	0.0%	0.0%

Figure 5.2: A wave diagram showing the occurrence of the wave height and period combinations.

Taking a wave scatter diagram that is typical to the northern part of the North Sea the most relevant wave heights and periods can be found for that region. In Figure 5.2 such a scatter diagram is shown. The largest vertical accelerations occur at short steep waves as was found by Keuning [20] and therefore these short steep waves are of most importance. From Figure 5.2 the following wave height and period relations where chosen for the construction of the database:

- Hs = 1 m, Tp = 7 sec.

- Hs = 1.5 m, Tp = 7 sec.
- Hs = 2 m, Tp = 7 sec.

Gathering statistically significant response data for each sea state at multiple speeds is time consuming. Therefore, a limited number of sea state conditions is used to provide a prove of principle of this way of providing speed advice. When using this model in real life it will be more valuable to have a larger database. However, in this case control over the wave height and period parameters is provided by the simulator.

Rayleigh plot

The simulated vessel responses to the sea states given above are measured for speeds ranging from 10 to 40 kts. These response statistics are used to construct Rayleigh plots. The Rayleigh plot is used as a tool to estimate the probability that the wave height will exceed a certain level. Assuming that the wave height is sufficiently narrow banded and normally distributed the wave crests and troughs follow a Rayleigh distribution as was found by Longuet-Higgens[32]. If a linear relation between the wave height and the accelerations is assumed then it follows that the accelerations also approximate the Rayleigh distribution. The nonlinear behavior will show up as deviations from the Rayleigh line. However, not all deviations are due to nonlinear behavior, in the tail the deviations can also occur due to the limited number of observations (also called vertical stack). The mathematical expression of the Rayleigh distribution is shown in Equation (5.3).

$$f(x) = \frac{x}{\sigma} exp(-\frac{x}{\sigma\sqrt{2}}) \tag{5.3}$$

Where,

- x is the signal assumed Rayleigh distributed.
- σ is the standard deviation of that signal.

Assuming the wave field is Rayleigh distributed in some cases can lead to an over-prediction of the actual wave elevation if the wave field is not sufficiently narrow banded. This phenomena is not really a problem because in most applications this overestimation is taken to be a safety factor. There are however some weaknesses in using Rayleigh distribution. Using linear analysis the extremes are neglected, which can lead exceedance of the threshold value eg Rayleigh method misses the highest of the peaks. Also it is difficult even when using independent regular wave components to relate the accelerations to the occurrence of peaks in a stochastic irregular sea. Furthermore, the difficulty with irregular seas is that a long time is needed to generate statistically reliable data.

Now to use the Rayleigh plot to provide a speed advice a threshold acceleration and a probability of exceedance need to be set. A threshold on the maximum allowed acceleration is found in literature. Using the work of Keuning and Walree [22] who found that the crew of small fast rescue craft tolerated vertical accelerations up to $13m/s^2$ at the wheelhouse and $25m/s^2$ at the bow. It has to be noted that the threshold acceleration is crew and mission dependent and therefore needs to be adjustable. However, for now the threshold is fixed at using the values above. A reasonable probability of exceedance was taken to be every 100 waves, although this value is also adjustable. Now the probability that acceleration x_n exceeds threshold value α is shown in Equation (5.4).

$$P(x_n > \alpha) = exp(\frac{-\alpha^2}{2\sigma_x^2}) \tag{5.4}$$

Where,

- x_n is the acceleration signal.
- α is the threshold.
- σ_x is the standard deviation of signal x.

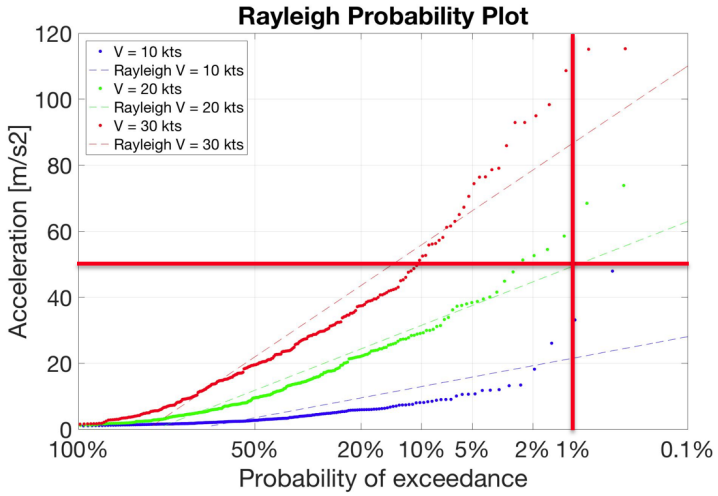

Figure 5.3: The Rayleigh plot of signals at different speeds containing the threshold and the probability of exceedance.

To make using the Rayleigh plot more straightforward the horizontal axis reversed and stretched in such a way that the Rayleigh distribution shows up as a straight line with a 100% probability of exceedance at the origin. Equation (5.4) is rewritten to Equation (5.5) to get this horizontal deformation of the axis. In Figure 5.3 an example of such a plot is given.

$$\alpha = \sigma_x \sqrt{-2ln(P(x_n > a))} \tag{5.5}$$

At the crossing of the red lines in Figure 5.3 the resulting advice speed is found using quadratic interpolation. Now it is known how the database needs to function it can be constructed using the ship responses that where collected for the three sea states mentioned above at ship speeds ranging from 10 to 40 knots.

5.4 Speed RPM relation

Once the advice speed is found, it has to be translated to a setpoint RPM. Due to the planing characteristics of the simulated FRISC this translation is not as straightforward as it might appear. Once the vessel starts planing the resistance drops significantly, as also happens in reality, before rising again as the speed increases further. In Figure 5.4 an approximation of the resistance curve of the FRISC model is shown. If this curve is compared to literature [10] on similar vessels as shown in Figure 5.5 it can be seen that the modelled FRISC resistance curve has an extreme dip. The result of this non-monotonously rising resistance curve is that the RPM-ship speed relation is not always defined unambiguously. Instead, a single RPM setpoint can result in multiple ship speed dependent on the RPM history. This obviously effects the translation from speed advice to RPM setpoint advice and therefore is analyzed further here.

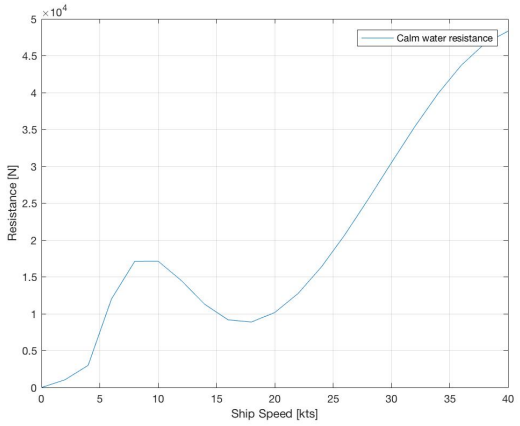

Figure 5.4: An approximation of the resistance curve of the FRISC model.

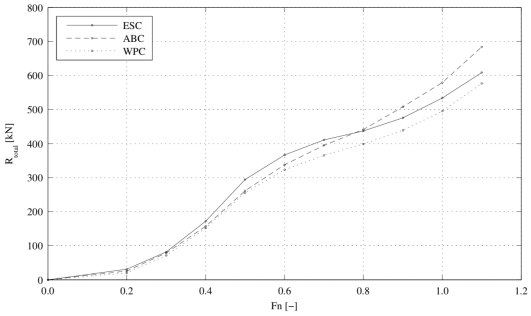

Figure 5.5: A resistance curve of larger but comparable vessels from de Jong [10], where the drop in resistance is also seen, however not as severe.

The problem becomes evident when the lines of constant RPM are plotted in the resistance curve of Figure 5.4 To obtain these RPM lines first the thrust needs to be written as a function of the resistance as in Equation (5.6).

$$T_{prop} = \frac{R}{(1-t)K_p} \tag{5.6}$$

where,

- T_{prop} is the total thrust delivered [N].
- R is the total resistance of the vessel [N].
- t is the thrust deduction fraction [-].
- K_p is the number of driving propellers.

Now the equation relating the thrust to the RPM needs to be used to be able to plot the lines of constant RPM in Figure 5.4. This is Equation (5.8) that describes the thrust delivered by each of the two propellers as a function of water density, propeller speed, propeller diameter and thrust coefficient $K_T(J)$.

$$T_{Prop} = \rho n_p^2 D^4 K_T(J) \tag{5.7}$$

$$J = \frac{v_s(1-w)}{n_p D} \tag{5.8}$$

where,

- J is the advance ratio [-].
- ρ water density $[kg/m^3]$.
- n_p is the propeller RPS [-].
- D is the propeller diameter [m].
- K_T is the dimensionless thrust coefficient as a function of advance ratio J [-].
- v_s is the ship speed [m/s].
- w wake fraction [-].

From FRISC documentation and simulations all parameters are known except for the thrust coefficient K_T. However, from a propeller open water diagram it can be derived that K_T will look like either the green line in Figure 5.6 or the blue line when assuming a linear relation. When using the linearized version of K_T only two unknowns are left in Equation (5.8), which are a and b. These unknowns can be found by solving the equation twice for different T values (T_{v1n1} and T_{v2n2}) as shown in Equations (5.9) and (5.10).

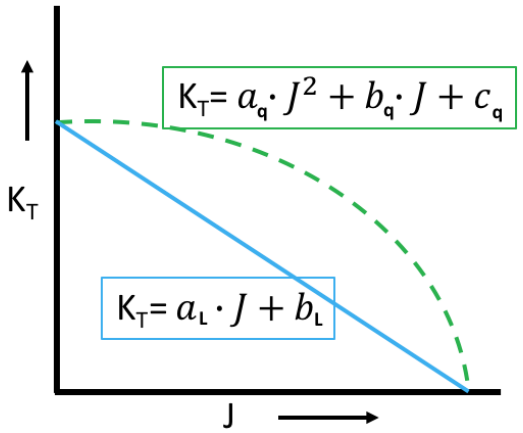

Figure 5.6: An typical propeller open water diagram.

$$\frac{T_{v_{s,1},n_{p,1}}}{\rho n_{p,1}^2 D^4} = a\left(\frac{v_{s,1}(1-w)}{n_{p,1}D}\right)^2 + b \tag{5.9}$$

$$\frac{T_{v_{s,2},n_{p,2}}}{\rho n_{p,2}^2 D^4} = a\left(\frac{v_{s,2}(1-w)}{n_{p,2}D}\right)^2 + b \tag{5.10}$$

Now all variables are known the lines of constant RPM can be drawn in Figure 5.4. The result of this can be found in Figure 5.8. From this figure it can also be seen that for a range of RPM values the lines intersect the calm water resistance curve in more than one place. What this means is that setting an RPM value when starting at low ship speed will result in a different steady state speed compared to having a high initial speed. This phenomena is best explained using Figures 5.7a and 5.7b. In Figure 5.7a a sketch of the intersection points that a line of constant RPM can have is given. Using Figure 5.7b it can be seen that point B is not a stable point and therefore the solution will always end up in either point A or point C.

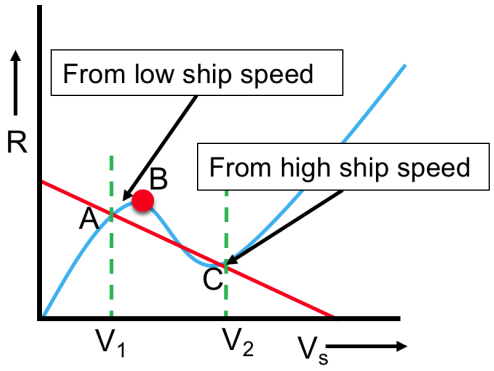

(a) An example showing that the same RPM line can have multiple solutions A, B or C depending on initial speed.

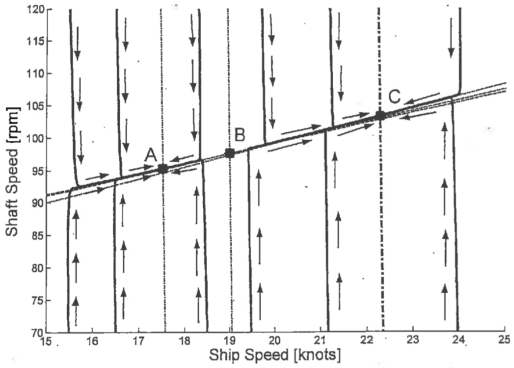

(b) The phase portrait for a fixed control parameter M_f from Figari [15].

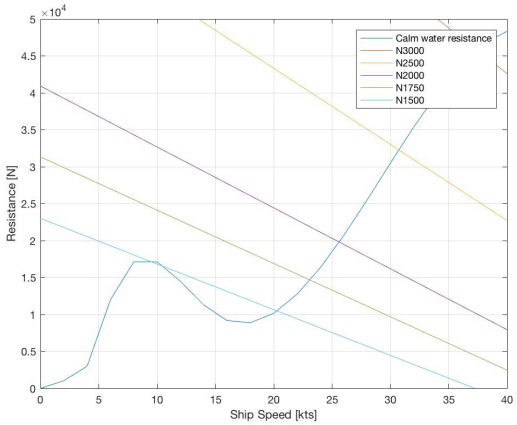

Figure 5.8: The resistance curve with the lines of constant RPM drawn.

Solution

Once this range of RPM values that does not lead to a unique solution are known it can be accounted for in the haptic algorithm. It has to be noted that this phenomenon only occurs at a very limited range of RPM values. Furthermore, in the calculations above are made using the calm water resistance while the FRISC considered will be sailing in waves, which is expected to influence the resistance curve. Rijkens [1] found that in simulations for a similar kind of vessel the increased resistance will only have a minor impact on the vertical accelerations therefore the resistance change is estimated to have a small effect.

For the construction of the Rayleigh database a fixed vessel speed was used, which means that when this conflict RPM region was reached the autopilot was continuously correcting. To solve the conflict for this region a choice between the left and the right solution needed to be made. After validation runs the right most solution (high speed) was chosen continuously when in this specific RPM region as the solution because it was at times only slightly above the true advice speed while the the left solution was found to be too conservative. The lower bound of the speed advice is around 12 m/s (or 23 kts) while the right solution is the same value.

5.5 RPM to lever position

First, the propeller RPM needs to be translated to engine RPM using the reduction ratio, which can be found in Chapter 2 and is (1:1.63). Next the advice RPM is known it needs to be translated to a maximum lever position. A look-up table was constructed by measuring the resulted RPM value from

the simulator for the full range of movement of the lever. Around 30 degrees lever angle only a small deviation in lever position can lead to a significant increase in vessel speed. This effect is explained by the planing behavior of the vessel. When the simulated vessel overcomes the resistance hump, the total resistance drops steeply, which results in significant ship speed increase.

5.6 Haptic Force

In order to have the levers feel as realistic as possible a motion damping is implemented in the form of a resistance force. This force makes sure that the levers remain in position after released. The speed advice that is communicated haptically to the operator resembles a virtual wall. This wall is implemented both on the maximum position and on the zero position to discourage thrust reverse. Thus the advice is only felt when the advised position is reached/exceeded. This way of providing only advise on the maximum position is done intentionally to give the operator the freedom to reduce speed freely if wanted. In Figure 5.9 the generated wall is shown schematically with X_{Adv} the advice position at time t and X_{Bound} are the limits of the advised position. It is possible to push through the advised position but if the lever is released past the advised position it will return to this position. This wall modeled by a simulated spring with spring stiffness K_s and damping coefficient D_s.

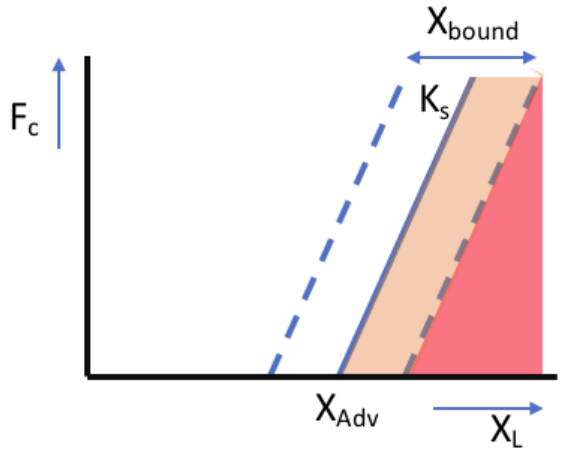

Figure 5.9: A schematic representation of the haptic force generation.

Next to the haptic speed advice a functionality is added to partly replace motions experienced when operating a real FRISC. Each time the defined threshold acceleration is exceeded, a vibration is felt in the levers. This functionality is separate from the haptic speed advice and only meant as a partial replacement of the vessel motions. All inputs and outputs of the haptic force block are shown in Figure 5.10.

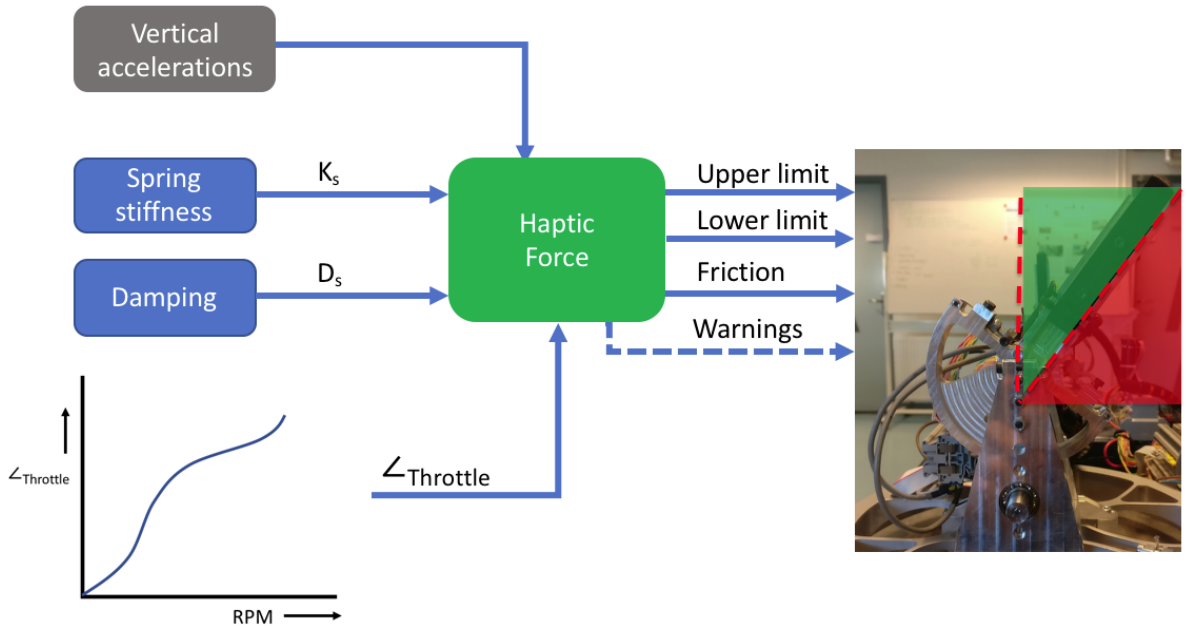

Figure 5.10: A schematic overview of the haptic force algorithm inputs and outputs.

Chapter 6

Experiment

Human subject research as an effective and proven method to test and develop assistance devices as known from the automotive and aviation industry. When designing an experiment it is recommended to think beforehand about the expected outcomes. From literature it is found that in a well designed experiment haptic feedback tents to reduce the workload and increase performance [3]. In this chapter the full experimental design is described. The human-in-the-loop haptic simulator test setup is described in Appendix B.

6.1 Experimental design

The choices made in designing the experiment will largely influence the outcome. In this section all choices made in designing the experiment are treated such as: type of experiment, experimental setup, environmental conditions, learning effects, training, subject selection, etc..

What to test

In this phase it is important to consider what needs to be tested to answer the research question as stated in Chapter 1. From the automotive domain it is known that if the right metrics are chosen and the experiment is well designed, then haptics assistance is likely to increase the performance and reduce the workload experienced by the participants. Therefore, the hypotheses reads: "Haptics assistance on the lever will help to reduce the vertical accelerations in head waves" and "The effect of reduced visibility increases the effect of shared control when mitigating the amount of excessive accelerations". From this hypothesis already some constraints can be formed, such as test with and without assistance to determine if there is an effect and test sailing in head waves thus no manoeuvring.

There are three types of metrics to be considered in this experiment, which are performance related, safety related or workload related. In the experiment the participant are asked to sail as fast as possible from location A to location B while experiencing as little excessive accelerations as possible. The performance metric in this experiment is the completion time and the ratio between the excessive accelerations and the completion time, while the safety metric has to do with the amount/magnitude of the accelerations. To get an estimate on the control effort both a NASA Task Load Index (NASA-TLX) [17] and the lever inputs are used. Furthermore, the ship speed, advice speed and the ship motions (roll/pitch/heave) are recorded. All metrics are sampled at 1 kHz and stored on the Real-Time controller until the trial is completed.

Environmental conditions

The length of the trial is determined by looking at the characteristics of the wave field. An expected average speed is set and the simulated FRISC's heave response is measured. From the heave motion a wave field pattern with wave groups can be distinguished. To have equal wave conditions for every participant an even number of wave groups need to be encountered. This resulted in a track length of 4 nautical miles (or 7.4km) of which a sketch is shown in Figure 6.1.

The wind, wave and current conditions are the next thing to be determined. For the wave conditions a significant wave height of 2 m and a peak period of 7 seconds was chosen to provide the participant with a challenging but realistic wave field. The wind speed is tuned using visual inspection, to see the behaviour of the capillary waves. These capillary waves are needed to give the participants a good depth perspective. Because for this experiment no maneuvering is required the current velocity is set to zero.

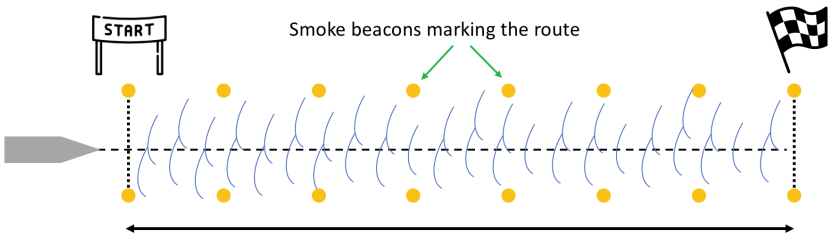

Figure 6.1: A sketch of the track.

For the experiment both a day time run (12:00 simulation time) and a night run (22:55 simulation time) are chosen. This is motivated by looking at the current operator strategy, where the operators looks ahead at the waves and acts if a wave is estimated to cause an excessive acceleration. It is hypothesized that if the operator looses most of the only source of information that his decisions are based upon the effect of shared control will be increased. The four experimental conditions are:

- Condition 1: Sailing manual during day time
- Condition 2: Sailing with shared control during day time
- Condition 3: Sailing manual during night time
- Condition 4: Sailing with shared control during night

A training track is sailed before the experiment starts in which the participant is free to gain a bit of experience. This is done in order to familiarize the participants with the ship dynamics and give a feel for under what combinations of ship speed and wave height an excessive acceleration is likely to occur. When the simulated ship experiences an excessive acceleration a vibration is felt in the levers that replaces the impact forces, which would normally be the result of such a slamming event.

6.2 Experimental choices

Now the length of the experiment and the experimental conditions are known the more fundamental experimentation choices are made. Because of time and resources constraints and given the fact that the main interest is the difference in behaviour when subjected to different treatments, a within-subject experiment is chosen. A within-subjects experiment generally has higher statistical power compared to between-subject experiments.

Next, the participants need to be selected. Due to time constraints, the large distance between Delft University and the Royal Netherlands Navy Academy and the size of the test setup it was deemed unrealistic to have only navy personnel as test subjects. Therefore, it was decided that the participants would be selected from among the students and staff of Delft University. These participants are expected to have little experience sailing fast ships in waves and thus the learning effects could be large between the first and the last trial. To counter this learning effect a fully counterbalanced Latin square test approach is used that counters the learning effects by giving each participant his/her own sequence of conditions. In the experiment proposed above four experimental conditions are given that leads to a test group of 24 participants according to Latin square (4! = 4x3x2x1 = 24) because there are 24 ways in which the experimental sequence can be varied.

Before the participants are allowed to partake in the experiment an informed consent form that explains the experimental procedure needs to be read carefully and signed. This form can be found in Appendix G.

6.3 Potential vulnerabilities

Potential vulnerabilities of this experiment could have as source the simulator setup (level of reality), the inexperience of the operators, the level of advice provided by the haptic levers and the lack of immersion due to the missing motion ques. To partly counter these effects a large HD screen is used for the visualization channel. Also the capillary waves and weather effects in the simulator are tuned to give the best possible viewer experience using the current software. The lack of experience of the participants is more difficult to counter, however, a small questionnaire to gain insight in their sailing experience is attached to the informed consent form. Due to time constraints and limited availability of the motion base platform of MARIN, the experiments are conducted without experiencing the vessel motions. The vibration on the levers is implemented to partly reduce the effect of these missing motions.

6.4 Pilot study

In order to test the haptic algorithm, the experimental setup and optimize the whole experimentation process a pilot study was used. In this study four participants were subjected to all four experimental conditions and the results are studied to find possible adjustments to the experiment.

From interviews conducted after the pilot study it was found that the participants lost focus and motivation as the trials progressed. Furthermore, the common complaint was that they had no idea about what their performance was. In an attempt to solve these problems a score-board that showed the completion time and the number of excessive accelerations was introduced. The first score on the board is set as an experienced navy officers' score to give the right level of motivation for the participants to approach that score. After every run the number of accelerations and the completion time will be written on the board and a quick feedback session on how that score compared to the other participants is provided. The competition is expected to keep the participants motivated and the feedback will give them a score to improve upon.

Chapter 7

Results

In this chapter the experimental results are presented. First the data will be presented in a raw form. The data will be split up in the performance, safety and effort metrics such as discussed in Chapter 6. Potential outliers will be located and if necessary removed from further analysis. Also the outcomes of the statistical tests will be presented. All data that is not shown in this chapter can be found in Appendix G.

Before going further into the data, the scores from the score board were plotted to get a measure of how the participants behaved in the different conditions. In Figure 7.1 the number of excessive accelerations is plotted against the completion time for day and night condition and the manual and shared control condition correspondingly.

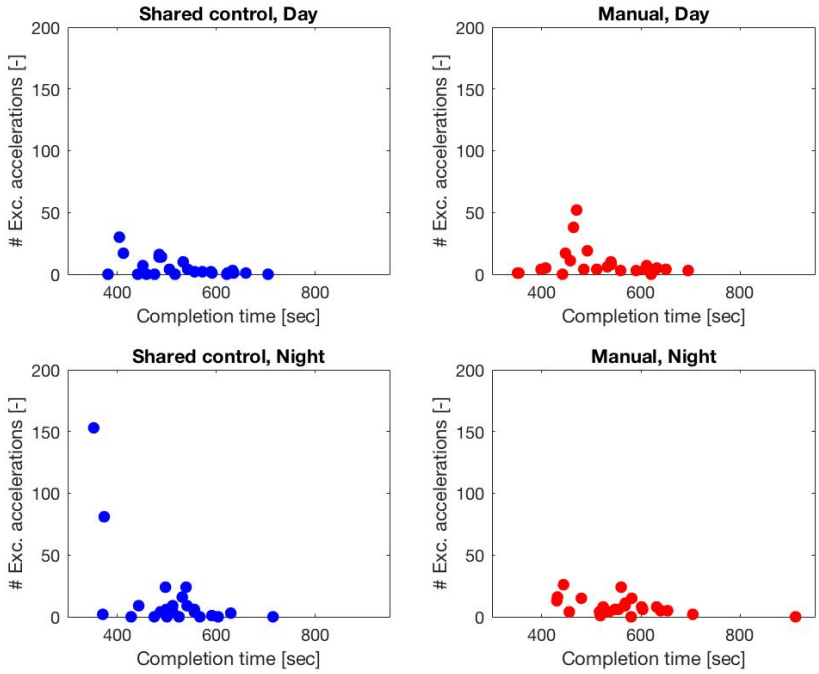

Figure 7.1: The completion time vs the number of excessive accelerations split up for the four conditions.

From Figure 7.1 it can be seen that there are clearly 2 distinct outliers, participant 9 and 10 who show excessive results with respect to the number of vertical accelerations experienced. During the night time trial with shared control switched on these participant show such clearly aberrant behaviour. It is decided to no longer use the results of any of the trials of these participants.

After excluding the outliers the different metrics for each participant are plotted. From these plots

it was seen that when the recordings started the speed advice had not always been fully initialized. The reason for this was that when the trial started most participants started of full throttle and therefore crossed the starting line faster than was calculated using average speed. Therefore, it was decided to exclude the first 10% of all participants at all trials. In Figure 7.2 the lever angle and the advised angle, the vessel speed and advised speed and the accelerations and threshold is plotted for a single participant.

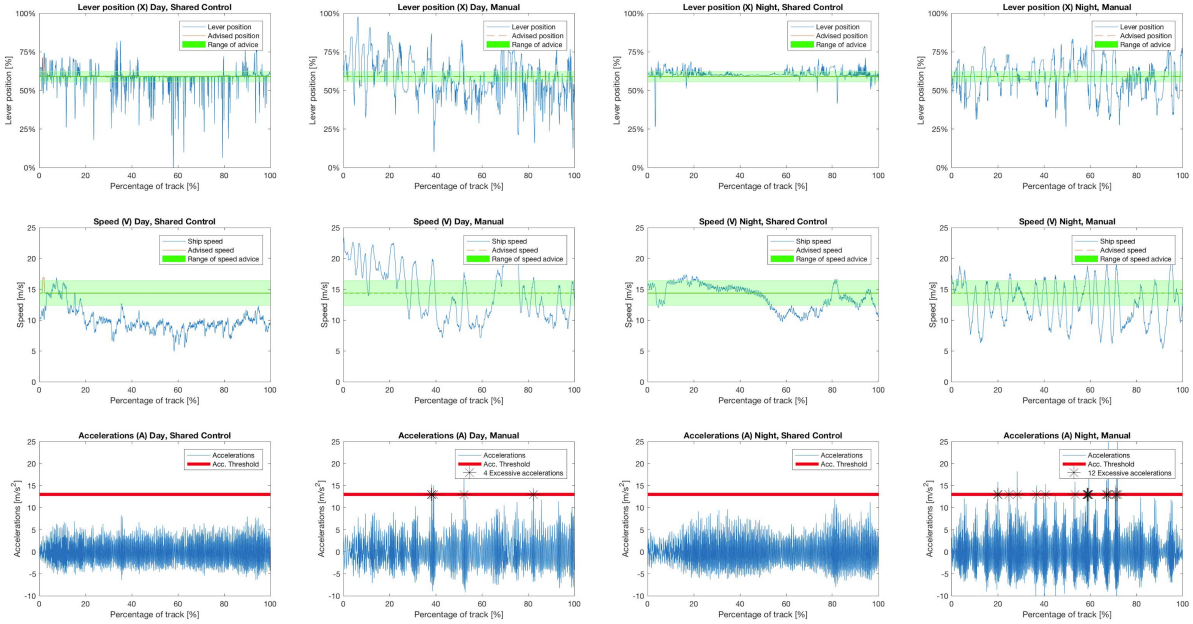

Figure 7.2: The measured lever angle (X), speed (V) and vertical acceleration (A) for a typical participant.

7.1 Performance, Safety and Effort

The large data files gathered during the experiment are split up into the corresponding metrics. However, first the raw signals themselves are analyzed to find out more about the behavior of the participants in the different conditions and to check the validity of the measured signals. The visualization method used for this is called not-a-box-plot. These plots show the same statistics as a regular box plot but also the individual scores are shown. This is done to visualize the distribution of the scores. The individual scores are presented as data points and given a jitter (distance from each other) to clearly show their value. These plots show the individual scores, the mean, standard error of the mean and 95% confidence interval denoted by the red dot, red line and blue line respectively.

Performance

To assess the performance of the participants the average speed over the trial is used. Average speed was taken because in literature on the mitigation of excessive accelerations [1][4] the difference in average speed is used as a measure of performance or effectiveness of the system. In Figures 7.3a and 7.3b the average speed of all participants during the day and the night condition is shown respectively. From these figures it can be seen that especially during night time a higher average speed is achieved using shared control.

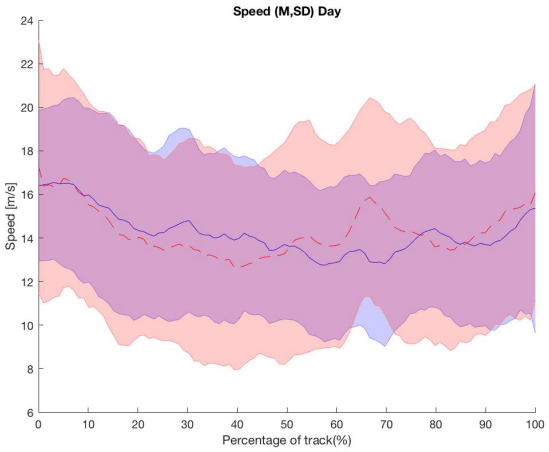

(a) The average speed and standard deviation during day time.

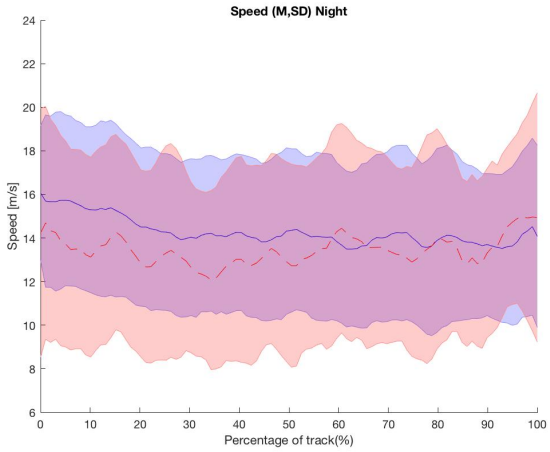

(b) The average speed and standard deviation during night time.

To assess the individual performance as well as the statistics of the participants Figure 7.4 is used. The average speed and standard deviation of all participants over all trials is $(M, SD)_1 = 14.3, 2.7$, $(M, SD)_2 = 14.2, 2.6$, $(M, SD)_3 = 13.4, 2.2$, $(M, SD)_4 = 14.3, 2.2$. During the day condition shared control has little effect on the average speed sailed. However, during night time an average speed increase of 7% was found using shared control.

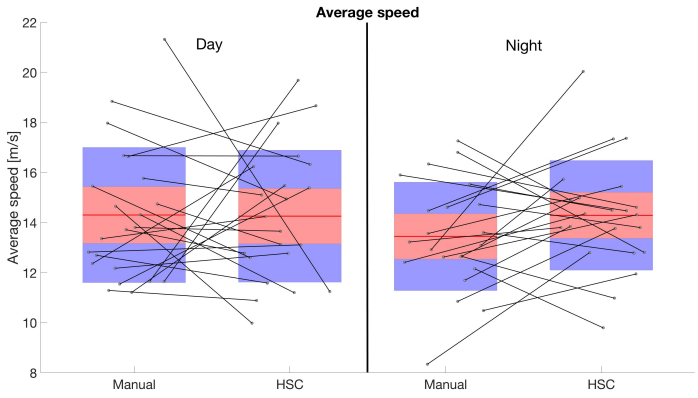

Figure 7.4: The average speed showing the groups of raw data, the mean (red line), the SEM (pink square) and the 95% confidence interval (blue square) for each of the four conditions. The lines show the difference for the same person due to different conditions.

Safety

For the safety metric the information contained within the acceleration signal is considered. From the raw data the following information needs to be obtained for each participant:

- The mean acceleration level.
- The accelerations above threshold value ($A > 13m/s^2$).
- The significant accelerations: $A_{(1/3)}$, $A_{(1/10)}$ and $A_{(1/100)}$.

The means are used to investigate the change of operator behaviour when using shared control. Because the advice is only generated when the system assumes the vessel is on the boundary of the threshold

acceleration level, the means give an indication if the acceleration levels are increasing on average. Secondly, the number of excessive accelerations is counted and compared because the shared control system was designed to mitigate these. If the participants would perfectly follow the shared control advice on average an excessive acceleration would be encountered every 1000 waves. The significant acceleration levels are used to gain insight in the distribution and the change in distribution of the acceleration levels. It is deemed important to investigate if/how this changes when implementing shared control.

The magnitude distribution of the accelerations is given in Figure 7.5. For each condition the distribution of the occurrence of the impacts is given together with green, black and red lines that denote the $A_{(1/3)}$, $A_{(1/10)}$ and $A_{(1/100)}$ respectively.

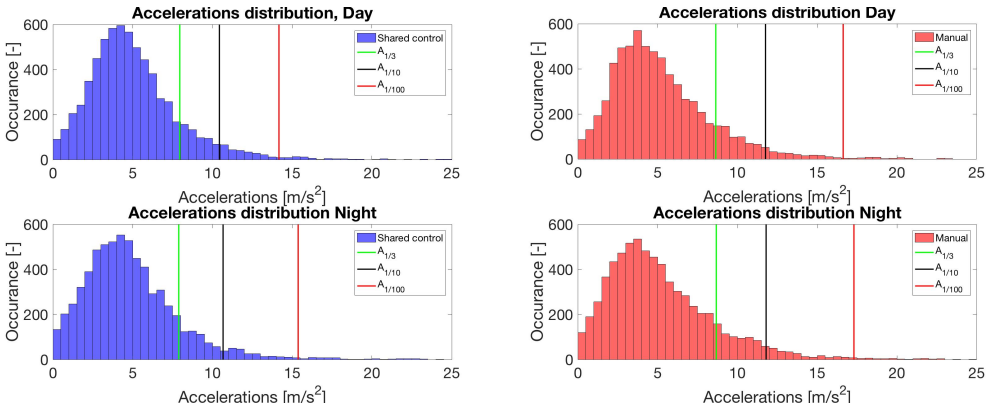

Figure 7.5: The distribution of the accelerations for all conditions.

Next, the number of excessive accelerations is presented in Figure 7.6. These are the number of accelerations that are above the threshold value of $13m/s^2$ for all participants. Both in the day and the night condition the mean number of excessive accelerations is less using shared control compared to manual. Also the confidence interval looks to be smaller.

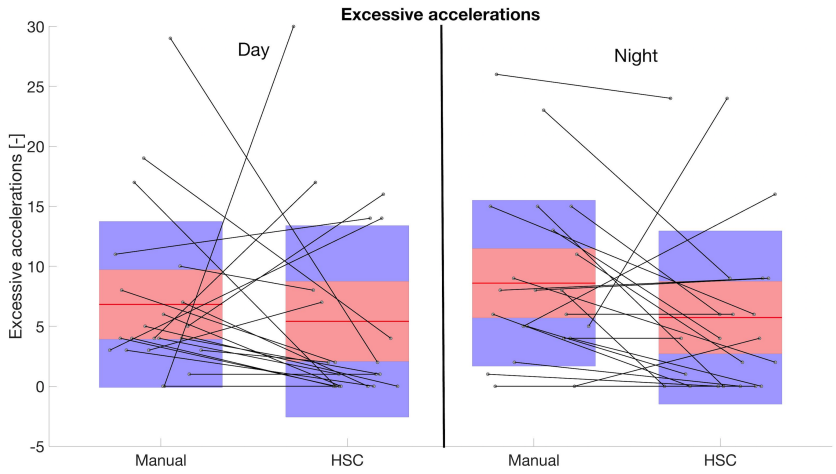

Figure 7.6: The number of excessive accelerations showing the groups of raw data, the mean (red line), the SEM (pink square) and the 95% confidence interval (blue square) for each of the four conditions. The lines show the difference for the same person due to different conditions.

In order to gain insight in how the participants behaved over the duration of the trial the magnitudes and locations of the excessive accelerations are investigated. In Figures 7.7a and 7.7b the magnitude and location distribution during the day time is given and in Figures 7.8a and 7.8b the distributions during

night are given. As can be seen the accelerations are spread quite evenly over the length of the track, with the exclusion of the first 20%, and no "sprint to the finish" occurs.

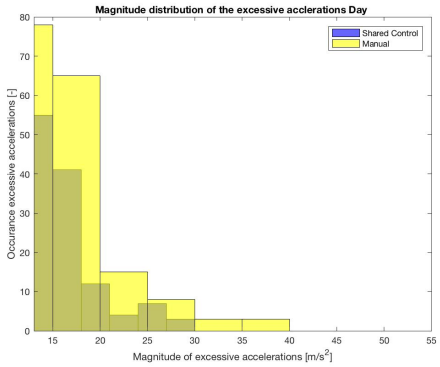

(a) The magnitude of the excessive accelerations for the day condition.

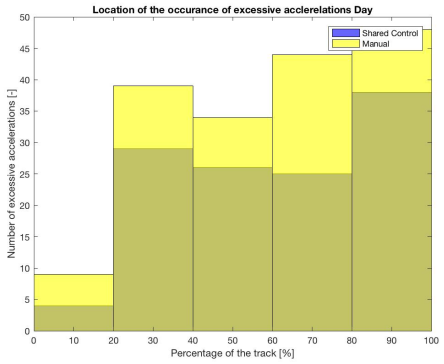

(b) The location of occurrence of the excessive accelerations for the day condition.

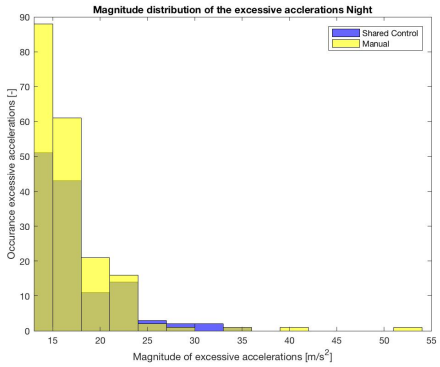

(a) The magnitude of the excessive accelerations for the night condition.

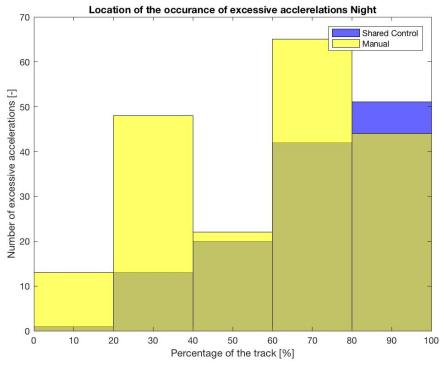

(b) The location of occurrence of the excessive accelerations for the night condition.

Workload

From literature it is known that shared control generally decreases the workload when compared to manual control. However, without respiratory or EEG measurements an alternative indication for workload experienced needs to be found. Johanson et al. [21] found for the automotive domain that when looking at user input on the system, the number of reversals and the reversal rate give an indication of the workload experienced by the participants. A reversal is signified by a significant change in the movement direction of the steering wheel (or in this case lever). To make sure the reversal is an intended movement instead of noise, a minimum difference between peaks is used. This is shown in Figure 7.9, where a reversal is counted each time the difference in the green and red x is larger than 2 degrees.

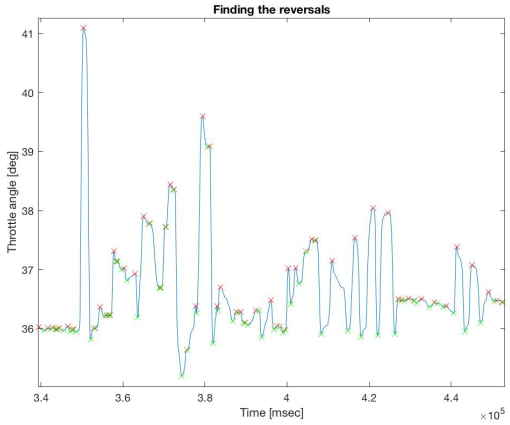

Figure 7.9: Finding the reversals from the lever angle signal and counting a reversal each time a peak through difference of more than 2 degrees is measured.

Now the definition of a reversal is given the lever angle measurements can be subjected to the process described above. In Figure 7.10 the reversals in the day and night conditions are shown for each participant for each trial. For this figure it can be seen that on average the manual conditions result in much more reversals. Besides being tiring for the operator these reversals also potentially decrease the lifetime of the drive train.

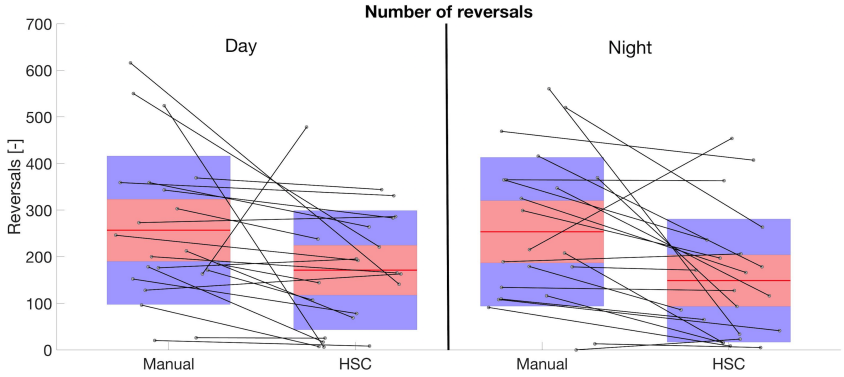

Figure 7.10: The reversals showing the groups of raw data, the mean (red line), the SEM (pink square) and the 95% confidence interval (blue square) for each of the four conditions. The lines show the difference for the same person due to different conditions.

In Figure 7.11 the histograms of the lever angle are given for the day condition and the night condition. Also the upper and lower boundary of the advised position is shown in red and green respectively. As can be seen from the figure the effect of applying shared control shows a significant change in behaviour. The mean advised lever position coincides with the position most used.

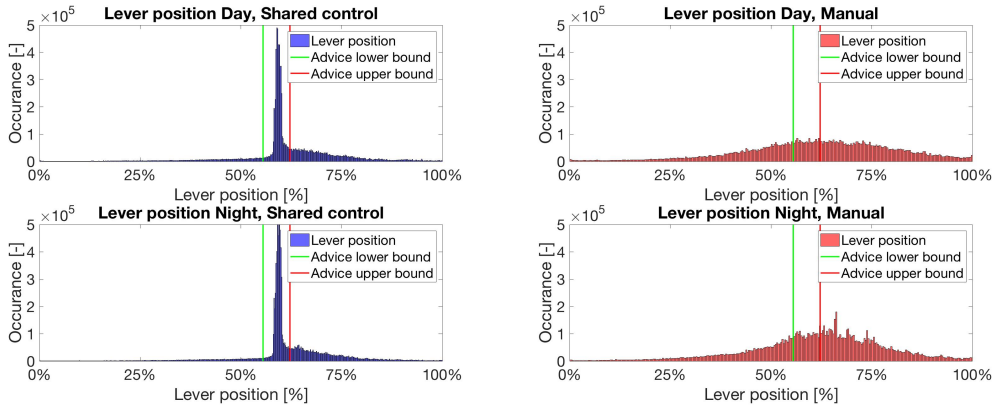

Figure 7.11: The histograms for the lever position for all participants over the different conditions.

Due to the relatively slow dynamics of the vessel and the response delays in the drive train system not all reversals will have a significant effect on the vessel speed. This effect can be investigated by comparing the distribution of lever position to the distribution of vessel speed, thus comparing Figures 7.11 to 7.12 for each condition respectively.

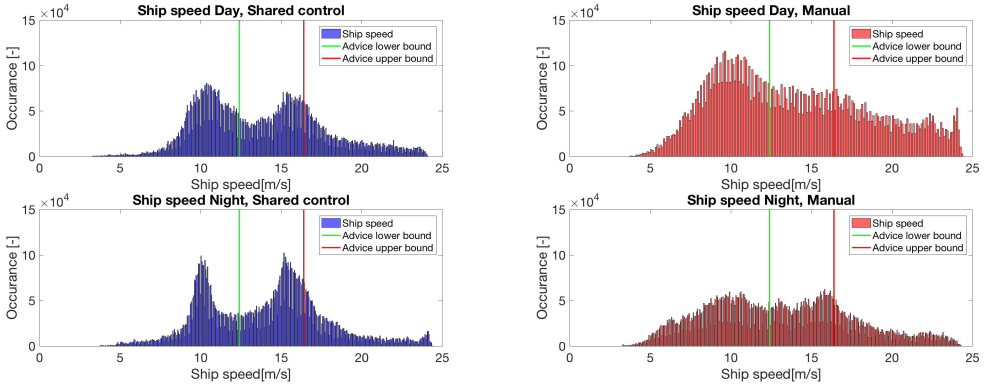

Figure 7.12: The histograms for the vessel speed for all participants over the different conditions.

After comparison it can be seen that there are some peaks in the vessel speed that are not directly translatable to the lever position plots. However, if the planing and resistance effects as explained in Chapter 5 are investigated this could provide a probable solution for these peaks. As the participants decelerated below the speed advice the vessel resistance increased and the speed lowered until the new steady state position was reached. Once the participants realized their speed was decreasing the vessel speed was increased again.

The NASA Task Load indeX (NASA-TLX) [17] is used to find the workload experienced in mental, physical and temporal sense as well as the amount of effort required and the performance estimate. After each experiment the participants grade their workload form 0 to 20 for each of the six topics. The results of the TLX are given in Figure 7.13 divided in the categories mental demand, physical demand, temporal demand, performance, effort and frustration.

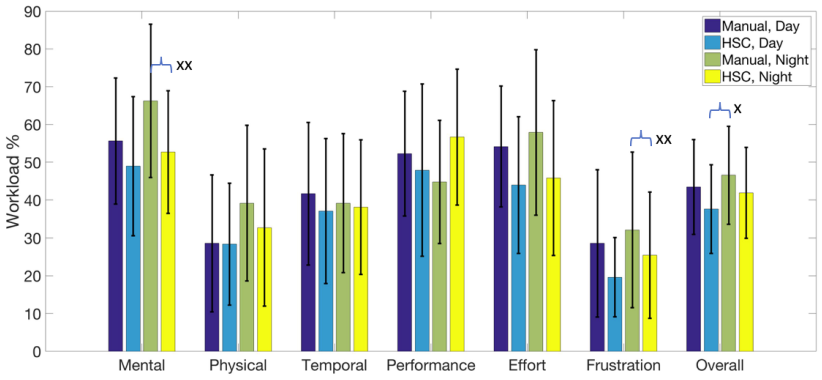

Figure 7.13: The results and the standard deviation of the NASA-TLX for all participants with x:p=0.01, xx:p=0.001.

From Figure 7.13 it can be seen that the participants felt a higher workload while operating manually compared to shared control. Also as the visibility decreases the workload experienced increased.

Order effects

For the experiment mostly inexperienced participants were selected. This is expected to have an effect on the validity of the results of the experiment. To counter this effect a training trial was used to familiarize the participants with the track, controls and the conditions. However, one training trial is not expected to completely replace the experience of a skilled operator. To investigate the effect of this limited training the order effects on the three metrics studied. The Latin-square approach randomized experimental order to counter the expected learning effects. Using the order effects the severity of the learning effects can be studies by plotting the scores of the participants trial in the same order as they were conducted. In Figure 7.14 the order effects for average speed, number of excessive accelerations and reversals is shown respectively. As can be seen only for the number of excessive accelerations there is a large learning effect.

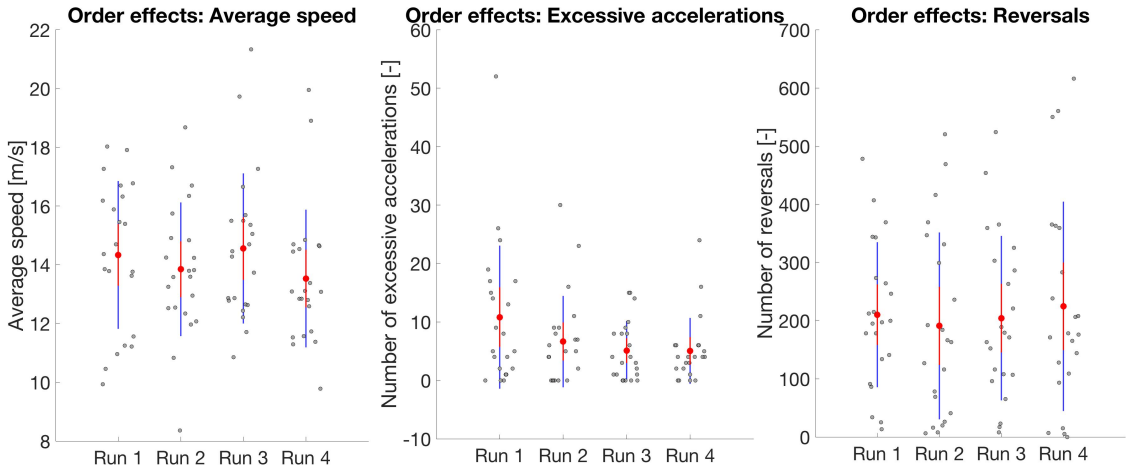

Figure 7.14: The order effects for average speed, number of excessive accelerations and number of reversals.

7.2 Statistics

In this section it is investigated if the results obtained from the different test scores show a significant effect. For each metric (dependent measure) a 22x4 matrix was constructed that held the test scores of each participant. Because the metrics possibly violate the assumption of normality that goes with parametric tests such as ANOVA and t-test it was chosen to rank transform the matrix. In this rank transformation each score is ranked on a scale of 1 to n, where n is the number of entries in the matrix (in this case 96) according to [8]. In this way all test scores can be considered for the statistical analysis and there is no need to discard the outliers or perform normality and variability checks. The matrix is submitted to a repeated measures ANOVA with the four experimental conditions as within-subject factor. The six pairwise comparisons between the conditions are subjected to Bonferroni corrections [1].

What to compare

Looking back at the research question the aim of the experiment is to find how the haptic assistance could assist the operator when operating in waves. The experiment that was conducted is to show the effect of shared control on the performance, safety and workload. Following from literature on shared control [3] [9] it was expected that the operator would perform better and more safe while also experiencing less workload when compared to manual control. To test this effect of shared control the conditions 1 and 2 are compared to see the effect of shared control during day time. The conditions 3 and 4 are compared to find what the effect of shared control during night time. Furthermore, the shared control during day time is compared to manual control during night time to investigate the best/worst case scenario. In Figure 7.15 an overview of the comparisons is given.

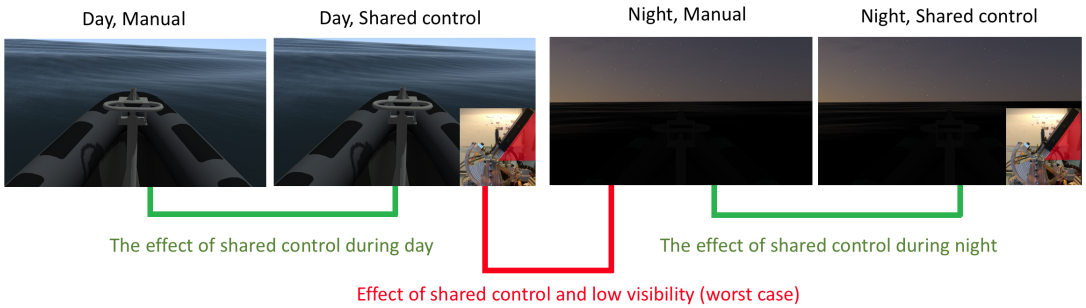

Figure 7.15: An overview of the different conditions and the comparisons.

$$d_z = \frac{|(\mu_{x-y})|}{\sigma_{x-y}} \tag{7.1}$$

Where,

- μ_{x-y} is the mean of the difference.
- σ_{x-y} is the standard deviation of the difference.

The results of the statistical analysis are presented in Table 7.1 where the metrics are grouped in the performance, safety and workload. A significant result is found if the p-value is less than 0.05, which means that if a random score is selected it can be said with 95% certainty that it is either from the shared control trial or the manual trial. For those calculations the ranked means and standard deviations where used.

The effect size calculated using Equation (7.1) gives a measure for the magnitude of the event in statistics. These are classified such that 0.2 is considered to be a small effect, 0.5 to be a medium effect and 0.8 to be a large effect. In general the effect sizes need to be large for such a limited amount of participants as is taken in this experiment.

[1] The chances of a rare event occurring increase if multiple hypothesis are tested, which also increases the likelihood of incorrectly rejecting the null hypothesis. Bonferroni corrections compensate for this phenomena by testing each individual hypothesis at a significance level of α/m, where α is the desired overall alpha level and m is the number of hypotheses

Performance

For all dependent measures the means, standard deviations, the results of the repeated measured ANOVA and the pairwise comparisons are provided in Table 7.1. No difference in average speed was found between the conditions.

Safety

When looking at safety the mean acceleration level, the number of excessive accelerations and the significant accelerations were considered. The mean acceleration level does not show a significant difference between the different condition. This is considered a positive outcome since the shared control system is only tuned to perform at the bounds of the threshold acceleration level. Therefore a potential outcome could have been that the mean acceleration level experienced went up because participants chose to operate more closely to the limits.

The number of excessive accelerations was found to vary significantly between the conditions. The effect size during night time was found to be medium and the a significant effect (p=0.039) was found when comparing the shared control day case to the manual night condition (best/worst comparison).

For the $A_{1/3}$ no significant effect of shared control was found. However, the same holds here as for the mean accelerations, the model was not designed to decrease these acceleration levels. When looking at the mean $A_{1/3}$ value the shared control conditions even scored a bit lower than the manual conditions.

The $A_{1/10}$ accelerations also do not show a significant effect of shared control. In the manual case the $A_{1/10}$ are about 10% higher on average.
In the tail of the acceleration distribution a significant effect is shown when comparing the different conditions. When comparing the best/worst case again a significant effect (p=0.034) was found. In general when approaching the tail of the acceleration distribution the effect sizes are observed to be growing for the different comparisons.

In general it can be concluded that the effect of shared control on the acceleration levels experienced is relatively low. In the next chapter it will be discussed what the reasons are for this.

Workload

For the workload the reversals, the reversal rate and the NASA TLX are investigated. The reversals show a strong effect of shared control, especially during night time. When comparing the night conditions a significant effect (p=0.009) of shared control was shown and a reduction of reversals of more than 42%.

The NASA TLX results are evaluated separately per item and also the arithmetic mean is taken. For the mental demand the participants reported significantly more mental load when comparing the night conditions (p=0.001) but also when comparing the best/worst condition (p = 0.0066). The physical demand did not lead to significant differences between the conditions. The same holds for the temporal demand. Participants felt significantly more confident regarding their performance when using shared control during night time (p=0.037), which indicates a level of trust in the system. The same holds for effort, the participants indicated that they had to put in significantly more effort when using manual control during night time compared to shared control (p=0.046) and for the best works case scenario even more (p=0.02). Finally, the participants reported significantly more stress/frustration in day time when using manual control compared to shared control. From the overall evaluation of the NASA-TLX the effect of shared control was found to be significant for the day (p=0.014), night (p=0.045) and best/worst case (p=0.007) pairwise comparisons. The results of the individual components of the NASA-TLX can be found in Appendix G.

Table 7.1: Means (M), standard deviations (SD), effect sizes (d_z), and results of the repeated measures ANOVA (F, p) per dependent measure.

	Manual Day M(SD)	Shared control Day M(SD)	Manual Night M(SD)	Shared Control Night M(SD)	p-value (F=3,94)	Pairs 1-2 $p(d_z)$	3-4 $p(d_z)$	2-3 $p(d_z)$
Performance								
Average speed	14.3(2.7)	14.2(2.6)	13.4(2.2)	14.3(2.2)	p=0.58 F=0.65	0.02	0.35	0.23
Safety								
Mean acc.	5.3 (1.2)	5.1 (1.1)	5.3 (1.2)	4.9 (1.1)	p=0.59 F=0.64	0.08	0.33	0.0.16
Excessive acc.	7.9 (11.0)	5.5 (8.0)	8.6 (6.9)	5.7 (7.2)	p=0.033 F=3.11	0.32	0.54	0.64 (x=0.039)
$A_{1/3}$	8.6 (2.1)	8.0 (1.9)	8.7 (1.9)	7.9 (1.6)	p=0.17 F=1.74	0.23	0.4	0.42
$A_{1/10}$	11.8 (3.7)	10.4 (2.8)	11.8 (2.7)	10.7 (3.0)	p=0.060 F=2.59	0.30	0.46	0.55
$A_{1/100}$	1.6.6 (6.5)	14.2 (5.0)	17.3 (5.6)	15.4 (5.3)	p=0.041 F=3.0	0.43	0.35	0.62 (x=0.034)
Workload								
Reversals	256.7 (159.2)	171.3 (127.8)	253.4 (159.6)	148.6 (132.0)	$p=1.39*10^{-4}$ F=7.9	0.56	0.78 (x=0.009)	0.53
NASA TLX (%)	45.1 (11.9)	36.4 (10.4)	47.4 (15.2)	42.2 (13.4)	$p=3.82*10^{-4}$ F=7.01	0.73 (x=0.014)	0.63 (x=0.045)	0.80 (x=0.007)

Chapter 8

Discussion

In the last chapter the results of the human-in-the-loop experiment that was conducted are presented. In this chapter these results are compared to the expectations from before the experiment commenced. The research question and the hypotheses are answered and it is discussed why the results are in accordance with the expectations or not. This study is the first study in the field of shared control for maritime applications and therefore the selection of the metrics and the experimental setup was not straightforward. In order to get a good estimate inspiration was drawn from the automotive industry where human-in-the-loop testing of feedback systems is more commonplace.

8.1 Results

The application of shared control in the experiment considered showed a reduction in both the reported workload (NASA-TLX), 20% in day and 10% in night, and the measured workload (reversals), 33% in day and 42% in night, without effecting the average speed or the number of excessive accelerations. This effect measured during an experiment with a limited duration could prove to be beneficial in reality since FRISC missions can consist of hours of sailing.

The fact that there was no significant difference between manual and shared control in terms average speed and number of reversals could be attributed to the large differences between individual subjects. For example Figure 7.6 in Chapter 7 shows the lines comparing individual performance, here it can be seen that 16 out of 22 tend to experience less excessive accelerations using haptic shared control during for the day condition and in the night condition this number is even 17 out of 22. However, for a few participants the lines go up, which indicates a different strategy, namely taking more risks by exceeding the speed advice more. For the average speed this effect is not observed, which indicates that taking more risk in the form of excessive accelerations does not always translate in a higher average speed.

Furthermore, the results do show a significant reduction of the number of excessive accelerations between manual night and haptic shared control day. This indicates that haptic shared control does influence the number of excessive accelerations, however, the effect size is low and thus only observable for the most extreme condition comparison (i.e. low visibility for manual and high visibility and haptic assistance). An increase in the number of participants could increase the statistical significance between the different runs.

It was found that when looking at the reversals metric a significant decrease was found during the night condition. The reversals seem to decrease when using haptic shared control compared to manual for both day an night. However, a only for night time a significant effect was found. The results from the NASA-TLX indicated that the participants experienced less control workload when using the shared control system compared manual control. This reduction in of both reported and measured workload corresponds to the expectations based on literature [2] on haptic shared control in other domains.

The haptic speed advice is felt once the maximum advised lever position and correspondingly the maximum safe speed is reached. The fact that the mean acceleration level, the $A_{1/3}$, and the $A_{1/10}$ accelerations did not vary significantly between the conditions is considered to be a positive outcome of the experiment, since an increase in these acceleration levels when using shared control could have meant an increase in acceleration dose sustained because participants choose to operate more closely to the limits.

8.2 Effect of experimental design choices

When preparing the experiment choices and simplifications needed to be made due to time and resources constraints. In this section the impact of these simplifications on the outcome of the experiment are discussed.

Simulator setup: From literature it is known that the operators tend to react after a (excessive) vertical acceleration is felt [20]. The lack of this motion cue in the current experimental setup could have had an effect on the results. The vibration that was implemented on the levers when an excessive acceleration was encountered is much more easily dismissed than a full body vibration. Using the FSSS motion platform at MARIN together with the haptic levers could lead to different results. However, the aim of the experiment to investigate the effect of applying haptic shared control when sailing in waves. If valuable insights could be gained using the current simplified setup it would be beneficial compared to a expensive motion platform.

Participants: For the experiment 24 conveniently sampled participants were selected from among the students and staff of Delft University of Technology. After analyzing the raw data two participants were excluded from further analysis. Of the remaining participants only two were in possession of a navigation license. The lack of sailing experience and the relatively small size of the group could have effected the outcome of the experiment. However, if experienced operators would have been selected for the current setup, the lack of motion cues and the presence of a navigator could have interfered with the operators strong internal model gained from experience. This could also have had a significant impact on the results.

Wave field: Although the wave characteristics in general, the peak period and significant wave height, are similar for every participant it can happen that some participants encounter somewhat more long and shallow waves rather than steep high waves. In some cases this could have lead to a more difficult wave environment. If full insight into the wave field components could have been provided it could be used to normalize the score of the participants with for example the spectral power of the wave signal. However, with the current simulator information available this was not possible.

Sea state estimator: The sea state estimation was kept simple to show the prove of principle of this method of providing advice based solely on the heave response of the vessel. However, if the pitch motion of the vessel would also be included in the estimation it could be used to estimate the wave steepness next to the wave height and base the sea state estimation on this combination. Experiments will need to show the usefulness of this combined method. Furthermore, the current approach makes use of simple sensors that are mostly available on the current vessels. However, using sensors that could potentially make a more precise estimate of the sea state, such as radar or smart camera's, could also increase the model quality in the future.

Warnings: To partly replace the missing motion cue a vibration signal was implemented on the lever when an excessive acceleration was reached. It could have happened that the vibration is easily dismissed or that the the signal did not carry enough information about the severity and the duration of the acceleration signal. Therefore, if the vibration would be made dependent on the severity and/or the duration of the excessive acceleration it could give the operator more information and potentially influence behavior. Conveying a signal that contains more information than a warning signal could be useful. However, this will also require more training and effort to get familiar with.

Order effects: When looking at the order effects, which can be found in Chapter 7, for number of

excessive accelerations it can be seen that a substantial decrease in the number excessive accelerations occurs when the participants become more experienced. This indicates that the participants are not fully trained when the experiment commenced. The large number of excessive accelerations could potentially partly be explained by training trials that were not recorded, so the participants did not get feedback on their performance before the experiment commenced. This was done intentionally because the participants were urged to explore the boundaries of what was possible with the simulated vessel and thereby get a feel for the dynamics and the acceleration and deceleration capabilities. However, providing feedback on the training run could have helped in avoiding the outliers that occurred during some of the first runs. To compensate for these learning effects the Latin-square approach was used. However, testing the model with experienced operators could reduce these differences in individual prior skill level. For future experiments a longer training run could also help to further mitigate the learning effects.

Headwaves: In the experiment is was chosen to sail in head waves because this is generally considered to be the most limiting condition. However, a much voiced argument, especially from the persons with sailing experience and a navigation licence, was that the inability to maneuver did not feel natural. What experienced operators tend to do is to maintain an angle of attack with respect to the approaching wave of about 30^o. This leads to a zigzag sailing pattern in which the chance of excessive vertical accelerations due to wave slamming is decreased. The reason to set the simulated ship to autopilot is to have similar conditions for every participant and make the experiment less sensitive to operator experience. In an experiment with experienced (FRISC) operators and a more realistic simulation environment it could be useful to have also manoeuvring capabilities.

Chapter 9

Conclusion

In the introduction the research question was posed which read: To what extend can haptic feedback on the lever assist the operator in mitigating the excessive vertical accelerations due to wave slamming? During this research it was investigated how haptic feedback could potentially assist the operators of small fast ships. From literature two potential mechanisms were identified: 1. Looking ahead to make a prediction of the wave field, the resulting ship motions and give feedback to the operator, or 2. Make a prediction of the movements to be encountered by the motions that are experienced and use that to give feedback to the operator. For a long time both methods were deemed interesting and developed further, however, due to time constraints only the second method was fully developed and used to perform experiments. In Chapter 10 recommendations as a set of steps to be taken are provided that would make further developing this model easier.

In order to test the effectiveness of the model that was developed an experiment was set up. In this experiment the participants were exposed to different environmental conditions both with and without shared control. The main aim was to see if the participants would achieve less excessive accelerations with the shared control condition compared to manual. To have the participants sail fast and take risks in the same way that operators are forced to in reality a time critical assignment was chosen. The participants needed to sail as fast as possible from A to B with as little excessive accelerations as possible. The hypotheses that resulted from this experimental setup read: "Haptic feedback on the lever will decrease the amount of excessive vertical accelerations due to wave slamming".
As shown in Chapter 7 a significant decrease in the number of excessive accelerations is only achieved when comparing the best/worst case scenario. However, 16 out of 22 participants experienced less excessive accelerations when sailing shared control. The lack of significance indicates a difference in control strategy between the participants. Furthermore, a significant decrease in the workload reported and the number of reversals was found when shared control was used.

To answer the research question to what extend can haptic feedback on the lever assist the operator in mitigating the excessive accelerations due to wave slamming it can be concluded that the workload is reduced significantly, especially during conditions with poor visibility. Furthermore, there seems to be a positive trend in the reduction of the acceleration levels using shared control.

This study is the first to consider human-in-the-loop experiments for reducing the vertical accelerations of small fast vessels. Furthermore, it was the first time a haptic ship simulator was used to perform experiments. Valuable insights were gained on operator response and applying human-in-the-loop experiments for maritime applications. Further research could expand the way operator response is measured and how best to apply shared control within the maritime domain.

Chapter 10

Recommendations

In Chapter 8 several potential sources of reduced experiment validity are identified. Due to time and resources constraints model and experimental choices needed to be made that potentially negatively effected the experimental results. In this chapter several recommendations are given that could improve the results of the experiment and more generally also the application of haptic interfaces in small fast ships.

10.1 The current model

Firstly some recommendations regarding the current model and experiment are given. These recommendations are meant as improvements to strengthen the current experiment.

- *Connect to motion base platform*
  Firstly, it is recommended to connect the existing haptic controls setup to the FSSS simulator with motion base platform, which currently based at Marin. The participants are expected to perform in a much more realistic manner when really feeling the effect that the waves have on the vessel.
- *Test with trained/experienced operators*
  The response to the feedback of the persons that will need to use this technology is very valuable. Also their feedback on how the system functions and what could be improved can be very useful. In this way the model can be tuned using the experience of the operators.
- *Test multiple conditions*
  For the experiment that was conducted in this research only a day and a night condition were used. It would be interesting to see the operators response in other conditions. Also the effect of sailing to and from sheltered positions would be interesting to measure.
- *Maneuvering*
  In the improved experiment it is recommended to allow the operator to maneuver up and down the waves as would also be done in reality. This will improve the operators sense of immersion in the simulation. Using the FSSS simulator from Marin the current steering wheel could be used to manoeuvre or it could even be extended with a haptic steering wheel that would help to navigate the waves.

10.2 The predictive model

In this section the steps that are needed to implement and test the predictive model are provided. During this research a significant amount of time was spend investigating the possibility of having a predictive model as well as a model based on statistics. The Marin simulator was adjusted such that the wave information could be send over NMEA to the model and the model could calculate at each location at any time the wave height. However, a large complication that was encountered was that a sufficiently accurate ship response model is needed to calculate the estimated ship responses seconds before the waves

are actually encountered. Understanding, implementing and tuning such a model was deemed outside of the scope of this project and therefore a guide on how to continue with this research is provided below.

- *Fully conveying the wave information*
  Find a suitable data type such that the Bachmann can handle the full NMEA sentence that contains the wave information. The current data type that is handled by the Bachmann is cut of after 76 bytes while the Marin Dolphin simulator can send strings of up to 1024 bytes. Once the wave information is fully conveyed the created wave reconstruction subsystem from the Simulink model can be used.

- *Ship response model*
  For the ship response model a trade-off needs to be made between accuracy and speed. It would be both elegant and robust to use a model that approaches the FSSS model as developed by Marin such that the visual and the haptic information has a high correlation.

- *Prediction window*
  A minimum prediction window of 5 seconds is recommended to allow the vessel to decelerate in time to have a significant effect on the predicted motions.

- *Forces*
  For the first tests use the vibration subsystem that was already developed in the current Simulink model. In a later stage also repulsive forces can be used to guide to operator to a new safe speed. It is not recommended to use a guidance force that encourages accelerating as well as decelerating. Better to let the operator him/her-self chose to set a speed, otherwise the system could become difficult to handle in reality.

- *Test procedure*
  When testing the predictive model the same test strategy and setup as was used for the current research can be used. If the model is fully functioning it can be tested on the FSSS simulator. It would then also be interesting to test the predictive and the statistics methods against each other and compare the operator responses.

10.3 Implementation of the current model

In this section the steps that are needed to implement the current model aboard the FRISC fleet is provided. Because this model is largely dependent on statistics the first step in the recommendation is to collect as much response data as possible. A system similar to what companies like Tesla use is recommended that would allow all FRISCs to share response and operator behaviour data. To be able to collect, store and share all this data the FRISCs need to be equipped with high precision sensors, robust shock resistance data storage units and a wireless vessel to vessel connection. As time goes on more data is gathered the system will become more precise and the operators more skilled in using it. Collecting all this data will not only strengthen the database but also grand and insight in operator behaviour, which could be very valuable when performing preventive maintenance, but also accident analysis and many other applications.

Developing a version of the haptic levers that is small but yet powerful enough to give feedback to the operator even when wearing protective gear could prove to be a challenge. The levers will also have to be redundant that when the haptic functionality fails the engines can still be controlled. It is recommended to first let an external party develop the actuated levers to investigate if the levers can be made small and powerful enough for the FRISC application.

Bibliography

[1] Rijkens A.A.K. *Proactive Control of Fast Ships: Improving the seakeeping behaviour in head waves.* PhD thesis, Delft University of Technology (2016).

[2] Boer E. R. Abbink D. A., Mulder M. Haptic shared control: smoothly shifting control authority? *Cognition, Technology Work 14.1 : 19-28 (2012).*

[3] Mulder M. Abbink D. A. Exploring the dimensions of haptic feedback support in manual control. *Journal of Computing and Information Science in Engineering 9.1: 011006 (2009).*

[4] Deyzen A.F.J. *Improving the operability of planing monohulls using proactive control: From idea to proof of concept.* PhD thesis, Delft University of Technology (2014).

[5] Allen R. Allen D.P., Taunton D.J. A study of shock impacts and vibration dose values onboard highspeed marine craft. *The Transactions of the Royal Institution of Naval Architects Part A: International Journal of Maritime Engineering 150.A3 : 1-10 (2008).*

[6] Hirst J. Coe T.E., Dyne. S. Whole body vibration mitigation: maintaining capability while complying with legislation and protecting crew from high speed craft motions. *Conference Proceedings of INEC (2012).*

[7] Hirst J. Coe T.E., King P.D. Understanding whole body vibration exposures on high speed marine craft. *Ocean Engineering 42: 126-134 (2012).*

[8] Iman R.L. Conover, W.J. Rank transformations as a bridge between parametric and nonparametric statistics. *Am. Stat. 35, 124129. (1981).*

[9] Cramer S. C. Reinkensmeyer D. J. Crespo L.M., McHughen S. The effect of haptic guidance, aging, and initial skill level on motor learning of a steering task. *Experimental Brain Research.*

[10] de Jong P. *Seakeeping behaviour of high speed ships.* PhD thesis, Delft University of Technology (2011).

[11] LTZ2OC de Waal. Systeemplan frisc sf1200 (2016).

[12] Defensie Materieel Organisatie (DMO). Binationaal gebruiksplan frisc (2013).

[13] Zarnick E.E. A nonlinear mathematical model of motions of a planing boat in regular head waves. *No. DTNSRDC-78/032. DAVID W TAYLOR NAVAL SHIP RESEARCH AND DEVELOPMENT CENTER BETHESDA MD (1978).*

[14] Coe T.E. et al. Development of an international standard for comparing shock mitigating boat seat performance. *Innovation in Small Craft Technology, London, UK (2012).*

[15] M. Figari and M. Altosole. Dynamic behaviour and stability of marine propulsion systems. *Proceedings of the Institution of Mechanical Engineers, Part M: Journal of Engineering for the Maritime Environment 221.4 (2007): 187-205.*

[16] International Organization for Standardization. Mechanical vibration and shock – evaluation of human exposure to whole-body vibration – part 1: General requirements.

[17] Staveland L.E. Hart, S.G. Development of nasa-tlx (task load index): results of emperical and theoretical research. *In: Meshkati, P.A.H.N. (Ed.), Human Mental Workload, vol. 1. (1988).*

[18] Abbink D.A. Hoeckx F., Vrijdag A. Developing of a test setup for exploring the potential of haptic feedback for maritime operations. *MECSS Conference Proceedings (2017).*

[19] Olander A. Huss M. Theoretical seakeeping predictions on board ships -a system for operational guidance and real time surveillance. *Naval Architecture, Department of Vehicle Engineering, Royal Inst. of Technology (1994).*

[20] Keuning J.A. *Nonlinear Behaviour of Fast Monohulls in Head Waves.* PhD thesis, Delft University of Technology (1994).

[21] Engstrm J. Cherri C. Nodari E. Toffetti A. Schind-helm R. Gelau C. Johansson, E. Review of existing techniques and metrics for ivis and adas assessment. *Adaptive Integrated Driver Vehicle Interface (AIDE) Product number: IST-1-507674-IP (2004).*

[22] Walree F. Keuning J.A. The comparison of the hydrodynamic behaviour of three fast patrol boats with special hull geometries. *In Proceedings of the 5th International Conference on High-Perfromance Marine Vehicles (2006).*

[23] Dunwoody A.B. Calisal S.M. Kose E., Gosine R.G. An expert system for monitoring dynamic stability of small craft. *IEEE Journal of Oceanic Engineering 20.1: 13-22 (1995).*

[24] Hirokawa S. Koyama T. On a micro-computer based capsize alarm system. *Proc. 2nd STAB, 1982: 329-339 (1982).*

[25] Marine Specialised Technology Limited. Operator manual fast raiding interception and special forces craft (2012).

[26] Koninklijke Marine. Instandhoudhoudingsanalyse frisc (2017).

[27] Riley M.R. A deterministic approach for characterizing wave impact response motions of a high-speed planing hull.

[28] Riley M.R. A generalized approach and interim criteria for computing a1/n accelerations using full-scale high- speed craft trials data. *No. NSWCCD-23-TM-2010/13. NAVAL SURFACE WARFARE CENTER CARDEROCK DIV NORFOLK VA COMBATANT CRAFT DEPT (2010).*

[29] Hill J. Dyson R. Myers S., Dobbins T. energy expenditure during transits in a 28 ft rib in varying sea states. *Proceedings of Human Performance at Sea, Influence of Ship Motions on Biomechanics and Fatigue- Panama City Florida (2006).*

[30] Directie operaties NLMF (2014). Voorschrift commando zeestrijdkrachten. *Zeemanschap deel 1.*

[31] Frank C. Peterson R., Wyman D. Drop test to support water-impact and planing boat dynamics. *No. CSS/TR-97/25. NAVAL SURFACE WARFARE CENTER PANAMA CITY FL, APA (1997).*

[32] Longuet-Higgins M. S. On the statistical distribution of the heights of sea waves. *Journal of Marine Research, 11: 245246 (1952).*

[33] Austen S. Townsend N.C., Wilson P.A. What influences rigid inflatable boat motion? *Proceedings of the Institution of Mechanical Engineers, Part M: Journal of Engineering for the Maritime Environment 222.4 : 207-217 (2008).*

[34] Commandant Zeestrijdkrachten. Operationele evaluatie frisc (2013).

Appendix A

Planning

MSc Thesis - R. Kok - Gantt Chart

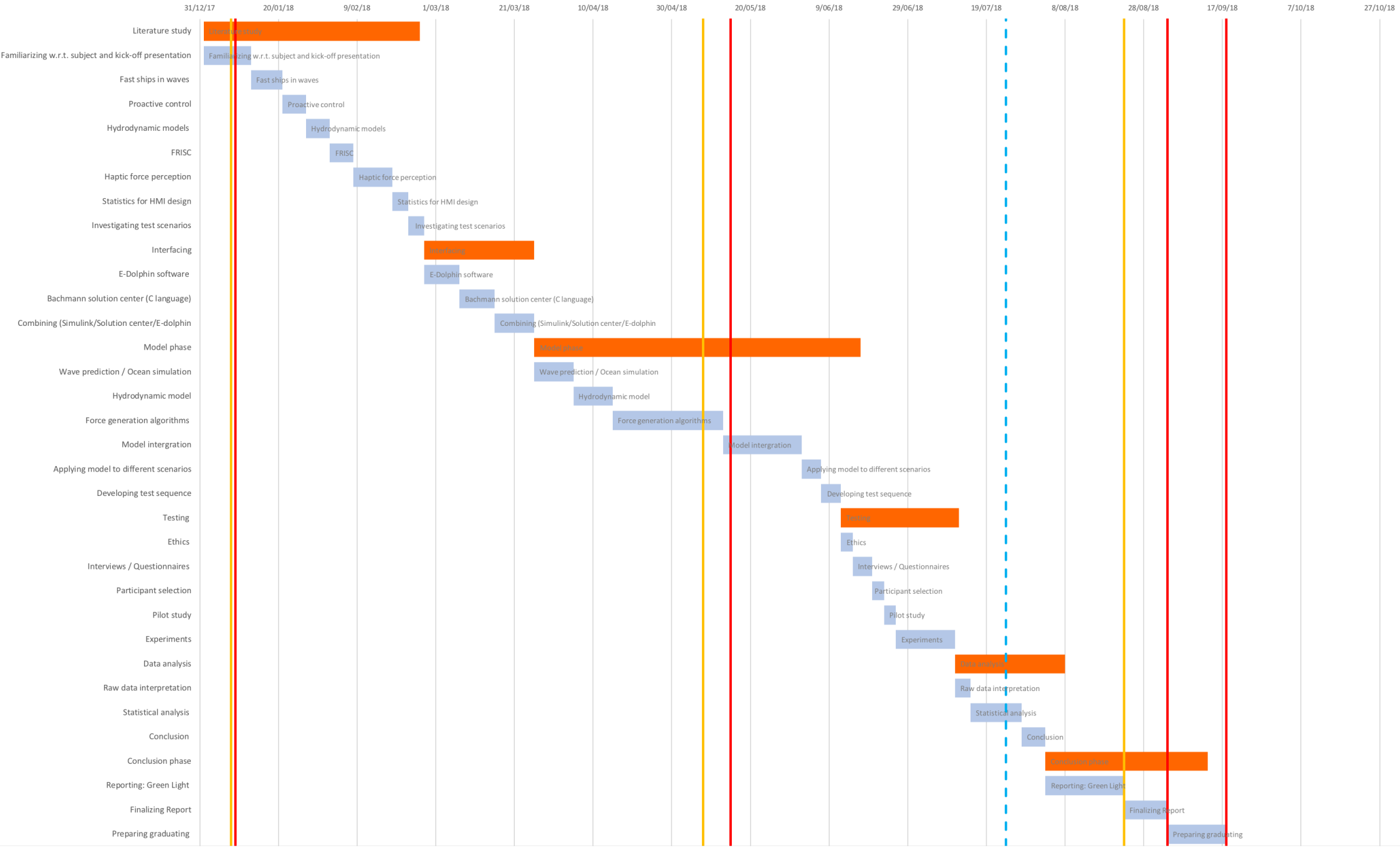

Appendix B

Experimental setup

In this chapter the haptic maritime simulator setup is discussed. The chapter is divided into 4 parts: the levers, the Real-Time controller (Bachmann), the central computers and the block diagram. The full setup is shown in Figure B.1.

B.1 The central computers

In the current setup two powerful computers are used to calculate, simulate and visualize the simulator output. The left most computer is fully dedicated to calculate all processes that occur in the simulation software. The right computer has a powerful graphics card (...), which is used to visualize the simulator output and control the settings of the Bachmann and the Matlab Simulink model.

Controlling the Matlab Simulink model is done via a dedicated created GUI (Graphical User Interface), which once created is an easy way to control and tune the model. In Figure B.2 the GUI is shown with on the top all essential buttons to activate and update the model and in the lower section all functions.

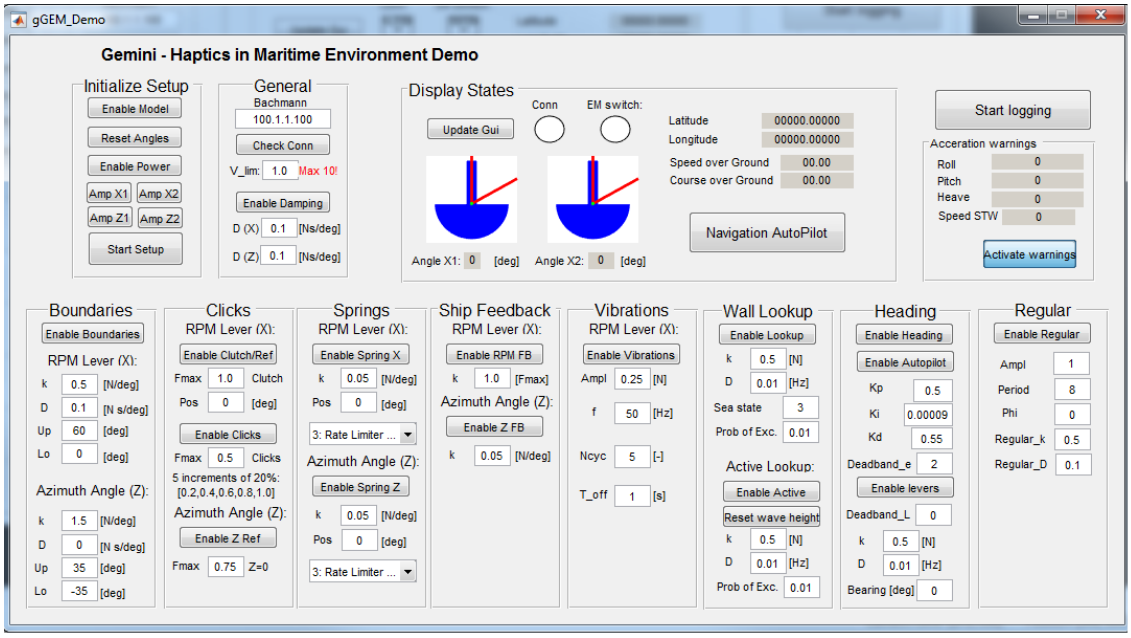

Figure B.2: The GUI interface to control the setting of the compiled Simulink model.

Figure B.1: The full haptic demonstrator setup.

A program called Solution Center is used to program and control the Bachmann directly using C/C++ language. This program is a custom made compiler that was created by Bachmann to control their CPU's directly over an FTP connection to the host PC. In Solution Center the software modules can be installed, deleted and controlled. The incoming communication, in the form of NMEA 0183 protocol, is received via a software module called Server. This module receives the NMEA sentences and processes them, such that the right information is assigned to each variable that is needed by the haptic algorithm. This Server module needs to be programmed by the user such that the right NMEA sentences are received and processed. The received information is translated to SVI (Standard Variable Interface) variables that can be used directly by the compiled haptic algorithm. The output of the model is send to the simulator and the levers using the Client software module. The Client translates the SVI variables back and packages them in a NMEA control sentence that can be received by the simulator. This setup is deliberately designed to communicate over NMEA to make the connection to a real ship relatively straightforward. In Figure B.3 the Solution Center interface is shown with on the top left the Server module, on the top right the Client module and on the lower part the variables view that shows all modules running at that time and the variables each receives.

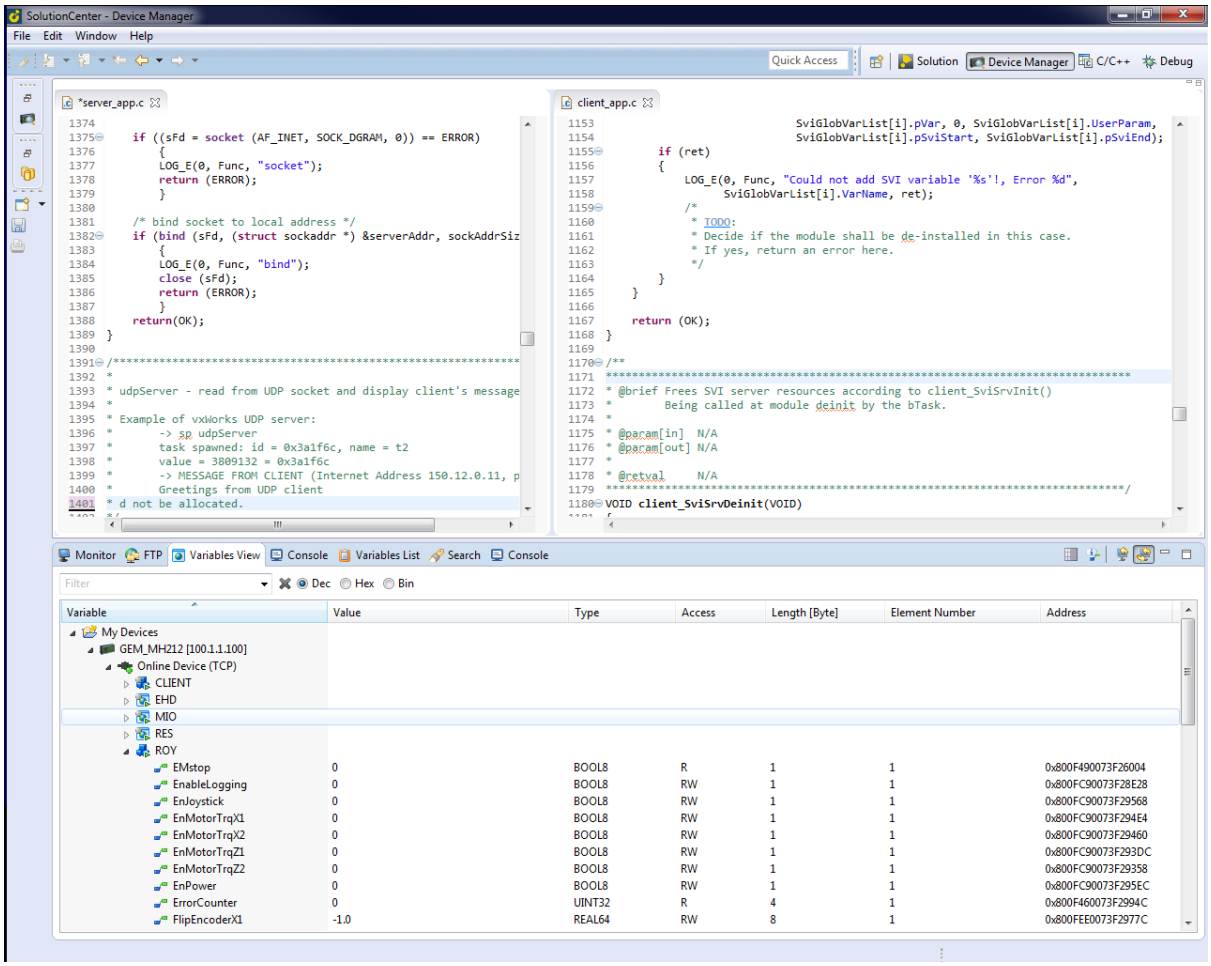

Figure B.3: The Solution Center interface.

B.2 The Bachmann Real-Time controller

The Real-Time controller is build by the Austrian company Bachmann Electronics. This company is well known for its modular designs that allow the user to add or remove parts relatively easily. To maintain haptic fidelity it is essential to have a control loop of at least 1kHz. For this setup a Bachmann processing unit was selected that can actively control the motor input signals up to 2.5kHz. The main components of the Bachmann assembly that is currently used are:

- Two counter modules (CNT204/R 1 and CNT204/R 2).
- One DIO module (DIO232): Digital input and output modules.
- One GIO module (GIO212): Universal (digital and analogue) input and output.
- One Central Processing Unit (CPU) MH212.
- One pulse generator.
- Four ESCON Pulse Width Modulation (PWM) modules: One for each motor that control the current that is fed to the motor.

B.3 The levers

Inspired from an azimuth lever the haptic feedback levers are the real interface between the user and the system to be controlled. The levers are two degrees of freedom and can be actuated each using two

electric (Maxon) motors connected to the levers via a capstan mechanism. In this mechanism the motor forces are transferred to the levers via steel cables with a significant moment arm such that an efficient force transfer is achieved. In Figure B.4 one of the levers is shown. For this research the azimuth angle of the levers is blocked because only RPM setpoint control in head waves is considered.

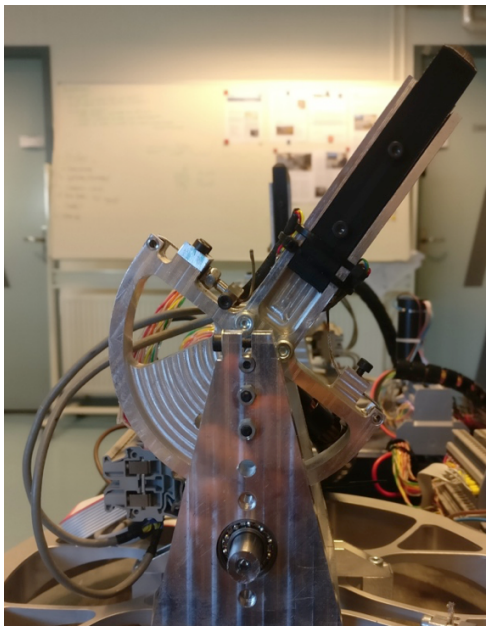

Figure B.4: One of the haptic levers.

The Haptic Feedback Project Setup System Block Diagram

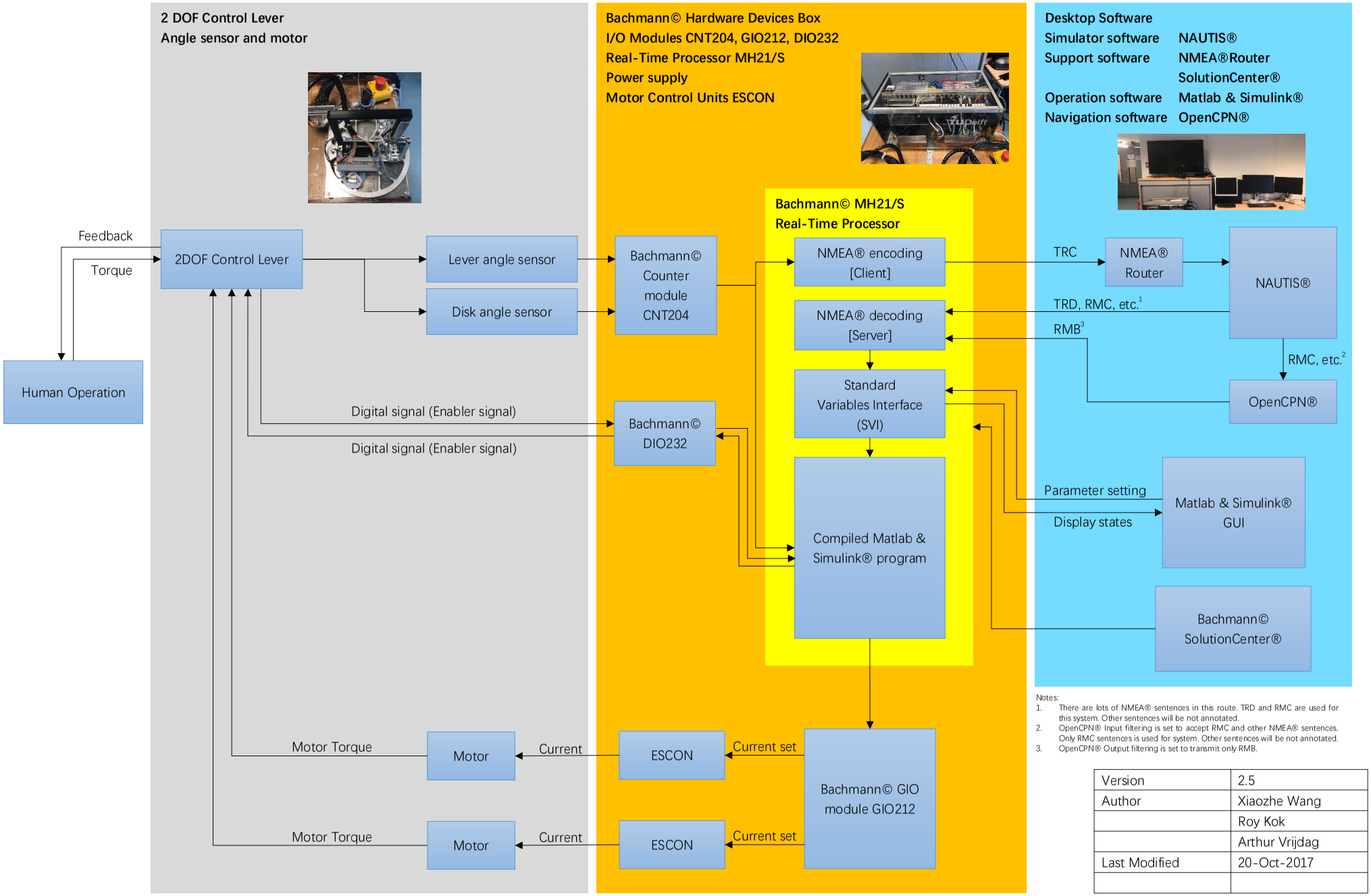

Notes:

1. There are lots of NMEA® sentences in this route. TRD and RMC are used for this system. Other sentences will be not annotated.
2. OpenCPN® Input filtering is set to accept RMC and other NMEA® sentences. Only RMC sentences is used for system. Other sentences will be not annotated.
3. OpenCPN® Output filtering is set to transmit only RMB.

Version	2.5
Author	Xiaozhe Wang
	Roy Kok
	Arthur Vrijdag
Last Modified	20-Oct-2017

Appendix C

Simulator validation

In this chapter the validation of the first FRISC simulator model (E-Dolphin 3.0) can be found. The sensor information available is determined by the FRISC model in the simulator. This sensor information can be recorded at different speeds and in varying sea states. In version 3.0 of the FSSS software only the roll, pitch and heave motions were available at a maximum frequency of 20 Hz. Taking the derivatives of these signals yield the response velocities and accelerations. Because the motions are expected to describe a sine wave like trajectory the calculated velocity and accelerations should compare to taking the derivative of a sine wave function. The accelerations are calculated on three points of the ship: at center of gravity (CoG) (C.1), at the side (C.2) and at the bow (C.3). For these calculations the ship dimensions and motions are needed. In Figure C.1 the heave displacement, velocity and acceleration are shown in one figure. It can be seen that the derived signal indeed resembles a sine wave derivative.

$$a_{z,cog} = \ddot{z} \tag{C.1}$$

$$a_{z,side} = \ddot{z} + \frac{W}{2} \cdot \ddot{\psi} \tag{C.2}$$

$$a_{z,bow} = \ddot{z} + \frac{2 \cdot L}{3} \cdot \ddot{\theta} \tag{C.3}$$

Where,

- z is the heave [m]
- W is the width of the vessel [m]
- L is the length of the vessel [m]
- ψ is the roll [deg]
- θ is the pitch [deg]

Model verification

The accuracy and limitations of the computational model are essential when comparing the usefulness of a potential haptic feedback solution. The first version of the simulator that was used is Dolphin 3.0. To check the behaviour of the model some basic system identifications checks were performed using a fixed ship speed and a regular wave field. While varying the period of the waves the response of the model was logged. The wave height that was selected for this system identification was 1 meter. From the heave, roll and pitch responses that are plotted in Figure C.2 it can be seen that something strange is happening in the model. At zero forward speed the heave movement of the vessel does not follow the wave but seems to be damped with a factor of 0.7.

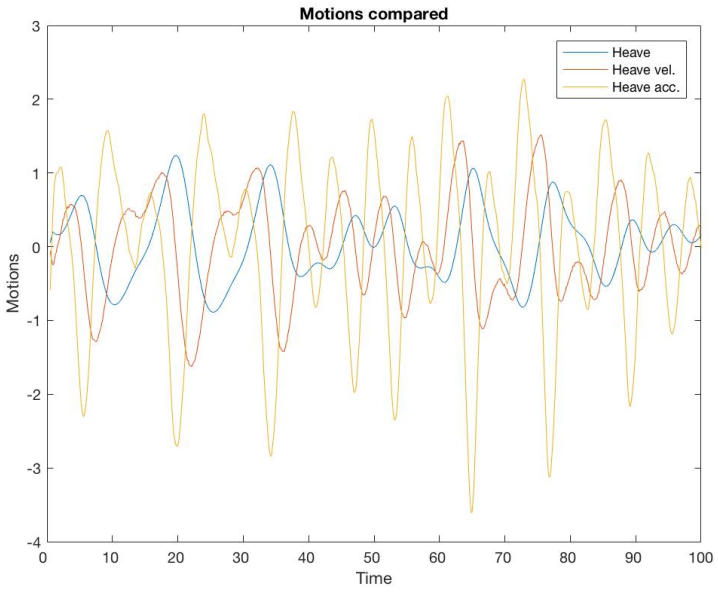

Figure C.1: The simulated heave motion and the calculated heave velocity and heave acceleration.

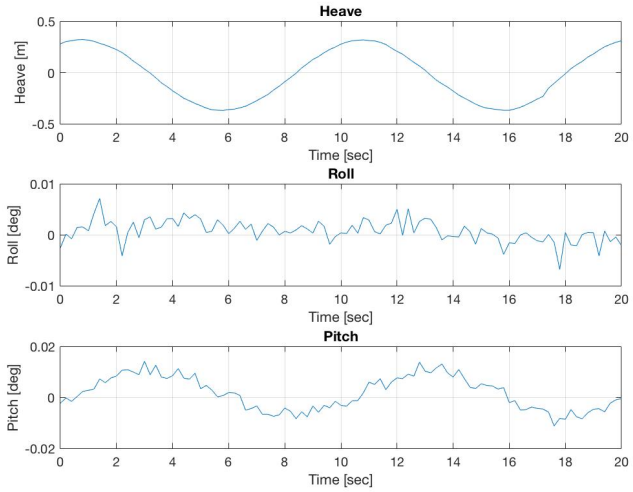

Figure C.2: The heave, roll and pitch from model version 3.0.

To perform further system identification the response amplitude operators (RAO's) are calculated and plotted. In Figure C.3a and C.3b the heave and pitch RAO's are given for different vessel speeds. As can be seen for the heave RAO something strange is happening here as well. At low encounter frequencies the response is expected to approach 1, however this is not the case as can be seen. The limited number of data points in the plot is caused by the limited number of wave frequencies that can be entered in this version of the model. The pitch RAO looks more like expected and no strange things are estimated to be happening there.

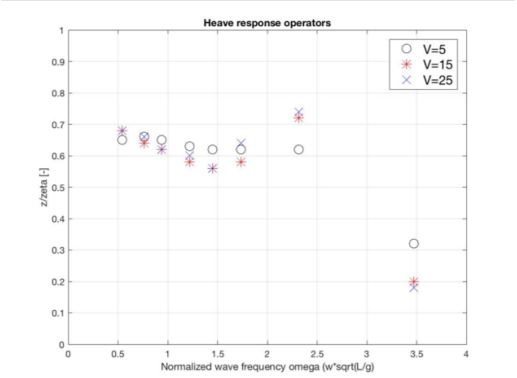

(a) The response amplitude operator for heave at a normalized wave frequency

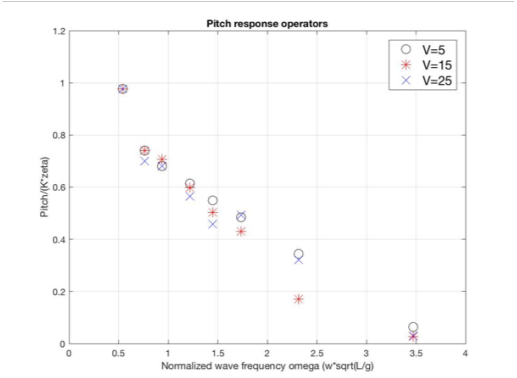

(b) The response amplitude operator for Pitch at normalized wave frequency.

Besides the inaccuracies in the hydrodynamic model the outside view of this version of the model is of low quality. It can be seen that the 1 meter significant wave height waves, which are shown in the figure, are hardly distinguishable. In Figure C.4a an example of the operator view is given and compared to the outside view of a later version in Figure C.4b is given.

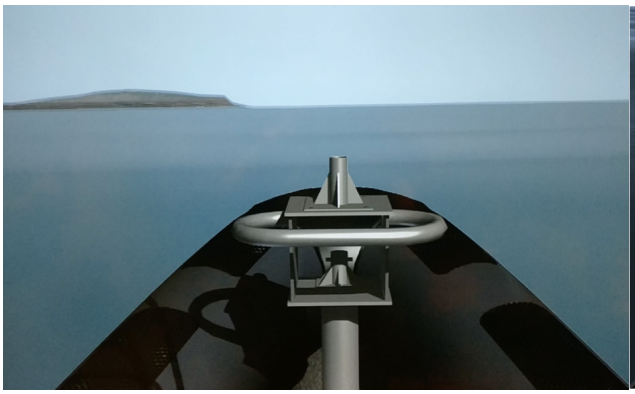

(a) The operator view of version 3.0.

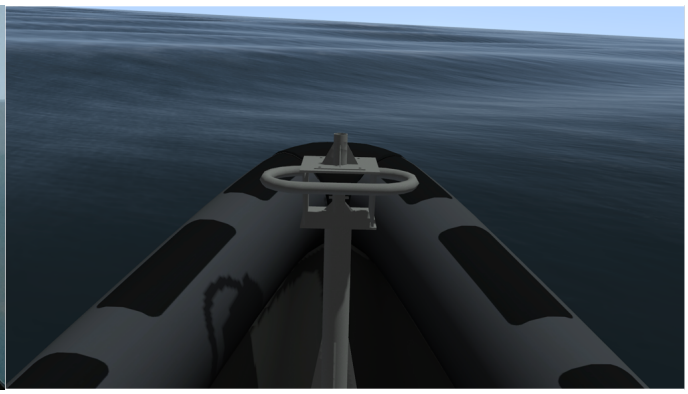

(b) The operator view of version 5.2.

In the same way as with the DMO signal also for the calculated signal the statistics are given below. The processed signal is used to construct a database that will eventually be used to provide a speed advice.

Table C.1: The statistics of the acceleration signal measured in Sea state 3.

Sea state 3	V = 15kts	V = 20kts	V = 25kts	V = 30kts	V = 35kts
RMS	1.7	2.4	3.0	6.1	5.0
$A_{\frac{1}{3}}$	2.4	3.5	4.3	8.7	7.0
$A_{\frac{1}{10}}$	3.2	4.3	5.2	11.2	8.5
$A_{\frac{1}{100}}$	3.8	5.0	6.0	13.3	9.6

Table C.2: The statistics of the acceleration signal measured in Sea state 4.

Sea state 4	V = 15kts	V = 20kts	V = 25kts
RMS	2.7	3.9	4.8
$A_{\frac{1}{3}}$	3.9	5.6	6.8
$A_{\frac{1}{10}}$	5.2	7.2	8.4
$A_{\frac{1}{100}}$	6.2	8.6	9.8

Table C.3: The statistics of the acceleration signal measured in Sea state 5.

Sea state 5	V = 15kts	V = 20kts	V = 25kts
RMS	3.6	5.3	6.4
$A_{\frac{1}{3}}$	5.4	7.9	9.3
$A_{\frac{1}{10}}$	7.9	10.0	11.2
$A_{\frac{1}{100}}$	9.4	11.8	12.5

C.1 Simulator data validation

Now the acceleration signals are known, the same signal processing steps as were used for the DMO signal in Chapter 3 can be applied. For these signals it is estimated that there will be little noise due to structural components because the calculation model does not cover this. To validate the quality of the simulator signal in this section it will be compared to the real measured data. As can be seen from Figure C.5 the simulated signal differs quite significantly from the measured DMO signal.

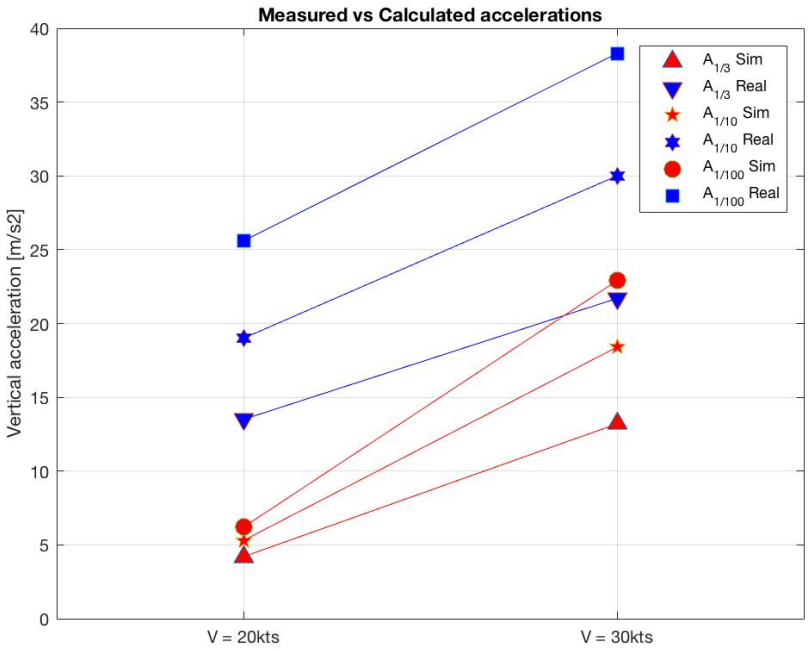

Figure C.5: Comparing the measured signal to the simulated signal for the significant accelerations levels.

Appendix D

Experiment

In this chapter the experimental order and the statistics of the participants are provided. In Figure D.1 the experimental order for each participant is given. All participant had to read and sign the informed consent form that can be found below. Also the NASA TLX that was to be filled in after each trial condition can be found below.

Experimental design				
latin square participant selection				
Participant	Order of conditions			
P1	4	3	2	1
P2	4	3	1	2
P3	4	2	3	1
P4	4	2	1	3
P5	4	1	3	2
P6	4	1	2	3
P7	3	4	2	1
P8	3	4	1	2
P9	3	2	4	1
P10	3	2	1	4
P11	3	1	4	2
P12	3	1	2	4
P13	2	4	3	1
P14	2	4	1	3
P15	2	3	4	1
P16	2	3	1	4
P17	2	1	4	3
P18	2	1	3	4
P19	1	4	3	2
P20	1	4	2	3
P21	1	3	4	2
P22	1	3	2	4
P23	1	2	4	3
P24	1	2	3	4

Figure D.1: The experimental order for each participant.

From the group of selected participants 16.6% (4) is female, which is about average for Delft University of Technology statistics. The average age is 26.9 years. Only 3 participants were in possession of a navigation license. However, more than half (58%) of the participants claimed they had a certain degree of sail experience.

Informed Consent Form for individuals interested in haptic feedback for ships we are inviting to participate in this research.

Principal Researcher:	R. Kok (r.kok-1@student.tudelft.nl)
Organization:	Delft University of Technology
Sponsors:	
-	Defensie Matrieel Organisatie (DMO),
-	Damen,
-	Alphatron Marine,
-	Marin,
-	St. Nederland maritiem land,
-	Ministerie van EZK

Project:	"Haptic assistance to mitigate the damaging vertical accelerations of small fast ships in waves"
Location:	Basement of tower B, 3ME faculty, TUD

This Consent form has two parts:

- Information Sheet (to share information about the study with you)
- Certificate of Consent (for signatures if you choose to participate)

You will be given a copy of the full Informed Consent Form

Part I: Information Sheet

Introduction:
Please read this consent form carefully before starting the experiment. This consent form will inform you of the purpose, procedures, duration and possible risks/benefits of this study. If anything is unclear now or in a later stage of the experiment please ask me to explain it to you.

Purpose of this research:
Operators of small fast ships can suffer discomfort or even serious injuries from impact forces caused by slamming of the hull of the ship on waves. An effective method to mitigate these slams is to reduce the speed of the ship several seconds before a large wave encountered. In this research a haptic feedback throttle is

used to warn or otherwise inform the operator about the environmental conditions such that timely action can be taken. The aim is to reduce the number of excessive vertical accelerations experienced.

Procedure and Instructions:
You will be asked to sail a FRISC (Fast Raiding Interception and Special forces Craft) in head waves in a simulation environment. You start with a training run where you will get a warning (vibration) when the ship reaches an excessive acceleration level. The goal of this training run is to learn to recognize the combinations of ship speed and wave height that cause an excessive acceleration. Both during training and during the experiment the ship will be steered by the autopilot and only throttle control is needed.

After you have gained some experience in sailing the simulated ship and what kind of wave height and ship speed combinations may cause excessive accelerations, you are asked to sail the ship as fast as possible from point A to B in a straight line while experiencing as little excessive accelerations as possible. Thus the main task is to keep the ratio of number of vertical accelerations over completion time to a minimum. This task will be repeated several times under varying conditions. The number and severity of the (excessive) accelerations will be recorded together with the completion time and any other relevant information. In total you will sail the same track five times.

Risks/Discomforts and Confidentiality:
There are no known risks during this experiment, however you may feel discomfort or nausea from the violent motions of the simulated ship. If at any point you feel nauseous or otherwise discomforted do not hesitate to say so and we can stop the experiment. All the data gathered in this study will remain confidential and will only be used for the scientific purposes. You will thus not be directly identifiable in any published results. If you are interested in our results they will be made available to you if you choose to leave your e-mail address, they will be made available around 2 months after this experiment is conducted.

Duration/Reimbursements and the Right to Refuse or Withdraw:
This whole session will take approximately 25 minutes and is entirely voluntary. You have the right to withdraw from the experiment at any time.

Questions and Contact:
As previously mentioned any questions will be answered whenever you have them during the session. If any questions remain you can contact me. (contact information is provided on the first page of the form).

Part II: Certificate of Consent

I have read the foregoing information, or it has been read to me. I have had the opportunity to ask questions about it and any questions I have asked have been answered to my satisfaction. I consent voluntarily to be a participant in this study.

Name:.....

Gender:.....

Age:.....

Are you in possession of a navigation license (vaarbewijs): YES / NO

Do you have experience on the water (sailing or otherwise): YES / NO

Date (D/M/Y):...../...../.....

Assigned experimental order: .....

(E-mail Address):.....(only fill in if you want to be informed of the results)

I have read and understood the information provided above
I give permission to process the data for the purpose described above
I voluntarily agree to participate in this study

Signature:.....

NASA-TLX

Participant No:	Experimental Conditions:	Date / Time of day:

The questions below are about your experience in the experiment (run) that you just performed. Put a cross on the line, not between them.

Mental Demand: How mentally demanding was the task?

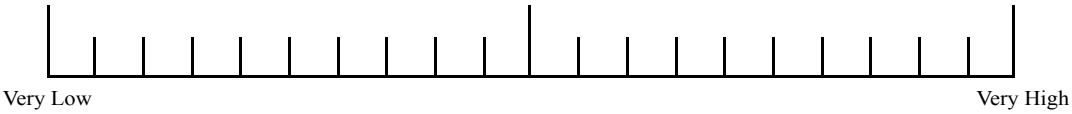

Physical Demand: How physically demanding was the task?

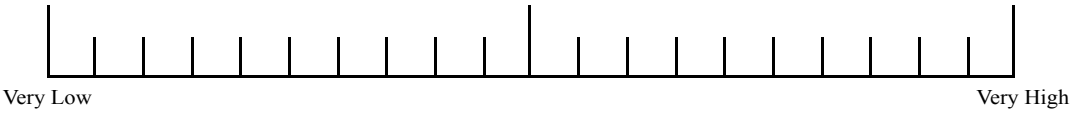

Temporal Demand: How hurried or rushed was the pace of the task?

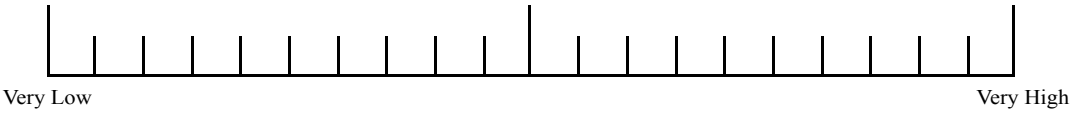

Performance: How successful were you in accomplishing what you were asked to do?

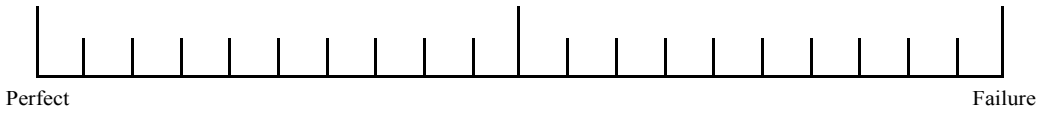

Effort: How hard did you have to work to accomplish your level of performance?

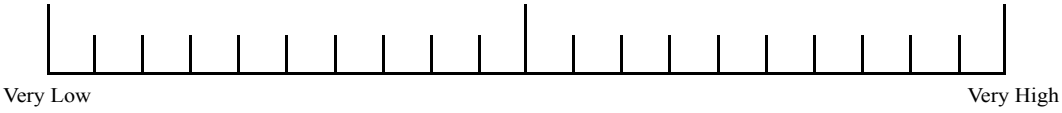

Frustration: How insecure, discouraged, irritated, stressed, and annoyed were you?

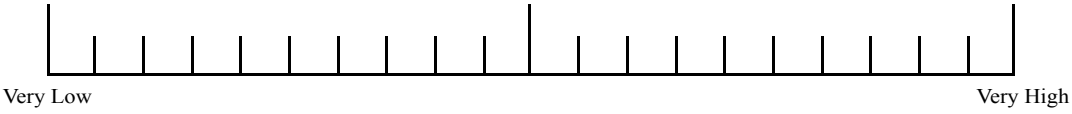

Nausea: To what extend do you experience nausea? *Please circle the statement that is most fitting to your condition.*

1. Not experiencing any nausea, no sign of symptoms.
2. Arising symptoms (like a feeling in the abdomen), but no nausea.
3. Slightly nauseous
4. Nauseous.
5. Very nauseous, retching.
6. Throwing up.

Appendix E

Planing hull

In this section the excel file that was used to calculate the planing behaviour of the FSSS model can be found. The workings of the model are already explained in 5.

The planing problem							
Constants							
D	0,285	Propeller diameter					
t	0,03	Thrust reduction factor much less than 0.12 *source mandieselturbos					
roh	1025	Water density					
w	0,2	Wake fraction effect					
a	-0,7461						
b	5,6139						
n_engine (RPS)	**n_prop (RPS)**	**v_ship**	**R**	**T_tot**	**T_prop**	**aJ+b**	**J**
64,2	39,4	46,9	57000,0	58762,9	14690,7	1,4	6,0
61,7	37,8	45,2	52000,0	53608,2	13402,1	1,4	6,0
58,3	35,8	42,9	45000,0	46391,8	11597,9	1,3	6,1
53,7	32,9	39,2	41000,0	42268,0	10567,0	1,4	6,0
50,0	30,7	36,3	36000,0	37113,4	9278,4	1,5	6,0
45,5	27,9	32,6	28500,0	29381,4	7345,4	1,4	5,9
40,0	24,5	25,3	17000,0	17525,8	4381,4	1,1	5,2
30,0	18,4	17,0	10500,0	10824,7	2706,2	1,2	4,7
26,7	16,4	12,0	14000,0	14433,0	3608,2	2,0	3,7
21,7	13,3	10,0	14500,0	14948,5	3737,1	3,1	3,8
15,5	9,5	8,0	13000,0	13402,1	3350,5	5,5	4,3
10,3	6,3	5,5	7000,0	7216,5	1804,1	6,6	4,4
0,0	0,0	0,0	0,0	0,0	0,0	0,0	0,0
10,0	6,1	5,3	7000,0	7216,5	1804,1	7,1	4,4
13,7	8,4	7,2	12500,0	12886,6	3221,6	6,8	4,3
16,0	9,8	8,2	13500,0	13917,5	3479,4	5,3	4,2
21,7	13,3	10,1	14500,0	14948,5	3737,1	3,1	3,8
26,7	16,4	12,5	13500,0	13917,5	3479,4	1,9	3,9
30,0	18,4	15,0	10000,0	10309,3	2577,3	1,1	4,1
33,8	20,8	18,6	10500,0	10824,7	2706,2	0,9	4,5
37,2	22,8	21,4	11500,0	11855,7	2963,9	0,8	4,7
45,0	27,6	32,4	28500,0	29381,4	7345,4	1,4	5,9
48,3	29,7	34,9	35000,0	36082,5	9020,6	1,5	5,9
53,3	32,7	39,2	41000,0	42268,0	10567,0	1,5	6,1
57,8	35,5	42,5	46500,0	47938,1	11984,5	1,4	6,1
61,7	37,8	45,2	52000,0	53608,2	13402,1	1,4	6,0
64,2	39,4	47,0	57000,0	58762,9	14690,7	1,4	6,0

n_prop = 3000			
R	a*J	v_ship kmh	v_ship kts
50000,0	-2,6	61,2	34,0
45000,0	-2,9	68,5	38,1
40000,0	-3,2	75,8	42,1
35000,0	-3,5	83,1	46,2
30000,0	-3,8	90,4	50,2
25000,0	-4,1	97,6	54,2
20000,0	-4,4	104,9	58,3
15000,0	-4,7	112,2	62,3
10000,0	-5,0	119,5	66,4
5000,0	-5,3	126,7	70,4
0,0	-5,6	134,0	74,5

n_prop = 2500			
R	a*J	v_ship kmh	v_ship kts
50000,0	-1,2	24,3	13,5
45000,0	-1,7	33,1	18,4
40000,0	-2,1	41,8	23,2
35000,0	-2,5	50,5	28,1
30000,0	-3,0	59,3	32,9
25000,0	-3,4	68,0	37,8
20000,0	-3,9	76,7	42,6
15000,0	-4,3	85,5	47,5
10000,0	-4,7	94,2	52,3
5000,0	-5,2	103,0	57,2
0,0	-5,6	111,7	62,0

n_prop = 2000			
R	a*J	v_ship kmh	v_ship kts
50000,0	1,2	-19,8	-11,0
45000,0	0,6	-8,9	-5,0
40000,0	-0,1	2,0	1,1
35000,0	-0,8	12,9	7,2
30000,0	-1,5	23,8	13,2
25000,0	-2,2	34,8	19,3
20000,0	-2,9	45,7	25,4
15000,0	-3,6	56,6	31,4
10000,0	-4,2	67,5	37,5
5000,0	-4,9	78,4	43,6
0,0	-5,6	89,4	49,6

n_prop = 1750			
R	a*J	v_ship kmh	v_ship kts
50000,0	3,3	-46,6	-25,9
45000,0	2,5	-34,1	-19,0
40000,0	1,6	-21,6	-12,0
35000,0	0,7	-9,2	-5,1
30000,0	-0,2	3,3	1,8
25000,0	-1,1	15,8	8,8
20000,0	-2,0	28,3	15,7
15000,0	-2,9	40,7	22,6
10000,0	-3,8	53,2	29,6
5000,0	-4,7	65,7	36,5
0,0	-5,6	78,2	43,4

n_prop = 1500			
R	a*J	v_ship kmh	v_ship kts
50000,0	6,6	-78,6	-43,7
45000,0	5,4	-64,0	-35,6
40000,0	4,1	-49,5	-27,5
35000,0	2,9	-34,9	-19,4
30000,0	1,7	-20,3	-11,3
25000,0	0,5	-5,8	-3,2
20000,0	-0,7	8,8	4,9
15000,0	-2,0	23,3	13,0
10000,0	-3,2	37,9	21,1
5000,0	-4,4	52,5	29,1
0,0	-5,6	67,0	37,2

n_prop = 1250			
50000,0	11,9	-118,9	-66,0
45000,0	10,2	-101,4	-56,3
40000,0	8,4	-83,9	-46,6
35000,0	6,7	-66,4	-36,9
30000,0	4,9	-49,0	-27,2
25000,0	3,2	-31,5	-17,5
20000,0	1,4	-14,0	-7,8
15000,0	-0,3	3,4	1,9
10000,0	-2,1	20,9	11,6
5000,0	-3,9	38,4	21,3
0,0	-5,6	55,8	31,0

IF IN DOUBT SHOUT

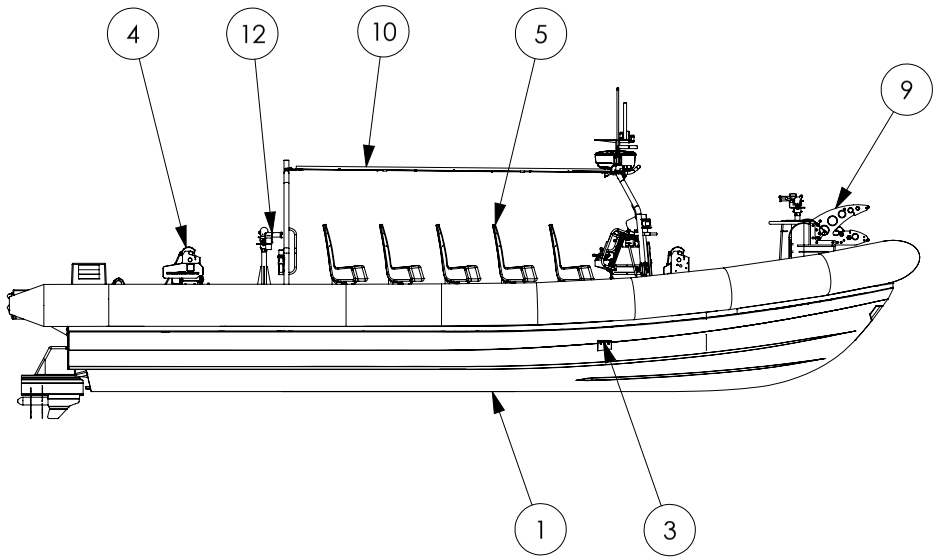

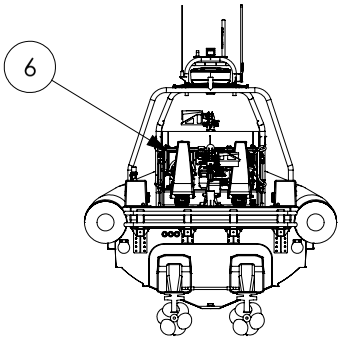

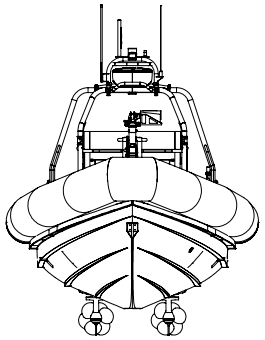

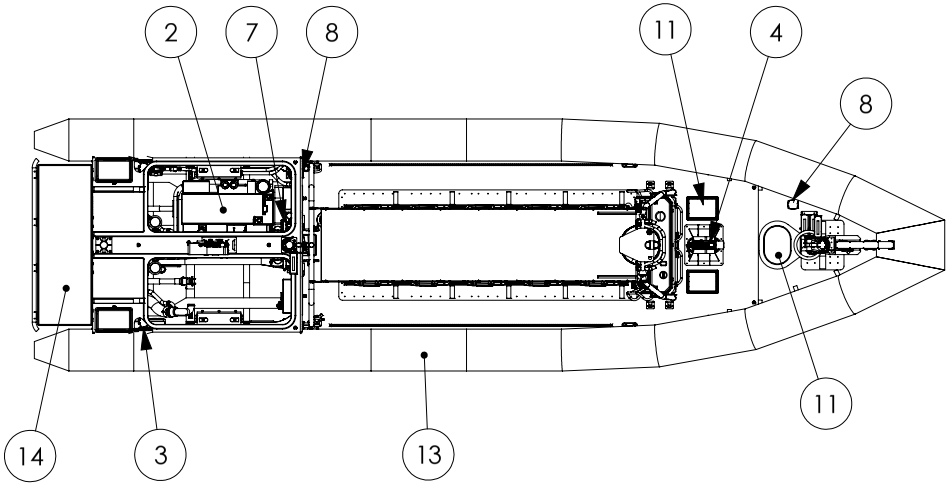

ITEM NO.	DESCRIPTION	PART No	QTY.
1	FRISC 1200 BC Hull Assembly	5066_(C)	1
2	FRISC 1200 BC Stern Drive Installation	4473_(B)	1
3	FRISC 4 Point Lift System	4909_(C)	1
4	FRISC 1200 BC Twin Fall Lift Assembly	4517_(B)	1
5	FRISC Deck Plate Assembly	4520_(A)	1
6	FRISC Console	3670_(C)	1
7	FRISC 1200 Fuel System	4524_(C)	1
8	FRISC 1200 Bilge System	4465_(C)	1
9	FRISC Arrestor System	4519_(B)	1
10	FRISC Bimini Assembly	4514_(B)	1
11	FRISC 1200 Deck Fittings Assembly	4523_(B)	1
12	FRISC AFT Gun Mount Assembly	4516_(B)	1
13	1200 Tubes (330 Beam) - Bluff Bow	4522_(A)	1
14	FRISC Self Righting Assembly Mk2	4247_(B)	1

Principle Dimensions			
Length Overall	12.0m	Fuel Capacity	2 x 480 Ltrs
Beam Overall	3.3m	Tube Diameter	0.55m
Internal Length	7.475		
Internal Beam	2.2m		

UNLESS OTHERWISE SPECIFIED:
DIMENSIONS ARE IN MILLIMETERS
SURFACE FINISH:
TOLERANCES:
LINEAR:
ANGULAR:

FINISH:

DEBUR AND BREAK SHARP EDGES

	NAME	DATE
DRAWN	A.MILLS	10/09/10
CHK'D	AP	
APPV'D	AP	

REV	ER No.	DATE	DESCRIPTION	DRAWN	CHK'D
C	1547	16/11/11	UPDATED VIEWS AS IT HAS CHANGED SINCE DRAWING WAS ISSUED	CJ	AP
B	1227	22/02/11	SECOND ISSUE-DRAWINGS REVISIONS UPDATED	AM	AP
A		10/09/10	FIRST ISSUE	AM	AP

MATERIAL:

WEIGHT:

TITLE:
FRISC 1200 BC-INT GENERAL ARRANGEMENT

Drawing No. 4507

Rev. C

Marine Specialised Technology Ltd.
Unit 1, Atlantic Way
Brunswick Business Park
Liverpool
L3 4BE
Tel: +44(0)151 708 4112
web: www.mstltd.com
email: sales@mstltd.com

SCALE:1:70 | SHEET 1 OF 1 | A3

Appendix F

Simulink

In this section the Simulink model that was created is explained. The whole model consists of roughly 6 parts:

1. *A parameter file*
   In this file all important basic settings of the levers are stored. Tuning this file lets the user change for example the angle ratio between the real and the simulated levers.
2. *Hardware inputs*
   All signals generated by the levers are processed in this block.
3. *Software inputs*
   All the signals received by the Bachmann from the control pc's are processed in this block.
4. *The Joystick block*
   In this block all modeling is done.
5. *Software outputs*
   This block sends the commands to the control pc's.
6. *Hardware outputs*
   This block sends the commands to the levers.

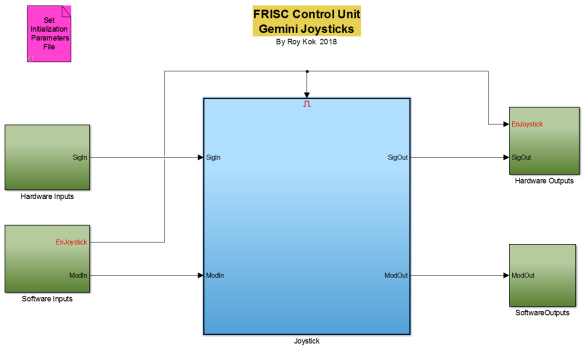

model.png

Figure F.1: An overview of the whole Simulink model.

The processes happening in the input and output blocks are relatively straightforward and will not be treated further. However, the joystick block is described in more detail due to its complexity. In Figure F.2 an overview of the blocks contained in the joystick model can be found. The following 4 blocks comprise the joystick block:

1. *Initialize motor angles*
   In this block the signals from the counter modules and the model settings are received and translated to motor position, speed and velocity. These then can be used in the rest of the model.

2. *Control*
   In this block all (haptic) functions are programmed. This is by far the largest and most complex block of the system. All functions are programmed in such a way that they are switched off by default. In this way one model that contains a large number of functions can be used in stead of creating separate models for each function.

3. *Overrule motor angles*
   The overrule functionality can be used when the operator prefers to let the autopilot control one or more degrees of freedom of the levers. The signal received from the levers is overruled by for example the signal generated by the autopilot.

4. *Motor safety*
   In this block the torque that has to be delivered by the model according to the function blocks compared to the maximum allowed torque to ensure the hardware is not damaged.

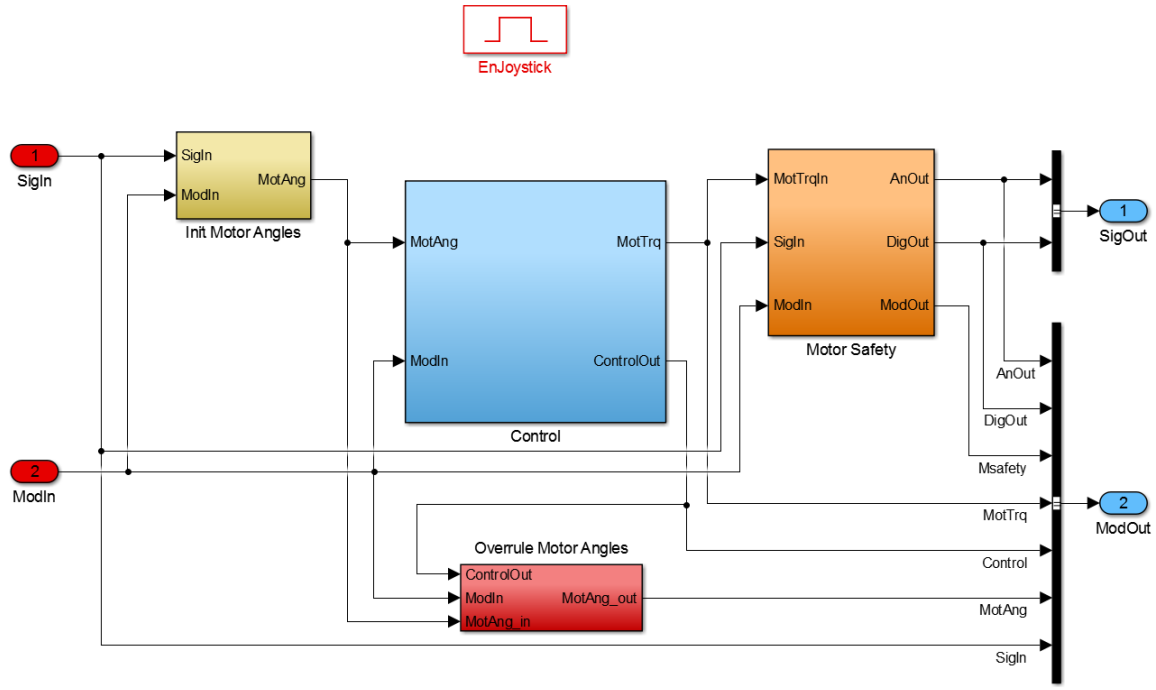

Figure F.2: The joystick functionality block.

The workings of the speed advice model are already described in Chapter 5. In Figure F.3 an overview of a part of the Matlab Simulink model is provided. Within the sea state estimation block the sea state is estimated using a 30 seconds running average time window. First for each upper and lower boundary of a sea state data is collected on the average vessel displacements at the estimated average speed. The generated database is used to find the average displacement boundaries within a sea state. Now the measured signal is compared in real-time to these boundaries to find in which sea state the vessel currently resides.

Knowing the sea state allows the system to select the corresponding look-up table. In this look-up table the advice speed is found by looking at the defined probability of exceedance and acceleration threshold. Quadratic interpolation is used to approximate the advice speed when the intersection of the threshold and Probability of Exceedance (PoE) lines does not occur precisely at one of the Rayleigh lines. This quadratic interpolation was used because it approximated the middle line the best when using three speed lines to tune the model.

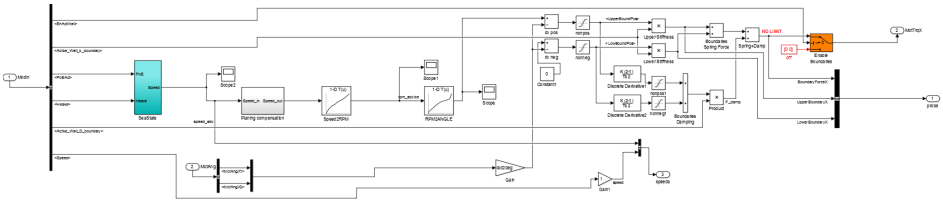

Figure F.3: The haptic speed advice model

The speed advice is communicated to the operator by placing a virtual wall at the maximum safe speed found by the model. This force is tuned such that the operator was aware of the advice provided but could push through if more calm seas were expected to be inbound. In Figure F.3 it can be seen how the speed advice is translated to a motor torque that is fed through to the operator.

Appendix G

Results

In this section all relevant plots and tables that were generated from the experimental data are provided. Because the update rate of the model is 1 kHz not all data generated by each participant could be provided. The storing of the experimental data resulted in data files with on average 600.000 data points per trial per metric for each of the 15 metrics. Therefore, it was chosen to visualize the data in a manner that does not show all points but shows the trends. The data is shown for all relevant metrics that are recorded.

1. Ship speed
2. Accelerations
3. Throttle angle

G.1 Ship speed

In Figures G.1 and G.2 the occurrence of the speeds during the day and night conditions are given. In these figures it can be seen that the range of speeds is much more narrow for the shared control condition compared to manual.

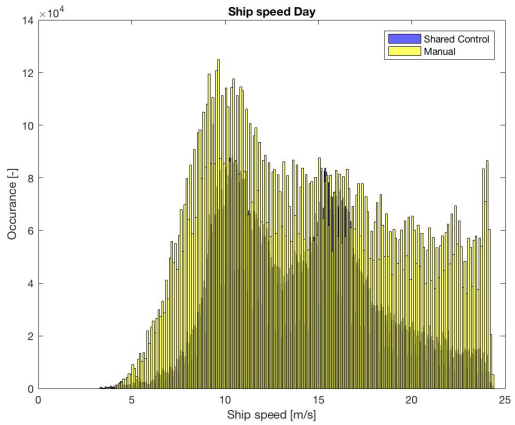

Figure G.1: The occurrence of ship speeds during day time.

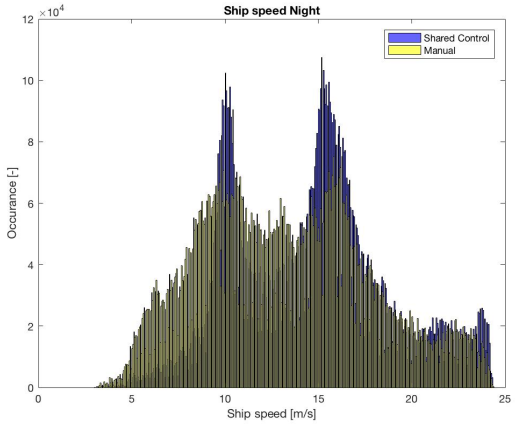

Figure G.2: The occurrence of ship speeds during night time.

G.2 Accelerations

In Figures G.3a, G.4a, G.5a G.6a the magnitude of the excessive accelerations are shown for the different conditions. Figures G.3b, G.4b, G.5b and G.6b show the location of the accelerations over the track.

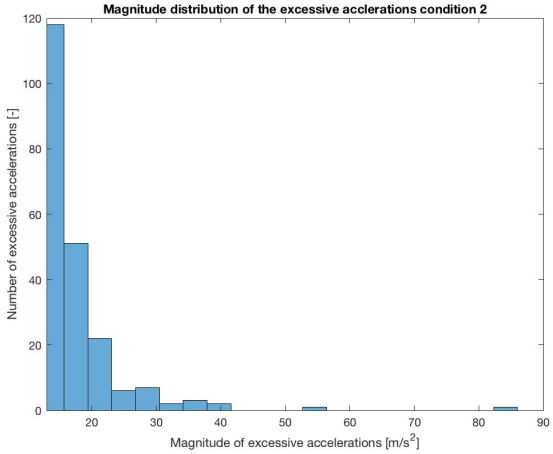

(a) Peak accelerations for the Manual day condition.

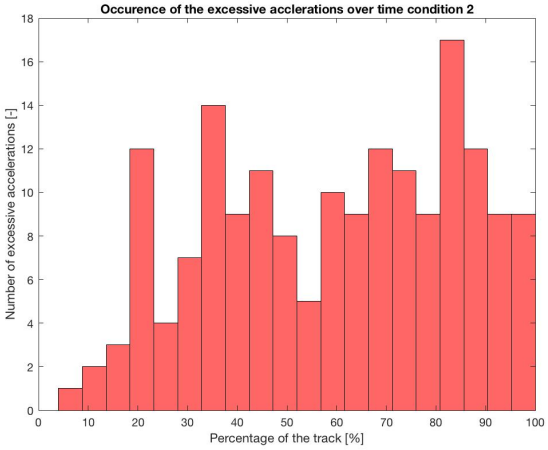

(b) Location of the peak accelerations for the Manual day condition.

In Figures G.7, G.8 and G.9 the not-a-box-plot of the $A_{1/3}$, $A_{1/10}$ and $A_{1/100}$ are shown for the different conditions.

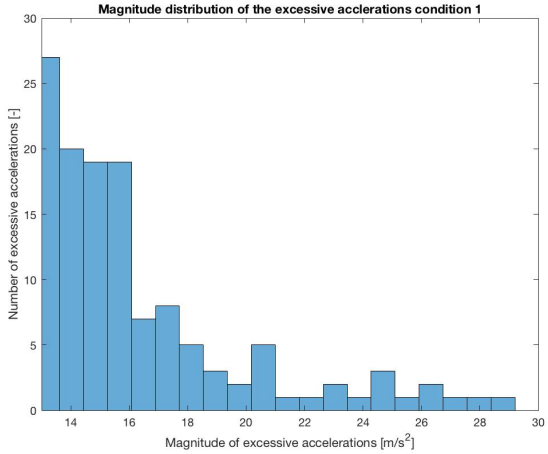

(a) Peak accelerations for the Shared control day condition.

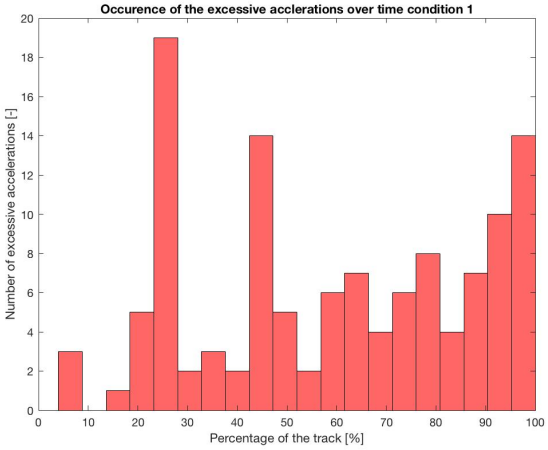

(b) Location of the peak accelerations for the Shared control day condition.

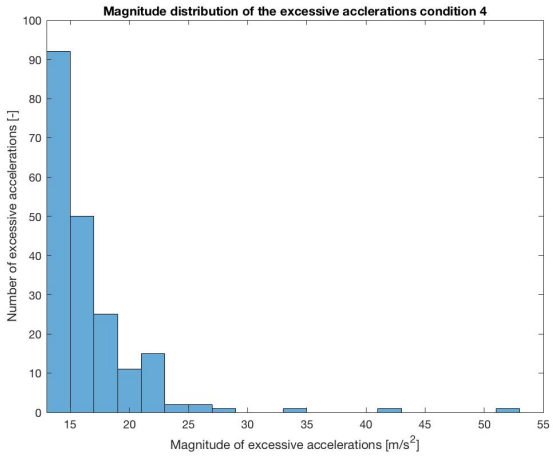

(a) Peak accelerations for the Manual night condition.

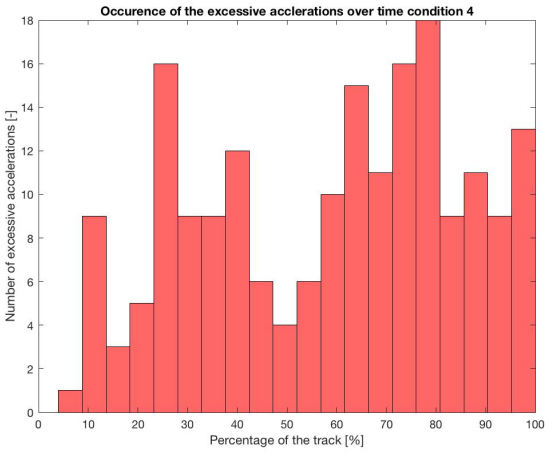

(b) Location of the peak accelerations for the Manual night condition.

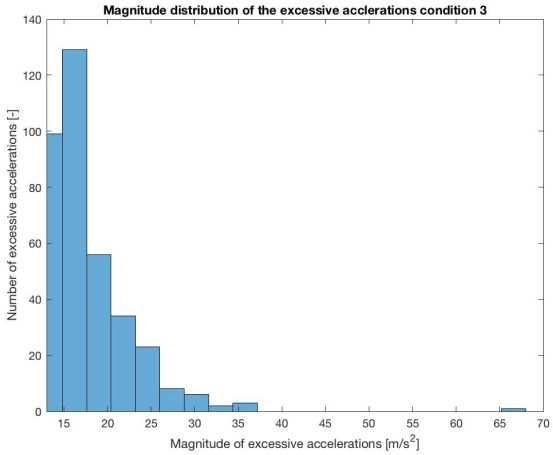

(a) Peak accelerations for the Shared control night condition.

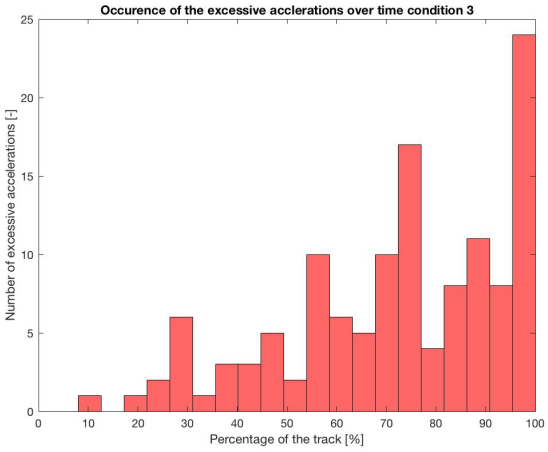

(b) Location of the peak accelerations for the Shared control night condition.

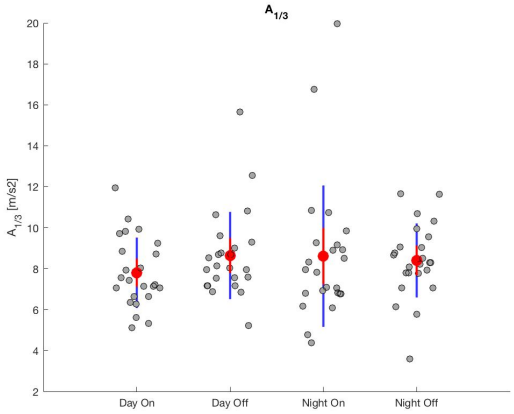

Figure G.7: The not-a-box-plots for $A_{1/3}$.

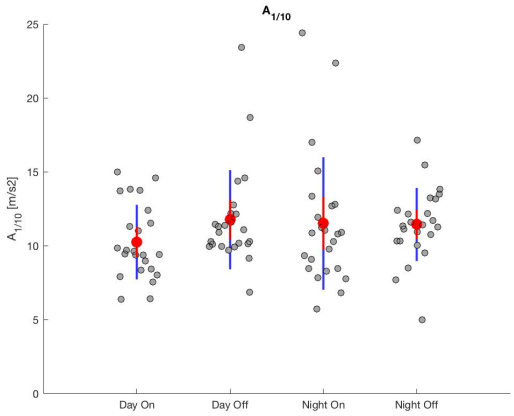

Figure G.8: The not-a-box-plots for $A_{1/10}$.

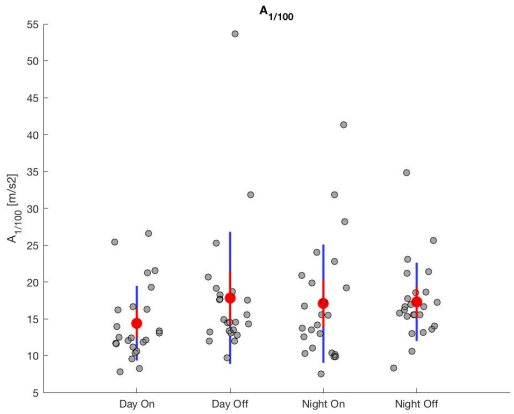

Figure G.9: The not-a-box-plots for $A_{1/100}$.

To gain an insight in the relations between the dependent variables the following plots are generated. First the relation between ship speed and acceleration is shown in Figures G.10a and G.10b

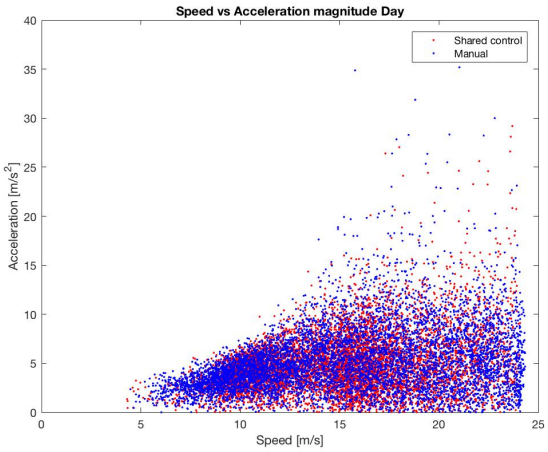

(a) Relation between ship speed and accelerations during day.

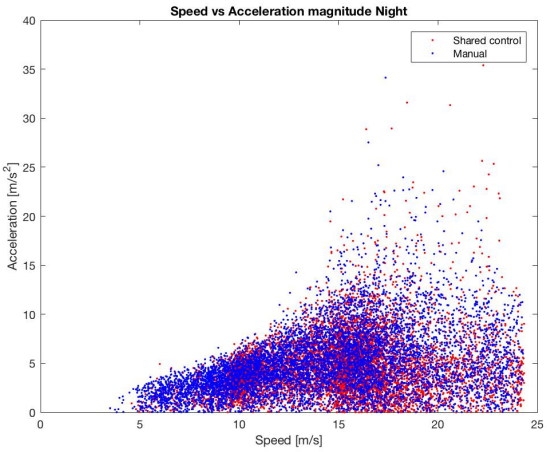

(b) Relation between ship speed and accelerations during night.

Also the relation between lever position and acceleration is investigated in Figure G.11a and G.11b. Using this figure it can be seen if the participants reacted before the impact occurred or after.

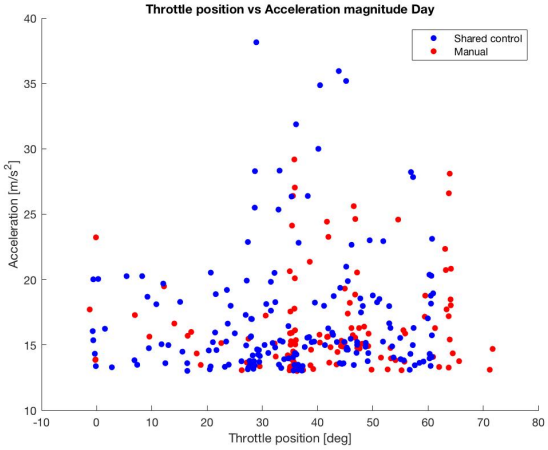

(a) Relation between lever position and accelerations during day.

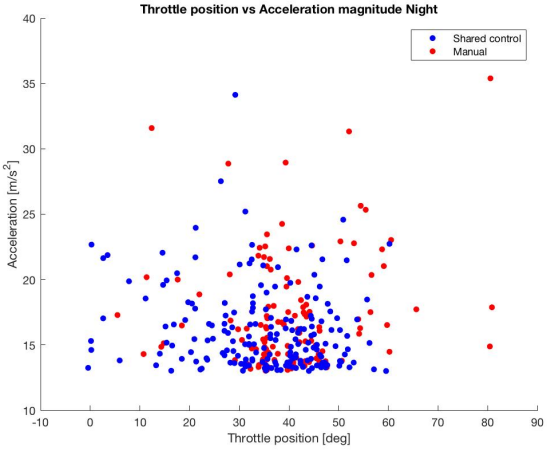

(b) Relation between lever position and accelerations during night.

In Figure G.12 the ship speed time trace is plotted together with the advised speed in one figure. This figure is then overlaid with the acceleration time trace and the peaks above threshold are identified by the blue arrows. It can be seen that most of the times when the ship speed becomes significantly higher than the advised speed an excessive acceleration is encountered. For conditions 2 and 4 the advice speed is plotted with a dashed line because this advice is not provided to the operator.

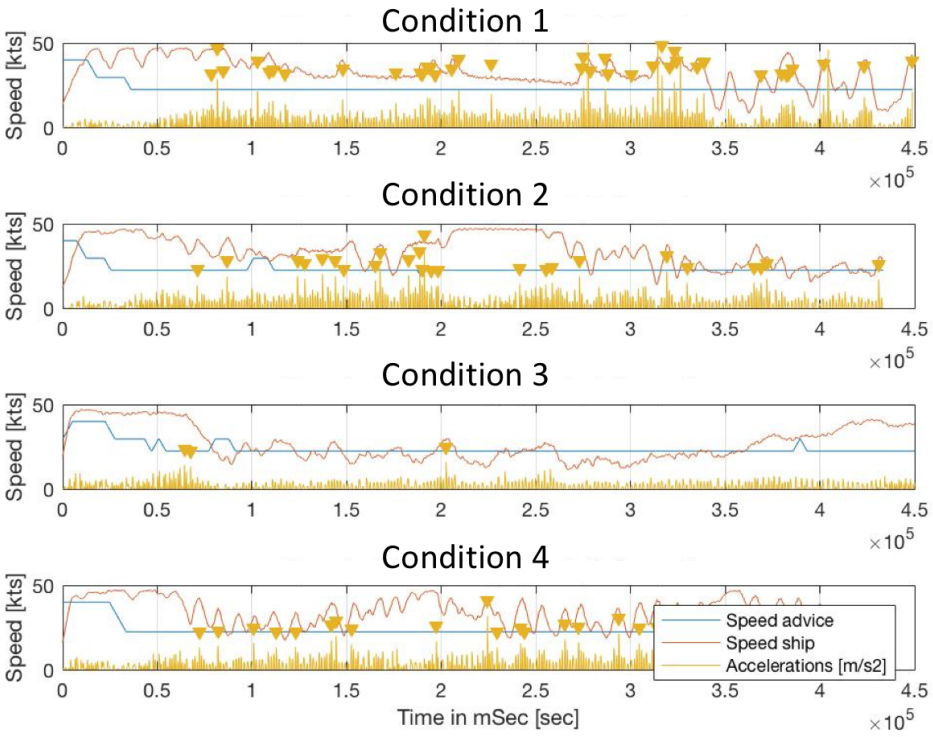

Figure G.12: The ship speed and advice speed from a random participant overlaid with the acceleration signal.

G.3 Different participants

The lever position in the different condition for two random participants is shown in Figure G.13. As can be seen the participants each had a different strategy. Where the right participant is moving much more without the speed advice, the left participant is trying to mimic the speed advice once it is taken away.

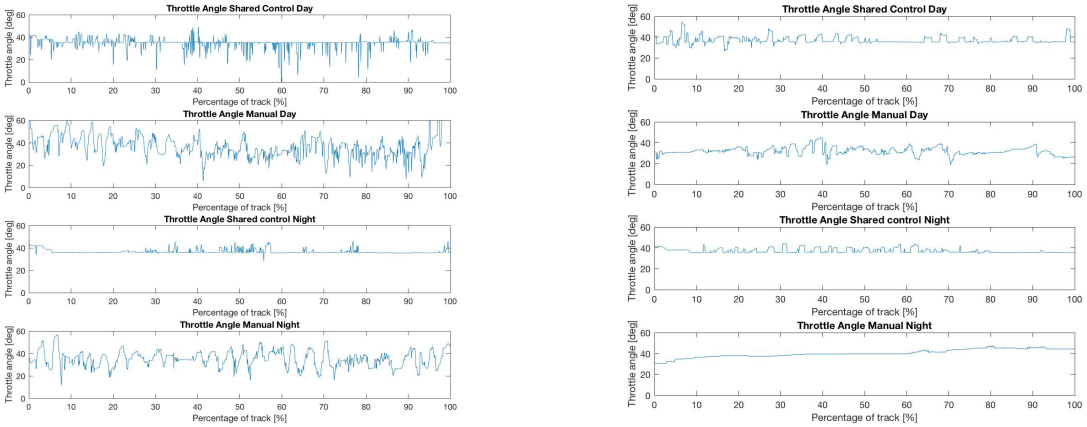

Figure G.13: The lever position over the duration of the track for different participants.

First part of the data

As discussed in Chapter 7 the first part (10%) of the data was discarded because the speed advice system was not fully initialized in all cases at the start of the measurements. In Figures G.14a and G.14b the advice speed for the day and the night condition is shown. It can be seen that in most of the cases the advice is not yet fully initialized.

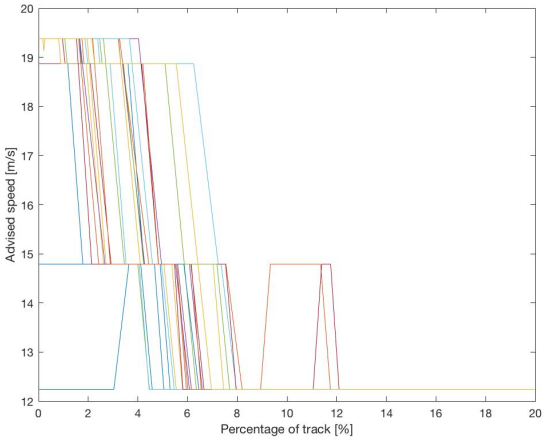

(a) The advised speed at the first 20% of the trial during the day condition.

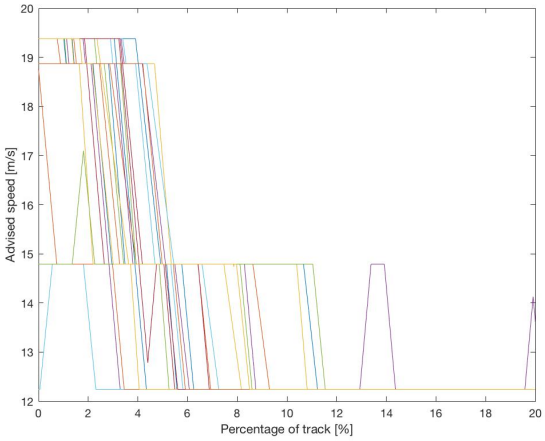

(b) The advised speed at the first 20% of the trial during the night condition.

The performance of one of the outliers is shown in Figure G.15. This figure can be used to to see what went wrong in that case. Clearly the participant disregarded the speed advice completely to achieve the highest possible speed and thereby also was subjected to the most violent accelerations.

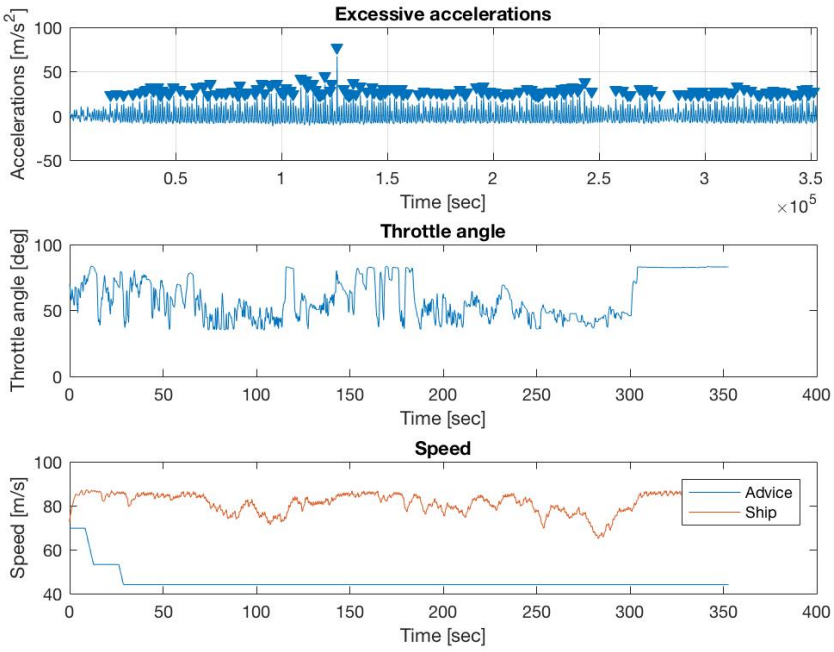

Figure G.15: The results of one of the outliers plotted for the different metrics.

The visualization of the difference in strategy is shown in Figure G.16, where the average speed is plotted against the number of excessive accelerations.

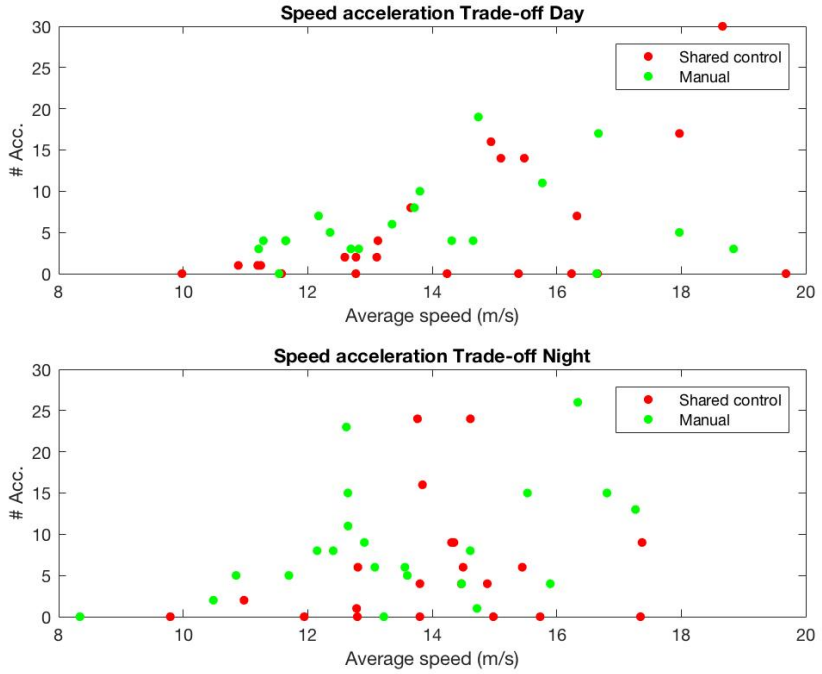

Figure G.16: The average speed plotted against the number of excessive accelerations.

Table G.1: Means (M), standard deviations (SD), effect sizes (d_z), and results of the repeated measures ANOVA (F, p) per item of the TLX.

	Manual Day M(SD)	Shared control Day M(SD)	Manual Night M(SD)	Shared Control Night M(SD)	p-value (F=3,94)	Pairs 1-2 $p(d_z)$	3-4 $p(d_z)$	2-3 $p(d_z)$
NASA-TLX								
Mental demand	57.9 (18.23)	46.1 (20.3)	67.7 (22.4)	53.0 (17.8)	p=$4.9 * 10^{-4}$ F=6.78	0.38	0.96 (x=0.001)	0.80 (p=0.0066)
Physical demand	29.1 (20.0)	23.6 (17.7)	38.0 (22.7)	33.4 (22.9)	p=0.03 F=3.12	0.27	0.21	0.60
Temporal demand	41.8 (20.8)	35.4 (21.1)	38.6 (20.0)	36.4 (19.5)	p=0.39 F=1.01	0.28	0.14	0.20
Performance	49.5 (18.2)	51.4 (25.1)	43.9 (18.0)	57.8 (19.8)	p=0.1 F=2.11	0.02	0.65 (x=0.037)	0.23
Effort	55.9 (17.6)	41.1 (19.9)	58.4 (24.0)	44.1 (22.6)	p=0.0017 F=5.68	0.58	0.63 (x=0.046)	0.70 (p=0.02)
Frustration	29.6 (21.4)	18.2 (11.6)	32.7 (22.7)	18.3 (18.3)	p=$4.26 * 10^{-4}$ F=6.91	0.70 (x=0.02)	0.58	0.96 (p=0.001)